Gallium: Inorganic Chemistry

Kulbinder Kumar Banger[1] & Aloysius F. Hepp[2]
[1]*Ohio Aerospace Institute & NASA Glenn Research Center, Cleveland, OH, USA*
[2]*NASA Glenn Research Center, Cleveland, OH, USA*

Based in part on the article Gallium: Inorganic Chemistry by Andrew R. Barron & Andrew N. MacInnes which appeared in the Encyclopedia of Inorganic Chemistry, First Edition.

1 INTRODUCTION

The element gallium was predicted, as eka-aluminum, by Mendeleev in 1870, and subsequently discovered by Lecoq de Boisbaudran in 1875. The new element was named in honor of France (Latin *Gallia*). The chemistry of gallium was reviewed by Gmelin in 1936,[1] and in the following year by Einecke.[2] Several general but informative chemistry publications/books have appeared that deal with certain aspects of the history, occurrence, extraction, purification, analysis, physical, and chemical properties, toxicology, or uses of the element,[3–5] while the industrial application[6–8] and coordination chemistry[9,10] of gallium has been extensively reviewed. In addition, the area has generally been reviewed and published in annual reviews.[11–21]

2 THE ELEMENT

2.1 Abundance

Gallium is very much less abundant than aluminum and tends to occur at low concentrations in sulfide minerals rather than as oxides, although gallium is also found associated with aluminum in bauxite. At 19 ppm, gallium is about as abundant as nitrogen, lithium, and lead; it is twice as abundant as boron (9 ppm), but is more difficult to extract owing to the lack of any major gallium-containing ore. Gallium always occurs in association either with zinc or germanium, its neighbors in the periodic table, or with aluminum in the same group. Thus, the highest concentrations (0.1–1%) are in the rare mineral germanite (a complex sulfide of Zn, Cu, Ge, and As); concentrations in sphalerite (ZnS), bauxite, or coal are a hundredfold less.

2.2 Preparation and Use

Gallium was originally recovered from flue dusts emitted during sulfide roasting or coal burning (up to 1.5% Ga), but is now obtained as a by-product of the aluminum industry. The Bayer process for obtaining alumina from bauxite gradually enriches the alkaline solutions from an initial weight ratio Ga:Al of about 1:5000 to about 1:300; electrolysis of these extracts with an Hg electrode gives further concentration, and the solution of sodium gallate is then electrolyzed with a stainless steel cathode to give gallium metal. Ultra high-purity gallium for semiconductor growth is obtained by further chemical treatment with acids and oxygen at high temperatures followed by crystallization and zone refining. Since bauxite (Al_2O_3) contain 0.003–0.01% gallium, complete recovery would yield some 500–1000 tons per year; however, present consumption, though growing rapidly, is only a small fraction of this being of the order of 10 tons per annum. This can be compared with the estimate of 5 tons for the total of Ga metal in the 90 years following its discovery (1875–1965).

Gallium's main use is in semiconductor technology. For example, GaAs can convert electricity directly into coherent light (laser diodes) and convert sunlight into electricity (solar cells), is employed in electroluminescent light-emitting diodes (LEDs); it is also used for doping other semiconductors and in solid-state devices such as heterojunction bipolar transistors (HBTs). The compound $MgGa_2O_4$ is used in ultraviolet-activated powders as a brilliant green phosphor used in copying machines. Another very important application is to improve the sensitivity of various bands used in the spectroscopic analysis of uranium. Minor uses are as high-temperature liquid seals, manometric fluids, and heat-transfer media, and for low-temperature solders.

2.3 Properties

Gallium has a beautiful silvery-blue appearance; it wets glass, porcelain, and most other surfaces (except quartz, graphite, and Teflon) and forms a brilliant mirror when painted onto glass. Selected physical constants of gallium are summarized in Table 1. The atomic radius and first ionization potential of gallium are almost identical with those of aluminum and the two elements frequently resemble each

Table 1 Physical properties of gallium metal

Atomic number	31	Melting point (°C)	29.75
Atomic weight	69.72	Boiling point (°C)	2227
Atomic radius (Å)	1.245	d_4^{20} (solid) (g mL^{-1})	5.907
Ionic radius (Å)	0.62	$d_4^{29.8}$ (liquid) (g mL^{-1})	6.0948
Ionization potential (eV)	6.00	Atomic volume (29 °C) (mL)	11.81
Standard electrode potential (volts)	0.52	Atomic volume (30 °C) (mL)	11.44

other in chemical properties. Both are amphoteric, but gallium is less electropositive as indicated by its lower electrode potential. Differences in the chemistry of the two elements can be related to the presence of a filled set of 3d orbitals in gallium.

The unusual physical properties of metallic gallium arise from its unique crystal structure which consists of Ga_2 units arranged in deformed sets of hexagonal rings, Figure 1.[6] The orthorhombic unit cell has four Ga_2 units lying symmetrically in the *ac* plane at angles of 17° to the *c*-axis, the spacing of these molecular planes being *b*/2. Each gallium atom has seven Ga···Ga interactions, one nearest neighbor at 2.44 Å, and three sets of two each at 2.71, 2.74, and 2.80 Å. This rather open structure collapses to a more nearly close-packed arrangement in the liquid state, and melting is accompanied by a contraction of 3.1% in atomic volume and by a considerable increase in electrical conductivity. Here gallium resembles its neighbor germanium, as well as antimony and bismuth. The structure of a denser form of gallium (orthorhombic) has been obtained by supercooling the liquid to −16.3 °C.[22] In this arrangement, the gallium atoms form zigzag chains along the *c*-axis. In a chain, the Ga–Ga distance is 2.68 Å, and the Ga–Ga–Ga angle is 72.3°. Between the chains, the gallium atoms have four additional neighbors at 2.87 Å, and two at 2.90 Å, making a total of eight Ga···Ga interactions.

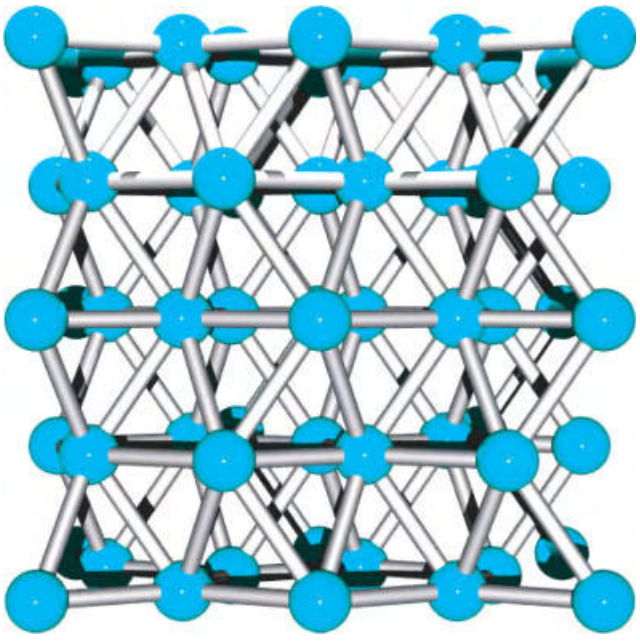

Figure 1 Unit cell of α-gallium metal

Elemental gallium has a very low-melting point, and an extraordinary low vapor pressure (less than 1 mmHg at 1300 °C). These factors combine to give gallium the longest liquid range of any known substance and form the basis of its (very limited) use in high-temperature thermometers.

3 SPECTROSCOPY

3.1 Gallium NMR

Gallium has two NMR-active isotopes (spin $I = 3/2$), ^{69}Ga and ^{71}Ga, with the latter possessing a higher receptivity in addition to narrower relative line width; however, NMR studies for both isotopes are equally reported and studied. Chemical shifts are generally reported with respect to either $Ga(NO_3)_3$ or $[Ga(H_2O)_6]^{3+}$ with the chemical shift window being approximately 1400 ppm (this follows suit with the corresponding Al compounds) (Table 2).

Ga NMR studies have received increased impetus as a viable probing tool for some key areas. ^{69}Ga NMR studies have been used to support and follow Ga antitumor agents and their mode of action and uptake into tumor cells. ^{71}Ga NMR has thus been used to study how various ligands may form complexes with the cation. In another area, the use of ^{69,71}Ga NMR has been used to examine defects in semiconductors, which can have a crucial influence on the semiconductors' electronic and optical properties.[23–25] In addition, a number of very useful web sites detailing Ga NMR related studies are available.[26–28]

3.2 Mass Spectroscopy

The two naturally occurring isotopes of Gallium Table 2 can be used as an aid in mass spectroscopic studies. Isotopic distribution patterns have been used to model the masses and abundances of the isotopes for a given formula, and as a 'fingerprinting' tool when used in a comparative analysis with the experimental data. This technique has recently been used for identifying the formation, mechanism, and the fragmentation pattern of Ga_n clusters (Figure 2),[29] and more recently to confirm the formation of the first Ga=As containing species.[30]

Table 2 Summary of properties for magnetically active quadruploar ga nuclei

Isotope	Spin	Natural abundance (%)	Quadrupole moment (10^{-28} m^2)	Relative sensitivity	Width Factor	Relative Intensity	Absolute sensitivity	NMR frequency (MHz)
^{69}Ga	3/2	60.4	0.178	6.91E-2	5.93	0.007	4.17E-2	24.003
^{71}Ga	3/2	39.6	0.112	0.14	2.34	0.024	5.62E-2	30.495

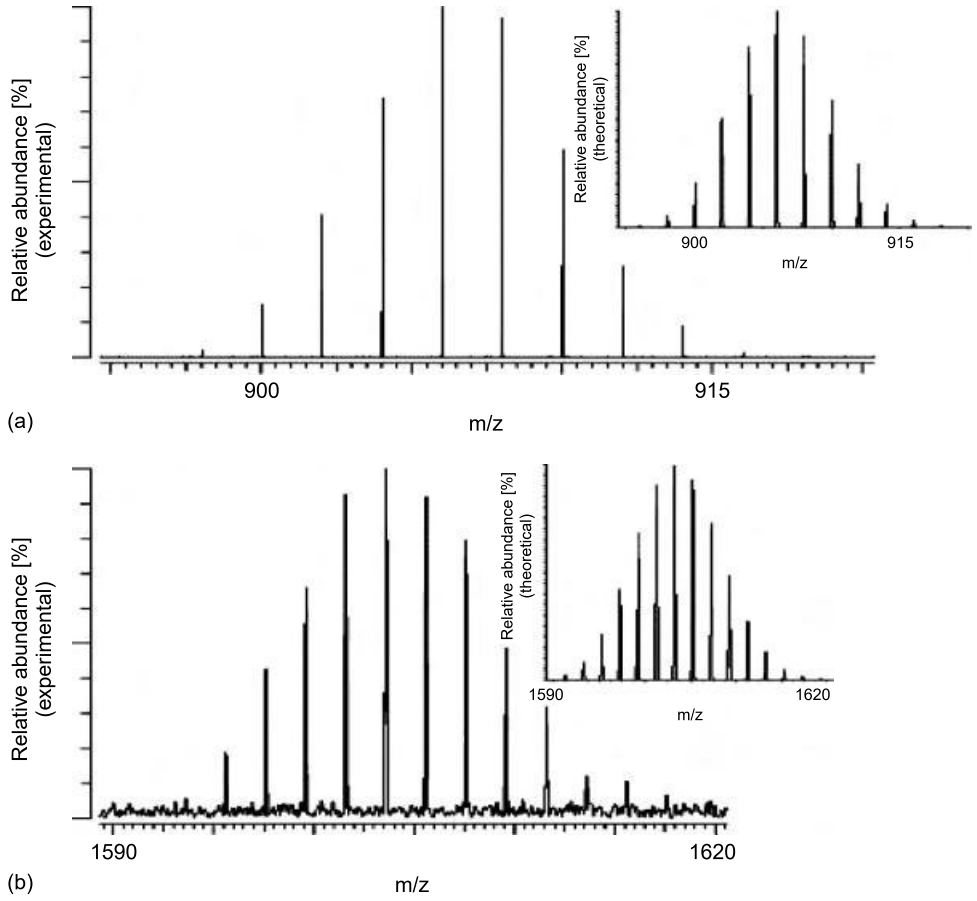

Figure 2 Mass spectra of the Ga_{13}^- cluster (a) and the Ga_{23}^- cluster (b) and the corresponding calculated spectra. (Reprinted from Ref. 29. © 2002, with permission from Elsevier)

4 BINARY COMPOUNDS

4.1 Gallium Pnictogens, (III-V)

Undoubtedly the binary compounds of gallium with the most industrial interest are those of the group 15 elements, GaE (E = N, P, As, Sb). The group 15 gallium alloys with nitrogen, phosphorus, arsenic, and antimony are isoelectronic with the group 14 elements. There has been considerable interest, particularly in the physical properties of these compounds, since 1952 when Welker first showed that they had semiconducting properties analogous to those of silicon and germanium.

4.1.1 Synthesis, Structure, and Physical Properties of Bulk Material

Gallium nitride is the only member of the group which cannot be prepared by direct reaction of the elements. It was first made by the reaction of gallium with ammonia at 1000 °C, but has also been prepared by the decomposition of either $[NH_4]_3[GaF_6]$ or the halide Lewis acid–base adduct $GaCl_3(NH_3)$. Gladfelter has shown that cubic GaN may be prepared by the low-temperature pyrolysis of the trimeric gallane compound $[H_2Ga(NH_2)]_3$ (equation 1).[31]

$$[H_2Ga(NH_2)]_3 \xrightarrow{\Delta} 3GaN + 6H_2 \quad (1)$$

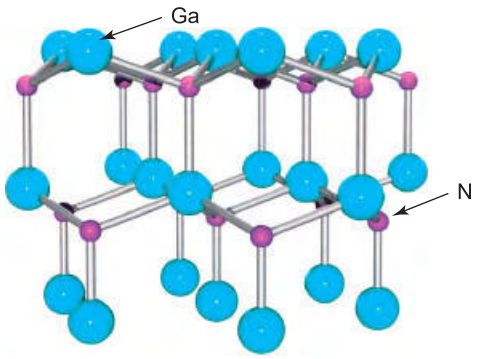

Figure 3 Lattice packing of würtzite GaN

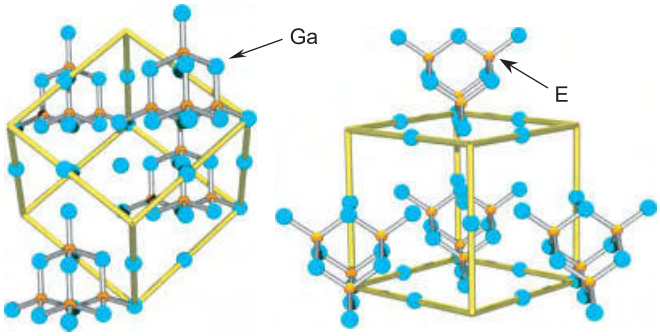

Figure 4 Unit cell structure of GaE (E = P, As, Sb); gallium atoms are cyan

Gallium nitride is commonly gray or yellow, diamagnetic, and crystallizes in the würtzite (ZnS) structure (Figure 3). Gallium nitride is not hydrolyzed by hot water or by acids such as dilute or concentrated hydrofluoric, hydrochloric, or nitric, or aqua regia. However, the compound dissolves slowly in hot concentrated sulfuric acid. With hot concentrated aqueous alkali, ammonia is evolved. There is no reaction with hydrogen at 800 °C but oxygen slowly reacts with gallium nitride at 900 °C over a period of days to give nitrogen and Ga_2O_3. The properties of GaN are summarized in Table 3.

Gallium phosphide, arsenide, and antimonide can all be prepared by direct reaction of the elements; this is normally done in sealed silica tubes or in a graphite crucible under hydrogen. Phase diagram data are hard to obtain in the gallium–phosphorus system because of loss of phosphorus from the bulk material at elevated temperatures. Thus, GaP has a vapor pressure of more than 13.5 atm at its melting point, compared to 0.89 atm for GaAs. The physical properties of these three compounds are compared with those of the nitride in Table 3. All three adopt the zinc blende crystal structure (Figure 4), and are more highly conducting than gallium nitride.

When considering the synthesis of group 13–15 compounds for electronic applications, the very nature of semiconductor behavior demands the use of high-purity single-crystal materials. The polycrystalline materials synthesized above are, therefore, of little use for 13–15 semiconductors but may, however, serve as the starting material for melt-grown single crystals. For gallium arsenide, undoubtedly the most important 13–15 semiconductor, melt-grown single crystals are achieved by one of two techniques: the Bridgman technique, and the Czochralski technique.

The Bridgman technique requires a two-zone furnace, of the type shown in Figure 5. The left-hand zone is maintained at a temperature of ca. 610 °C, allowing sufficient overpressure of arsenic within the sealed system to prevent arsenic loss from the gallium arsenide. The right-hand side of the furnace contains the polycrystalline GaAs raw material held at a temperature just above its melting point (ca. 1240 °C). As the furnace moves from left to right, the melt cools and solidifies. If a seed crystal is placed at the left-hand side of the melt (at a point where the temperature gradient is such that only the end melts), a specific orientation of the single crystal may be propagated at the liquid–solid interface eventually to produce a single crystal.

The Czochralski technique shown in Figure 6 relies on the controlled withdrawal of a seed crystal from a liquid melt. As the seed is lowered into the melt, partial melting of the tip occurs, creating the liquid–solid interface required for crystal growth. As the seed is withdrawn, solidification occurs and the seed orientation is propagated into the grown material. The

Table 3 Physical properties of group 13–15 compound semiconductors

Property	GaN	GaP	GaAs	GaSb
Melting point (°C)	>1250 (dec)	1350	1240	712
Density (g cm^{-3})	–	4.138	5.3176	5.6137
Crystal structure	Würtzite	Zinc blende	Zinc blende	Zinc blende
Cell dimen. (Å)[a]	$a = 3.187$ $c = 5.186$	$a = 5.4505$	$a = 5.6532$	$a = 6.0959$
Refractive index[b]	2.35	3.178	3.666	4.388
κ (ohm^{-1} cm^{-1})	10^{-9}–10^{-7}	10^{-2}–10^{2}	10^{-6}–10^{3}	6–13
Band gap (eV)[c]	3.44	2.24	1.424	0.71

[a]Values given for 300 K. [b]Dependent on photon energy; values given for 1.5 eV incident photons. [c]Dependent on temperature; values given for 300 K.

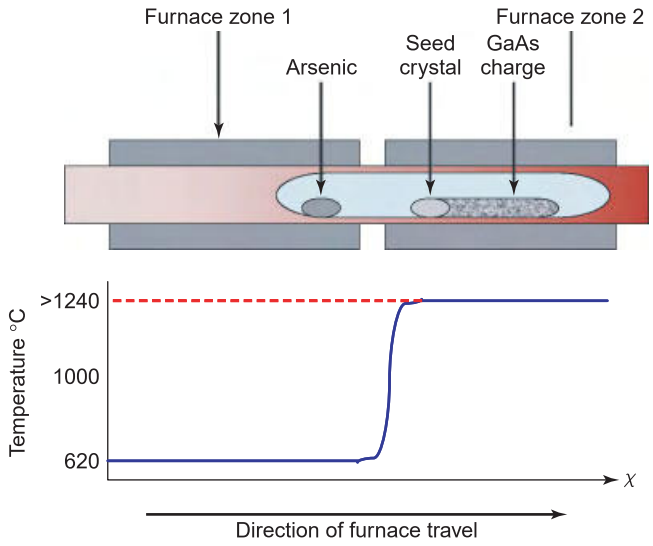

Figure 5 Schematic diagram of a Bridgman two-zone furnace used for melt growths of single-crystal GaAs

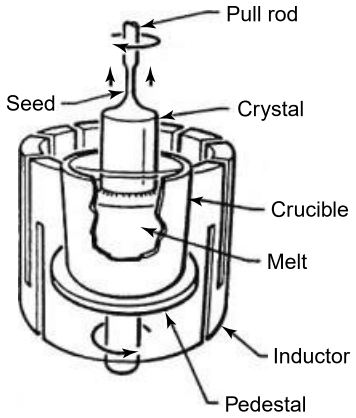

Figure 6 Schematic diagram of the Czochralski technique as used for the growth of single-crystal GaAs

variable parameters of rate of withdrawal and rotation rate can control crystal diameter and purity. The gallium arsenide melt is capped by boron trioxide (B_2O_3). The capping layer, which is inert to gallium arsenide, prevents arsenic loss when the pressure on the surface is above atmospheric pressure. The growth of gallium arsenide by this technique is thus termed liquid encapsulated Czochralski (LEC) growth.

While the Bridgman technique is largely favored for GaAs growth, larger diameter wafers can be obtained by the Czochralski method. Both of these melt techniques produce materials heavily contaminated by the crucible, making them suitable almost exclusively as substrate material. The methods by which higher purity single crystal of epitaxial GaAs can be obtained are therefore discussed below.

Table 4 Comparison of physical and semiconductor properties of GaAs and Si

Properties	GaAs	Si
Physical		
Formula weight	144.63	28.09
Crystal structure	Zinc blende	Diamond
Lattice constant	5.6532	5.43095
Melting point (°C)	1238	1415
Density (g cm^{-3})	5.32	2.328
Thermal conductivity (W cm^{-1} K^{-1})	0.46	1.5
Electronic		
Band gap (eV) at 300 K	1.424	1.12
Intrinsic carrier conc. (cm^{-3})	1.79×10^6	1.45×10^{10}
Intrinsic resistivity (Ω cm)	10^8	2.3×10^5
Breakdown field (V cm^{-1})	4×10^5	3×10^5
Minority carrier lifetime (s)	10^{-8}	2.5×10^{-3}
Mobility (cm^2 V^{-1} s^{-1})	8500	1500

4.1.2 Electronic Applications of GaAs

Gallium arsenide is a compound semiconductor with a combination of physical properties that has made it an attractive candidate for many electronic applications. From a comparison of various physical and electronic properties of GaAs with those of Si (Table 4), the advantages of GaAs over Si can be readily ascertained.

1. The band gap of GaAs is 1.42 eV, resulting in photon emission in the infrared range. Alloying GaAs with Al to give $Al_xGa_{1-x}As$ can extend the band gap into the visible red range. Unlike Si, the band gap of GaAs is direct, that is, the transition between the valence band maximum and conduction band minimum involves no momentum change and hence does not require a collaborative particle interaction to occur. Photon generation by interband radiative recombination is therefore possible in GaAs, whereas for Si, with an indirect band gap, this process is too inefficient to be of use. The ability to convert electrical energy into light forms the basis of the use of GaAs, and its alloys, in optoelectronics, for example, in LEDs (Figure 7), solid-state LASERs (light amplification by the stimulated emission of radiation), and solar cells.
   A significant drawback of small band-gap semiconductors, such as Si, is that electrons may be thermally promoted from the valence band to the conduction band. Thus, with increasing temperature the thermal generation of carriers eventually becomes dominant over the intentionally doped level of carriers. The wider band gap of GaAs gives it the ability to remain 'intentionally' semiconducting at higher temperatures; GaAs devices are generally more stable to high temperatures than are similar Si devices.
2. The low intrinsic carrier density of GaAs in a pure (undoped) form indicates that GaAs is intrinsically a very poor conductor and is commonly referred to as being semi-insulating. This property allows many active

Figure 7 III-V based light-emitting diodes

devices to be grown on a single substrate, where the semi-insulating GaAs provides the electrical isolation of each device; this is an important feature in the miniaturization of electronic circuitry, that is, VLSI (very large-scale integration) involving over 100 000 components per chip (one chip is typically between 1 and 10 mm^2).

3. The higher electron mobility in GaAs than in Si potentially means that in devices where electron transit time is the critical performance parameter, GaAs devices will operate with higher response times than equivalent Si devices. However, the fact that hole mobility is similar for both GaAs and Si means that devices relying on cooperative electron and hole movement, or hole movement alone, show no improvement in response time when GaAs based.

The many desirable properties of gallium arsenide are offset to a great extent by a number of undesirable properties, which have limited the applications of GaAs-based devices to date.

1. The bulk crystal growth of GaAs (see Section 4.1.1) presents a problem of stoichiometric control owing to the loss, by evaporation, of arsenic both in the melt and the growing crystal (>ca. 600 °C). Melt-growth techniques are, therefore, designed to enable an overpressure of arsenic above the melt to be maintained, thus preventing evaporative losses. The loss of arsenic also negates diffusion techniques commonly used for wafer doping in Si technology, since the diffusion temperatures required exceed that of arsenic loss.
2. The thermal gradient and, hence, stress generated in melt-grown crystals have limited the maximum diameter of GaAs wafers (currently 3–4 inch diameter compared to over 12 inch for Si), because with increased wafer diameters the thermal stress-generated dislocation (crystal imperfection) densities eventually becomes unacceptable for device applications.
3. Gallium arsenide single crystals are very brittle, requiring considerably thicker substrates than those employed for Si devices.
4. Gallium arsenide's native oxide is found to be a mixture of nonstoichiometric gallium and arsenic oxides and elemental arsenic. Thus, the electronic band structure is found to be severely disrupted, causing a breakdown in 'normal' semiconductor behavior on the GaAs surface. As a consequence, the GaAs MISFET (metal–insulator semiconductor field-effect transistor) equivalent to the technologically important Si-based MOSFET (metal–oxide semiconductor field-effect transistor) is, therefore, presently unavailable.

4.1.3 Gallium Arsenide-Based Devices

The considerable difficulty of growing GaAs single crystals, added to the higher cost of the raw materials gallium and arsenic compared to silicon, has resulted in GaAs technology only being used where Si-based technology is impractical, that is, application areas utilize either the high-speed or light-emitting properties of GaAs. Two areas where GaAs-based devices display properties unobtainable in Si-based devices are in microwave and photonic devices. To illustrate the basic operating principles and complex structures involved in such devices, we can consider two currently operational devices.

1. The MESFET (metal–semiconductor field-effect transistor) is a GaAs device capable of operating at microwave frequencies (1–100 GHz) and in its simplest form is shown schematically (Figure 8). A lightly doped *n*-type (electrons as majority carriers) GaAs layer is grown on a semi-insulating (i.e. high purity) GaAs substrate. Source and drain contacts (Au/Ge alloy) are termed ohmic, that is, there is negligible contact resistance between metallization and semiconductor. The gate contact (Al) is rectifying and creates what is termed a Schottky diode with the *n*-type GaAs. Under appropriate applied voltage or biasing conditions, the gate contact can reduce or maintain conductance in the underlying layer between source and drain and can thus modulate current flow through the

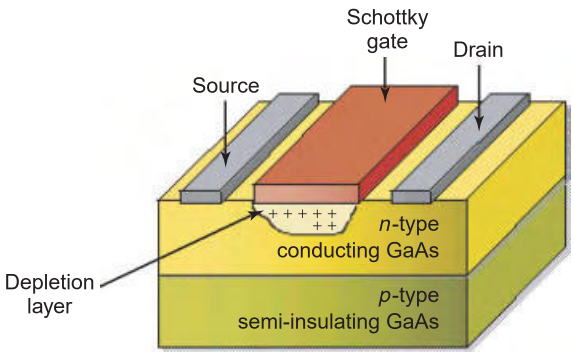

Figure 8 Schematic diagram of a GaAs-based MESFET device

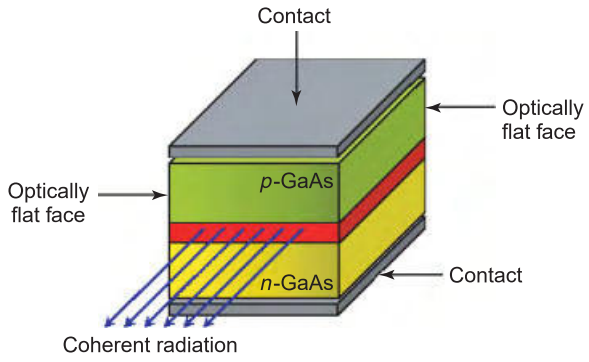

Figure 9 Schematic diagram of a GaAs-based solid-state laser

semiconducting layer. It is this high-speed switching that is utilized in microwave devices.

2. A schematic of a GaAs-based semiconductor laser structure is shown in Figure 9. The basic operating principle of this device is that a forward-biased p–n junction injects charged pairs (holes and electrons) into the 'active' region of the laser. Within this region, carrier recombination occurs, generating light. The injected charge carriers and generated light are confined within this active layer by the surrounding layer possessing both energy band discontinuities and high refractive indices. By this optical and carrier confinement method, stimulated emission of radiation can occur, that is, a generated photon can stimulate electron–hole recombination to produce a further photon in phase with the original. The laser structure thus generates a flux of coherent light. The absence of a direct band gap makes such a device impractical for silicon.

4.1.4 Epitaxial Growth of GaAs

The continuing drive for the scaling down of electronic device dimensions has necessitated the introduction of a new class of growth techniques where high-purity thin single-crystal layers are grown on a single-crystal substrate. The techniques of epitaxial growth (from the Greek *epi taxis* meaning *arrangement on*) are classified as either homo- or heteroepitaxy, depending on whether the base substrate is the same as or different from the growing film. The advantages of using epitaxial growth techniques include control of layer thicknesses, interfacial structure, material composition, and impurity concentration. Homoepitaxy, that is, GaAs on GaAs, is generally employed to provide either doping junctions, for example, *p*-type on *n*-type GaAs, or to allow low-impurity GaAs to be grown on considerably less pure substrates, whereby only the thin (high purity) epitaxial layer is electrically active in the device. Heteroepitaxy, that is, AlGaAs on GaAs, provides junctions with band discontinuities (conduction or valence) that can present either a barrier or enhancement to electron and hole mobility (and therefore current flow) depending on the appropriate doping and electronic biasing conditions. The techniques of epitaxy are discussed below.

4.1.5 Liquid Phase Epitaxy (LPE)

Liquid phase epitaxy (LPE) involves the growth of thin epitaxial layers on a crystalline substrate by direct precipitation from the liquid phase. The requirement for this process is that a suitable solvent for the film material can be obtained that provides a saturated melt solution at a temperature well below the melting point of the substrate. Gallium metal is used as the solvent for LPE of GaAs. A saturated solution of GaAs in gallium metal is introduced on to a substrate of GaAs and allowed to cool below the equilibrium saturation temperature. The melt solution becomes supersaturated, causing precipitation of GaAs on the GaAs substrate. As the melt temperature decreases, the precipitation reaction continues. Impurity additions can similarly be added to the melt to provide *n*- or *p*-type doping by segregation from the melt into the growing film.

4.1.6 Metal-Organic Vapor-phase Epitaxy (MOVPE)

Metal-organic Vapor-phase epitaxy (MOVPE) and what is commonly termed MOCVD (*metal–organic chemical vapor deposition*) are essentially the same technique whereby organometallic compounds, in the form of volatile liquids or sublimable solids, are transported via the vapor phase on to a heated substrate and decomposed alone or in combination with other vapors or gases to give the desired film (Figure 10). The vapor-phase techniques offer the advantages of low growth temperatures substantially below the melting point of the grown film, the ability to grow irregular shaped substrates with conformal, uniform growth, and in some instances the ability to selectively deposit only on desired areas of a substrate surface.

For the growth of group 13–15 compounds, the general embodiment of the vapor-phase process is that liquid

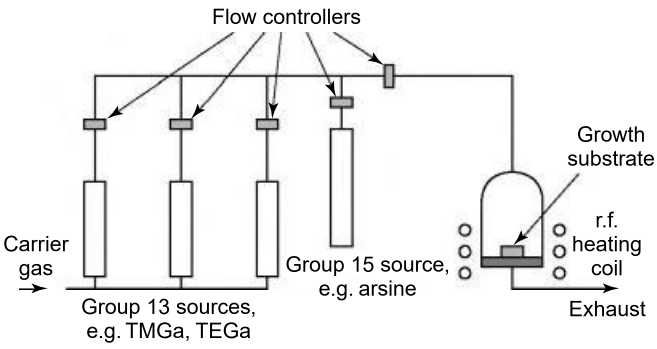

Figure 10 Schematic diagram of a typical MOVPE chamber

organometallic group 13 compounds react with group 15 hydrides at elevated temperatures (equation 2).

$$Me_3Ga + AsH_2 \xrightarrow{H_2} GaAs + 3MeH \qquad (2)$$

There are a number of properties required for compounds to be suitable as precursors for MOVPE; these include sufficient vapor pressure to allow suitable growth rates, ability to be highly purified, controllable deposition behavior, stability in storage, and stability with other species during vapor-phase transport.

Trimethylgallium is the most commonly used precursor owing to its relatively high vapor pressure (182 Torr at 20 °C) at both atmospheric and low pressure. Conversely, Et_3Ga, with both a lower vapor pressure (5.1 Torr at 20 °C) and lower thermal stability is used when higher purity films of GaAs are required. The increased purity of films grown from Et_3Ga, when compared to those grown from Me_3Ga, is a result of lower carbon incorporation (carbon is a *p*-dopant) in the growing film. Mechanistic studies reveal the differing carbon incorporation levels being due to

1. a decrease in Ga–C bond strength for Et_3Ga (52 kcal mol^{-1}) when compared to Me_3Ga (58 kcal mol^{-1}) allows for a lower temperature being required for the homolytic fission of the Ga–C bond in Et_3Ga
2. the ability of Et_3Ga to undergo a *β-Hydride Elimination* step involving the 'clean' elimination of an alkene also contributes to lower carbon incorporation (*see* ***Gallium: Organometallic Chemistry***).

The incorporation of a β-hydride elimination step into precursor pyrolysis has focused attention on alternative organometallic precursors for gallium. However, only limited success has been achieved. Other routes to 'clean' precursor decomposition include the pyrolysis of gallane adducts, that is, the gallane–trimethylamine adduct $H_3Ga(NMe_3)$; however, this and other related gallane compounds are thermally unstable and decompose at room temperature. Storage at low temperatures (−15 °C) and the difficulty of large-scale purification are some of the factors that limit the utility of such adducts. Several studies reported the presence of polymeric contaminant in MOVPE chambers in which the source vapors were allowed to react prior to the deposition zone. While this has now been circumvented by changes in reactor design, precursor compounds of the form $R_3Ga(AsR'_3)$ were found to provide a source of gallium alkyl without the unwanted prereaction with AsH_3. However, AsH_3 was still required as the arsenic source. Recently, many workers have focused on GaAs single-source precursors, with the general formula $[R_2Ga(\mu\text{-}AsR'_2)]_n$; however, the quality of films grown from these compounds still needs to be further improved for microelectronic applications.[9,10]

4.1.7 Molecular Beam Epitaxy

Molecular Beam Epitaxy (MBE) is essentially a modified and highly controllable form of vacuum evaporation, whereby elemental gallium and arsenic sources are held in effusion cells and heated in ultra-high vacuum (UHV) conditions to produce molecular fluxes. Under the UHV conditions, the molecular beams impinge on a heated rotating growth surface with no prior gas-phase collisions to produce precise epitaxial films. The advantages of MBE over vapor-phase techniques include the highly controlled growth that can be obtained, enabling structures of a few atomic layers to be grown, and with that multilayers and quantum-well structure where the layer thickness is less than the mean free path of an electron's travel. The UHV conditions (ca. 10^{-10} Torr) allow both films of the highest purity to be grown and also enable diagnostic and growth monitoring techniques to be employed in situ, that is, reflection high energy electron diffraction (RHEED), low-energy electron diffraction (LEED), and others.

A variation of MBE utilizes organometallic rather than elemental sources for the molecular beams and is termed metal–organic molecular beam epitaxy (MOMBE) or chemical beam epitaxy (CBE). The molecular sources are commonly those used in vapor-phase epitaxy, that is, R_3Ga and AsH_3, and are generally gaseous under UHV conditions. The MOMBE technique offers several advantages over conventional MBE, including lower growth temperatures with concomitant control of layer and doping profiles by lowering interdiffusion processes. The gaseous sources (in UHV) also mean that precursor reservoirs can be externally connected to the UHV chamber, providing 'constant' operational capability. The use of organometallics, however, inevitably introduces impurities (mainly carbon) into the growth system.

4.1.8 Passivation of GaAs

As discussed earlier, GaAs has the potential to be widely used in high-speed electronics and optoelectronics, but its implementation is somewhat hampered by difficulties in reproducibility controlling surface composition and electrical properties. From the earliest days of solid-state electronics, it has been recognized that the presence or absence of surface states plays a decisive role in the usefulness of any semiconductor material. It is desirable to covalently satisfy all surface bonds, thereby shifting the surface states out of the band gap and into the valence and conduction bands. Owing to the high surface-state density of GaAs, and its inability to form a stable native oxide overlayer (see above), there has been much work investigating the chemical passivation of the surface.

Oxide layers on GaAs have been grown by exposure of the GaAs surface to water,[9] or hydrogen peroxide,[32] aniodic oxidation,[33] and oxidation by high kinetic energy atomic oxygen beams.[34] The first effective passivation layer was reported in 1987 by Sandroff and coworkers.[35] They

discovered that a class of inorganic sulfides (Li_2S, $(NH_4)_2S$, $Na_2S{\cdot}9H_2O$, etc.) imparts excellent properties to GaAs surfaces. The surface recombination velocity (SRV) at the interface between $Na_2S{\cdot}9H_2O$ and GaAs begins to approach that of the nearly ideal AlGaAs/GaAs interface. These workers proposed, and this was confirmed by many subsequent studies, that a sulfide layer was covalently bonded to the GaAs surface. While these sulfide films result in a marked decrease in the SRV of GaAs, the effects are only temporary; after 18 h the SRV have returned to their pretreatment values. It is this lack of permanency that has prompted several groups to propose that MOCVD-grown films would make ideal passivation coatings.

The recently reported MOCVD-grown metastable cubic phase of gallium sulfide (GaS),[36] which forms a nearly lattice-matched layer on GaAs, shows promise as a stable commercially viable passivation layer for GaAs-based devices.[37,38] In addition, electrical characterization of the cubic GaS/GaAs interface shows that the Fermi level in both *n*- and *p*-type GaAs is completely unpinned, with the capacitance versus voltage curves showing well-defined accumulation and depletion regions.

4.2 Gallium Chalcogenides

4.2.1 Oxides and Hydroxides

The gallium oxide system is somewhat similar to that of aluminum, affording a high-temperature (α) and a low-temperature γ-Ga_2O_3, each having the same structure as their aluminum counterparts. β-Ga_2O_3 is the most stable crystalline modification (mp 1740 °C); it has a unique crystal structure with the oxide ions in distorted ccp and Ga^{III} in distorted tetrahedral and octahedral sites, with Ga-O distances of 1.83 and 2.00 Å, respectively (Figure 11).[39]

The structure appears to owe its stability to these distortions and, because of the lower coordination of half the Ga^{III}, the density is ca. 10% less than for the α (corundum-type) form. This preference of Ga^{III} for fourfold coordination, despite the fact that it is larger than Al^{III}, may indicate the polarizing

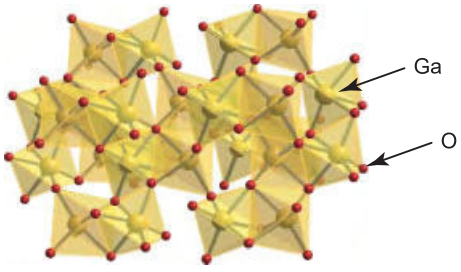

Figure 11 Structure of β-Ga_2O_3; oxygen atoms are shown red. (Ref. 27. Reproduced by permission from Dr Mark J Winter/WebElements. Source: WebElements [http://www.webelements.com/]; http://www.webelements.com/webelements/compounds/text/Ga/Ga2O3-12024214.html)

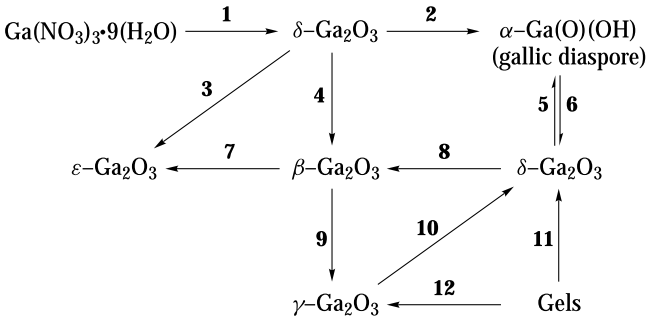

Scheme 1 Transformation relationships among the forms of gallium oxide and its hydrate. (1), 200 °C overnight; (2), <300 °C; (3), dry >500 °C, dry; (4), 300 °C wet; (5), 12 h, 500 °C, wet; (6), <300 °C, wet; (7), 870 °C, dry; (8), 300 °C wet, 600 °C, dry; (9), 650 °C, dry, 300 °C, wet; (10), 500 °C, few h; (11), 500 °C, 12 h, 400–500 °C, very rapid

influence of the d^{10} core; a similar tetrahedral site preference is observed for Fe^{III}. The trioxide is formed by heating the nitrate, the sulfate, or the hydrous oxides that are precipitated from Ga^{III} solutions by the action of ammonia. A summary of the transformations in the gallium oxide (and hydroxide) system is given in Scheme 1.

β-Ga_2O_3 is classified as a transparent conducting oxide (TCO), that is, materials that, though having a wide band gap, are electrically conductive, and exhibits the largest band gap among TCOs with $E_g = 4.8$ eV.[40] Consequently, it has a unique transparency from the visible into the UV wavelength region and is a viable candidate for the next generation of optoelectronic devices operating at shorter wavelengths. Large-size single crystals of high quality β-Ga_2O_3 (>2 cm diam.) have been grown by the floating zone technique.[41] Processed, cut, and polished wafers were found to be highly transparent in the visible and near UV, as well as electrically conductive, hence supporting its potential as a substrate for optoelectronic devices operating in the visible/near UV and with vertical current flow. Additionally, investigation into the formation of β-Ga_2O_3 nanocrystals has also been pursued.

A departure from the similarity of gallium oxides with those of aluminum is the stability of the gallium(I) oxide, which is made by high-temperature reactions (e.g. equations 3–5).

$$Ga_2O_3 + 4Ga \xrightarrow{700\,^\circ C} 3Ga_2O \quad (3)$$

$$2Ga + CO_2 \rightleftharpoons Ga_2O + CO \quad (4)$$

$$4Ga + SiO_2 \rightleftharpoons Si/Ga + 2Ga_2O \quad (5)$$

The dark brown, diamagnetic powder is stable in dry air and may be purified by vacuum sublimation at 500 °C, but undergoes surface oxidation at higher temperatures. Above 800 °C it disproportionates according to the reverse of equation (3). The hydrous oxides Ga(O)OH and $Ga(OH)_3$ are similar to their aluminum analogs. Thus gallium hydroxide

is amphoteric, but a much stronger acid than aluminum hydroxide; for $Ga(OH)_3$ the first acid dissociation constant is 1.4×10^{-7}, while for $Al(OH)_3$ the value is 2×10^{-11}.

On heating with other metal oxides, gallium oxide forms gallates $M^{I}GaO_2$, $M^{II}Ga_2O_4$ (spinels), and $M^{III}GaO_3$. The latter include the solid solutions $M^{III}_{2-x}Ga_xO_3$ (M = Al, In). Mixed oxide stoichiometries other than 1:1 (O^{2-}; Ga_2O_3) are quite common. With sodium, there are complex gallates: $NaGaO_2$, Na_3GaO_3, $Na_8Ga_2O_7$, and Na_5GaO_4. The structures of these last two are built up from effectively isolated $[Ga_2O_7]^{8-}$ and $[GaO_4]^{5-}$ units. Some hydrated forms have also been studied, for example, $LiGaO_2 \cdot 6H_2O$, effectively $[Li(OH_2)_4][GaO_2(OH_2)_2]$. The compound $NaGa_{11}O_{16}(OH)_2$ has a complicated structure in which both GaO_4 tetrahedra and GaO_6 octahedra are present. Structures based on GaO_4 tetrahedra prevail among gallates of the divalent metals, for example, $SrGa_2O_4$, $CaGa_2O_4$, $Ca_3Ga_4O_9$, and $Pb_9Ga_8O_{21}$.

4.2.2 *Sulfides and Selenides*

Although not as extensively studied as the group 13–15 compound semiconductors, there has been increasing interest in the heavier gallium chalcogenides because of their possible application as semiconductors,[39] semimetals, photoconductors, and light emitters.[42,43] The gallium sulfides, GaS and Ga_2S_3, are wide band-gap semiconductors (3.05 and 2.85 eV respectively), and are, therefore, considered to hold promise as optoelectronic and photovoltaic materials. Additional work on gallium sulfide has been prompted by its application as passivation layers on GaAs. The chalcogenides of Ga are much more numerous than that of aluminum,[44] and are listed in Table 5.

The hexagonal α- and β-forms of Ga_2S_3 are isostructural with the aluminum analog, having a würtzite structure, while γ-Ga_2S_3 adopts the defect sphalerite structure derived from cubic ZnS (zinc blende). This latter structure is the only type found for Ga_2Se_3 and Ga_2Te_3. It is the isomorphism of γ-Ga_2S_3 with ZnS that is believed to account for the specific enrichment of gallium in sphalerite minerals. All three chalcogenides, Ga_2E_3, are readily prepared from the direct reaction of the elements at high temperature. In addition, Ga_2S_3 can be prepared by the solid-state reaction of $GaCl_3$ and sodium sulfide (equation 6).[45,46] Ga_2S_3 disproportionates at high temperatures to give a nonstoichiometric sulfide, $Ga_4S_{4.8-5.2}$ (equation 7).

$$2GaCl_3 + 3Na_2S \longrightarrow Ga_2S_3 + 6NaCl \quad (6)$$

$$2Ga_2S_3 \rightleftharpoons Ga_4S_5 + \tfrac{1}{2}S_2 \quad (7)$$

Unlike the chalcogenides of aluminum, those of gallium form subvalent compounds (i.e. those in which the metal is formally of an oxidation state less than +3). Of these subchalcogenides, the (formally) divalent compounds are of the most interest. The thermodynamic phase of GaS has a hexagonal layer structure (Figure 12) with Ga-Ga bonds (2.48 Å).[47] Each Ga is coordinated by 3 S and 1 Ga, and the sequence of layers along the z-axis is $\cdots$SGaGaS, SGaGaS$\cdots$. The compound can therefore be considered as an example of Ga^{II}, while the presence of Ga-Ga bonding accounts for the diamagnetism of the compound.

Two other phases of GaS are known. The first is a rhombohedral phase,[48] similar in structure to the hexagonal phase, found as an impurity in Ga_2S_3. The second is a metastable fcc phase prepared by MOCVD from the cubane precursor $[(t\text{-Bu})GaS]_4$.[36] The latter phase does not contain any Ga–Ga interactions and is therefore most probably a mixed valence Ga^{I}/Ga^{III} compound. However, while the electronic structure of the cubic phase is not fully understood, it does have significant applications as a passivation layer on GaAs and other group 13–15 materials. The structures of GaSe and GaTe are similar to the hexagonal phase of the sulfide.

Gallium(I) sulfide cannot be prepared directly from the elements, but is obtained from the thermal decomposition of the higher sulfides. Thus when gallium(II) sulfide is heated at 1100 °C for several hours in a stream of nitrogen, Ga_2S sublimes quantitatively as green hexagonal prisms or yellow–green plates. The compound is in fact a phase of variable composition, $Ga_2S_{0.8-1.1}$, and has a hexagonal lattice similar to that of gallium(II) sulfide (see above). Above

Table 5 Stoichiometries and structures of the crystalline chalcogenides of gallium

Sulfide	Selenide	Telluride
Ga_2S green prisms	Ga_2Se	
GaS hexagonal layered structure, Ga–Ga bonds	GaSe like GaS	GaTe like GaS
GaS cubic (ZnS)		
Ga_4S_5		Ga_3Te_2
α-Ga_2S_3 würtzite (ZnS)		
β-Ga_2S_3 defect würtzite		
γ-Ga_2S_3 defect sphalerite	Ga_2Se_3 defect sphalerite	Ga_2Te_3 defect sphalerite Ga_2Te_5 chains of $GaTe_4$ plus Te atoms

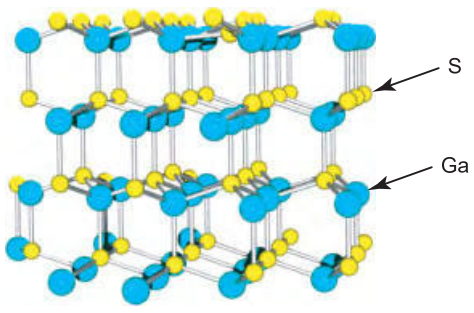

Figure 12 Lattice structure for hexagonal GaS

950 °C, pure Ga_2S decomposes to a liquid mixture of GaS and metallic gallium which becomes homogeneous above 1150 °C (equation 8).

$$Ga_2S(s) \longrightarrow GaS(l) + Ga(l) \rightleftharpoons Ga_2S(g) \qquad (8)$$

Gallium(I) selenide and gallium(I) telluride can be made by melting the elements together in evacuated quartz tubes for prolonged periods; their X-ray powder diffraction patterns have been recorded and indexed.

4.2.3 Chalcogenide Salts

Gallium forms a variety of ternary sulfides and selenides. Common types are $M^{I}GaS_2$, $M^{II}Ga_2S_4$, and $M^{III}GaS_3$; examples of each are $CuGaS_2$, $CdGa_2S_4$, and $LaGaS_3$, respectively. Owing to the unusual electrical properties of these and the corresponding indium compounds, there is an extensive literature concerned with their preparation, physical properties, growth as single crystals, and X-ray studies. Compounds of other stoichiometries occur in mixed sulfide systems involving gallium, for example, $Pb_2Ga_2S_4$ (or $2PbS{\cdot}Ga_2S_3$). All of these compounds have the common structural feature of extended lattices composed of linked GaS_4 tetrahedra, with Ga–S bond distances in the range 2.18–2.36 Å. The tetragallium anion $[Ga_4S_{10}]^{8-}$ has been isolated from the reaction of Ga_2S_3 with aqueous metal sulfides (e.g. equation 9).

$$2Ga_2S_3 + 4K_2S \longrightarrow K_8GaS_{10} \qquad (9)$$

The structure of the hydrated salt, $K_8Ga_4S_{10}{\cdot}14H_2O$, has been determined by X-ray crystallography (Figure 13).[49] The analogous seleno compound has been synthesized, as have the indium species, and all the structures have high thermal and solvolytic stability. Layers of isostructural Ga_4Se_{10} groups, linked through corners, comprise the structure of the ternary selenide $TlGaSe_2$.

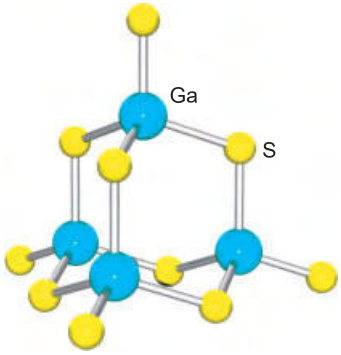

Figure 13 $[Ga_4S_{10}]^{8-}$ anion; Ga–S distances are 2.28 Å (bridging) and 2.25 Å (terminal)

Other gallium–chalcogenide anions are observed in the solid state, that is, discrete $[Ga_6Se_{10}]^{8-}$ anions occur in $Cs_5Ga_3Se_7$, while $Cs_6Ga_2Se_6$, obtained as moisture-sensitive crystals by the reaction of Cs_2Se with Ga_2Se_3, contains the $[Ga_2Se_6]^{6-}$ anion.

5 I-III-VI_2 TERNARY COMPOUNDS

The crystal structure of I-III-VI_2 ternary materials is common to the cubic zinc blende structure of II-VI material's (i.e. ZnS), but differs by group I and III atoms occupying the Zn sites alternatively. Consequently, each group I or III atom has a connectivity of four bonds to the group VI atom, hence each VI atom has two VI-I and two VI-III bonds (Figure 14). Owing to the different bond lengths of I & III with the group VI, atom lattice distortion is evident.

The most prevalent ternary chalcopyrite materials are *p*-type $Cu(In{:}Ga)(S{:}Se)_2$ (CIGS), which crystallize in the tetragonal chalcopyrite structure and are used in the photovoltaic modules. The complexity of the phase diagrams for Cu-III-VI materials results in a large number of intrinsic

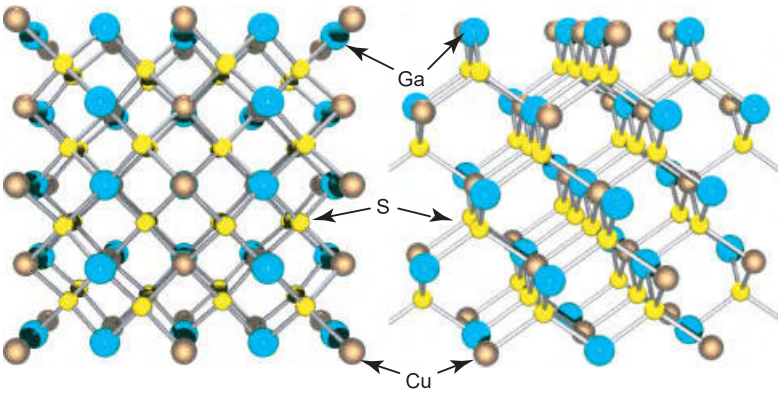

Figure 14 Structural representation of lattice packing for I-III-VI_2 materials

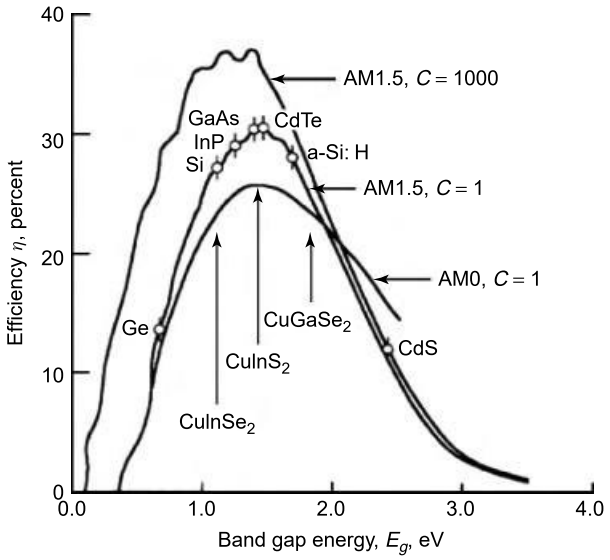

Figure 15 Predicted efficiency versus band gap for thin-film photovoltaic materials for solar spectra in space (AM0) and on the surface of the Earth (AM1.5) at 300 K compared with bandgaps of other PV materials with unconcentrated (C = 1) and high concentration (C = 1000) sunlight

defects in the semiconductor, which can influence the doping of the alloy and has been recently studied by Burgelman and Zhang.[50–53] The conductivity of the *p*-type CIGS is mainly due to copper atoms residing on indium vacant sites, whilst a deficiency in group VI atoms is considered to contribute to *n*-type doping. The use of a chalcopyrite semiconducting material is highly appealing since the band gap correlate well to the maximum photon power density in the solar spectrum for both terrestrial (AM 1.5), and space applications (AM0) (Figure 15), while displaying long-term stability and excellent radiation tolerance.[54] Furthermore, the band gap can be tuned from 1.0 eV to 2.4 eV, by adjusting the percent atomic composition of either Ga for In and S for Se.[55] The schematic of typical CIGS solar cell is shown in Figure 16.

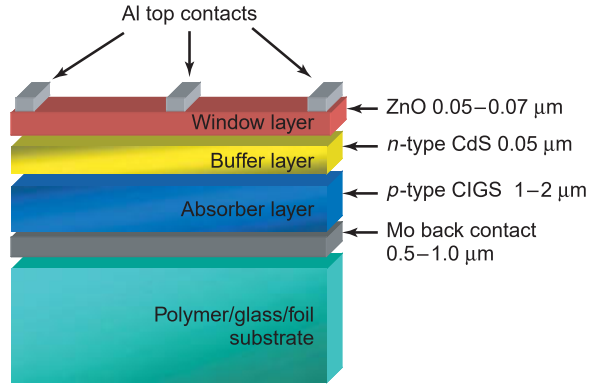

Figure 16 Schematic representation of a typical CIGS solar cell

Current methods for depositing ternary crystallite compounds include coevaporation of elements,[56] or alloys,[57] electrodeposition,[58] reactive-sintering,[59] and flash evaporation,[60] which are often followed by sulphurization/selenization steps, at elevated temperatures. The current world record cell has been reported by NREL with an efficiency of 19.2% based on their patented three-stage process.[55]

A more chemistry-based route to I-III-VI alloys is one that encompasses the design of molecular 'single-source precursors'. Two such routes are those involving the codeposition of two binary single-source precursors, namely, metal dithiocarbamates, and more recently the use of ternary single-source precursors. The first example of a ternary $CuGaS_2$ single-source precursor was recently reported, and although the exact molecular structure of the ternary precursor could not determined, well adhering stoichiometric thin films of $CuGaS_2$ were successfully deposited in an Aerosol Assisted CVD process.[61] Additionally, codeposition of Ga and In ternary single-source precursor to CIGS was also realized. Ternary single-source precursors of the form $[M^{(I)}(ER)_2Ga^{(III)}(ER)_2]$ ($M^{(I)}$ = Cu, Ag), to afford the semiconductor $CuGaS_2$ $AgGaS_2$ have also been designed, and their molecular structure have been elucidated[62] (Figure 17).

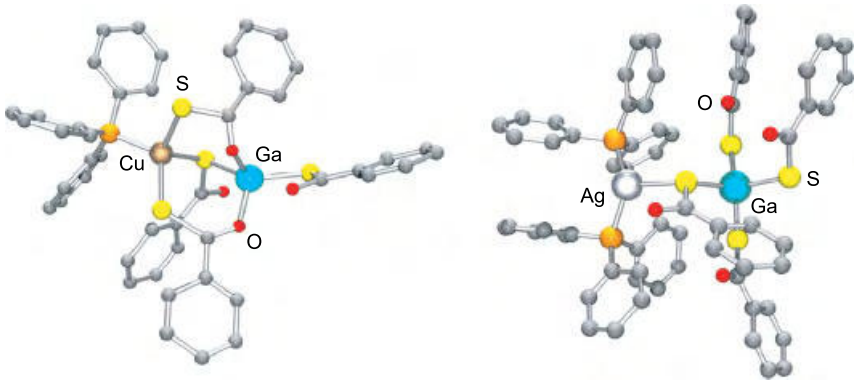

Figure 17 Molecular structure of $[\{PPh_3\}Cu(\mu\text{-}SC\{O\}Ph)_4Ga(SC\{O\}Ph)_2]$, $[\{PPh_3\}_2Ag(\mu\text{-}SC\{O\}Ph)_4Ga(SC\{O\}Ph)_2]$

Thermogravimetry and pyrolysis studies at 300 °C, (0.5 mmHg) for 30 min revealed that these compounds decompose to give the corresponding ternary metal sulfide materials, but thin-film deposition studies for the Ga derivatives are yet to be studied.

A series of trialkylammonium salts of indium and gallium thiocarboxylates, $[Et_3NH][M(SC\{O\}Ph)_4]\cdot H_2O$ (M = In, Ga) were synthesized and characterized for their use as precursors to metal chalcopyrite structures.[63] Thermogravimetric and pyrolysis experiments of these compounds showed the formation of tetragonal β-In_2S_3 and poorly crystalline monoclinic Ga_2S_3, respectively. In similar MOCVD studies, deposition on a nickel substrate gave thin films of cubic γ-Ga_2S_3 and hexagonal $Ni_{0.96}S$. Whereas deposition onto a Cu coated Si substrate afforded thin films of tetragonal $CuInS_2$, the gallium derivative furnished a mixture of tetragonal $Cu_{1.96}S$ and $CuGaS_2$. The composition of the thin films was found to be temperature-dependent during the growth process and the formation of $Cu_{1.96}S$ and $CuGaS_2$ results by the reaction of the group III compounds with the copper substrate to form the metal sulfide thin films.

6 GALLIUM NANOCRYSTALLITES

6.1 Introduction

Over the decade, there has been an immense drive to develop synthetic processes, and characterize binary nanocrystalline semiconducting material. The size dependent luminescence of these materials is a result of quantum confinement within the nanosized particulate resulting in an engineered band gap (eV) through the formation of discreet bonding/antibonding orbitals. As discussed earlier, many of the III-V materials are direct band-gap semiconductors, which have led to their increased use in optoelectronics and telecommunications. Consequently, it is the most frequently studied group of Ga nanocrystallites, but still falls well short of the number of studies for its Indium analogs. A few detailed reviews[9,64,65] and book chapters[66,67] have recently covered this area in depth.

6.2 III-V

Unlike the synthetic procedure established for fabricating II-VI semiconducting nanocrystallites, the use of a similar synthetic procedure cannot be directly translated for the synthesis of gallium pnictogens nanocrystallites, but requires modification. This is attributed to the reactivity of the gallium reagents, the greater covalent bonding nature of III-V material and the higher energetic barriers in the formation of the semiconductor from suitable precursors. The current reported methods that have been used are shown in equations (10–13).

$$GaCl_3 + As(SiMe_3)_3 \longrightarrow GaAs + 3ClSiMe_3 \quad (10)$$

$$Ga(CH_3(CO)CH(CO)CH_3)_3 + As(SiMe_3)_3 \xrightarrow{\text{triglyme}} GaAs \quad (11)$$

$$GaCl_3 + M_3E \xrightarrow[\substack{M=K,\ Na\\ E=P,\ As}]{\text{glymes}} GaE + 3ClSiMe_3 \quad (12)$$

$$2GaCl_3 + 2InCl_3 + P(SiMe_3)_3 \xrightarrow{\text{TOPO}} GaInP_2 + 3ClSiMe_3 \quad (13)$$

GaAs nanocrystals have been prepared by dehalosilyation reaction (equation 10), with the driving force being the high propensity for the formation of the Si–Cl bond.[68–70] In order to limit nucleation and particle growth via Ostwald ripening, coordinating ligands are used, which are commonly referred to a capping or passivating group/ligand. Initial studies using the dehalosilyation route where quinoline was used as both the solvent and capping ligand afforded 3–4 nm sized nanocrystals. However, optical interference from by-products during the synthesis was prevalent. Alternatively, the use of coordinating compounds such $Ga(acac)_3$ (acac = $CH_3(CO)CH(CO)CH_3$) has been studied (equation 11). However, size distribution control of the GaAs nanocrystals was not achievable owing to the large number of nucleation centers formed.[71] In the presence of a trioctylphosphine oxide (TOPO), which serves to passivate dangling surface bonds, nanocrystals of GaP and $GaInP_2$ were realized with good size distribution and optical properties.[64,72] In the continued pursuit of greater size distribution control and crystal quality, a polymeric Ga imide precursor $[Ga(NH_3)_{3/2}]_n$ heated in trioctylamine at 360 °C for one day was investigated.[73] The purified GaN particles, when partially dispersed in a nonpolar solvent, yielded transparent colloidal solution that consisted of individual spherical GaN particles (3 nm). The photoluminescence spectrum at 10 K (excited at 310 nm) showed a band edge emission with several emission peaks at 3.2–3.8 eV, while the photoluminescence excitation spectrum studies showed two excited-state transitions at higher energies.

A thermal reaction preparative route reacting Li_3N and $GaCl_3$ in benzene under pressure was successfully demonstrated to afford GaN 30 nm particles at low temperatures (280 °C) in high bulk yields of approximately 80%. Structural characterization revealed the sample was mainly hexagonal-phase GaN with a small fraction of rocksalt-phase GaN, which has a lattice constant of 4.100 Å. This rocksalt structure has been observed previously only under high pressure (>37 gigapascals).[74]

An interesting variation to this benzene thermal route is the preparation of GaN nanoparticles from the conversion of Ga_2S_3, as shown in equation (14). At 180 °C, a size distribution of 10–15 nm is achieved, whereas at 230 °C, a size distribution of 15–25 is achieved; however, crystal quality is poor at best or amorphous at the lower temperatures.[75]

$$Ga_2S_3 + 2Na_3N \xrightarrow{\text{benzene}} 2GaN + 3Na_2S \quad (14)$$

A novel method receiving great interest is the use of binary III-V single-source precursors, for example, the controlled pyrolysis of the inorganic polymer $[(Cl_3Ga_2P)]_n$ or $[X_2GaP(SiMe_3)_2]_2$ at reduced temperatures and pressures affords GaP nanocrystallites.[65] Additionally, the hydride analog $[H_2GaE(SiMe_3)_2]_2$ (E = As, P) was also successfully decomposed in xylenes (450 °C) to form III-V particles (5 nm).[76] Thermolysis of $M(PBu^t_2)_3$ (M = Ga, In) in hot 4-ethylpyridine afforded InP and GaP nanocrystals.[65] Investigations into the thermal decomposition mechanisms have suggested three major processes, two of which are temperature dependent; reductive elimination and β-hydrogen elimination, and the third a minor pathway involving free-radical formation. Attempts to prepare III-V nanocrystallites from either $Ga(PBu^t_2)_3$ and $In(PBu^t_2)_3$ in TOPO failed to yield the desired product. The fabrication of nanoparticles using this method has been recently been published.[77]

A non-chemical solution route for nanocrystallites formation is via Stranski-Krastinow Epitaxial Growth.[78] The nanocrystallites are formed by epitaxial growth by either MBE or MOCVD. The principle behind the formation of nanocrystallites is the controlled deposition onto a semiconducting substrate with a differing lattice constant, then the III-V material being deposited. When the lattice mismatch is sufficiently high, after the deposition of the first few monolayers, small islands of nanocrystallites are formed. This technique has focused primarily on Ga_xInAs_{1-x} grown on GaAs. A number of reports have focused on the preparation of β-Ga_2O_3 nano derivatives. A patented high-temperature method involves heating (1600 °C), a mixture of boron powder and bulk Ga_2O_3 in a 2:1 ratio in an inert atmosphere to yield Ga_2O_3 nanowires with a diameter of 15–100 nm, coated with 3–5 nm of BN layer.[79] In a similar process, substituting activated carbon for boron affords β-Ga_2O_3 nanowhiskers ($\leq$50-mm length, diameter 10–100 nm).[80]

Nanocrystal shape engineering has been demonstrated via a novel technique for the preparation of α-Ga_2O_3 nanoparticles, nano-hollow-particles, or nanorods and nanotubes via oxidation of nanocrystalline GaP at 400 °C for 30 min in dry O_2.[81] Additionally, a chemical vapor deposition process has been used to fabricate β-Ga_2O_3 from a gallium/gallium oxide mixture and oxygen. The diameter of the single-crystalline monoclinic nanowires were 30–80 nm with an average value of 50 nm. Nanowires grown without catalyst exhibited a significant planar defect, whereas the nanowires grown with nickel catalytic nanoparticles were reported to be almost defect-free.[82]

6.3 III-VI & I-III-VI_2

Binary III-VI alloys crystallize in a variety of forms such as defect wurtzite (Ga_2E_3), layered structures GaE, and a novel cubic form, whereas α, β, and γ – Ga_2S_3 are reported to have a wurtzite, hexagonal, and monoclinic phase respectively.[83] The two predominant binary stoichiometries are AB and A_2B_3, and these are categorized as mentioned earlier as mid to wide band-gap semiconductors. In comparison with II-VI and III-V nanocrystallites, there is a paucity of reports on preparation of III-VI and I-III-VI_2 nano derivatives, and of those they mostly focus on Indium derivatives (*see* ***Indium: Inorganic Chemistry***). The most widely used methods are pyrolysis of single-source precursors such as carbamate coordination compounds, selenolate thiolate complexes, and solvothermal high-temperature procedures of metal salts.

Although there are a limited number of reports for the preparation of InS and InSe nanoparticles via the use of single-source precursors such as $[In(S_2CNEt_2)_3]$ and $[In(Se_2CNEt_2)_3]$ respectively, there are no reported studies for their Gallium counterparts. However, decomposition of $[Bu^tGaSe]_4$ clusters under CVD condition has been shown to afford GaSe pseudo-spherical nanoparticles with a mean diameter of 42 ± 13 nm.[84] In addition, the use of ternary single-source precursors such as $[(PPh_3)_2CuIn(SEt)_4]$ and $[(PPh_3)_2CuIn(SePh)_4]$ have been successfully shown to yield I-III-VI_2 nanoparticles via pyrolysis in dioctyl phthalate at 200–300 °C (forming aggregated cluster with nanoparticles of size from 3 to 30 nm);[85,86] however, similar gallium derivatives remain to be studied for their potential use for the formation of Ga based I-III-IV_2 nanoparticles via this route.

Solvothermal routes have been used to realize the formation of I-III-VI_2 nanoparticles.[87–89] Aqueous and nonaqueous colloids, $CuInS_2$, $CuInSe_2$, $CuGaS_2$, $CuFeS_2$, $AgInS_2$, were prepared by the reaction of the respective metal salts in either water or $CNMe_3$ that has been saturated with H_2E, (E = S, Se) and stabilized with polyvinylalcohol (1%). For the formation of nanoparticle $CuGaS_2$ clusters, these were synthesized exclusively from a CuI solution in acetonitrile (0.01 mol/l and below) and gallium nitrate. Spherical $CuGaS_2$ particles (35-nm diameter) have been synthesized by adapting a low-temperature autoclave method used for preparing III-V nanoparticles. The reaction of CuCl with elemental Ga with excess sulfur at 200 °C for 12 h affords the crude product. Treatment of the precipitate, by washing with dilute acid, distilled water, and absolute ethanol, respectively, and drying under vacuum at 50 °C for 4 h gave the final nanocrystalline semiconductor. The synthesis of a number of analogous Ga-containing clusters has been reported, with the potential to afford ternary semiconducting alloys.[90]

7 HYDRIDES AND HYDRIDE COMPLEXES

The chemistry of the group 13 hydrides originated in 1912 with Alfred Stock's classic investigations into the synthesis and characterization of numerous boron hydrides (boranes) including the parent diborane, B_2H_6 (*see* ***Boron Hydrides***). Unlike boron, aluminum does not form a low-molecular weight hydride analogous to diborane, but a polymeric species $[AlH_3]_x$, in which each aluminum is surrounded octahedrally

by six hydrogens. As early as 1941, the isolation of both $[GaH_3]_x$[91] and Ga_2H_6[92] was claimed, but failure to repeat this work and the anomalously high thermal stability of the compounds caused researchers to question the existence of these compounds. However, a recent series of definitive studies not only showed that gallane does indeed exist in both oligomeric, $[GaH_3]_x$, and dimeric, Ga_2H_6, forms, but also confirms that the previous synthetic claims were incorrect. The low thermal stability ($<-20\,^{\circ}C$) of gallane is consistent, however, with the periodic decrease in the M–H bond strength.

The presence of a stable diborane-like molecule $[H_2Ga(\mu\text{-}H)]_2$ in both solution and the vapor phase suggests that the chemistry of gallane has a marked similarity to that of diborane, that is, (**1**). The analogy between the gallium and boron hydrides is extended by the synthesis and structural characterization of the mixed gallaborane, $GaBH_6$ (**1**).

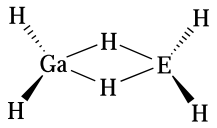

(**1**) E = B, Ga

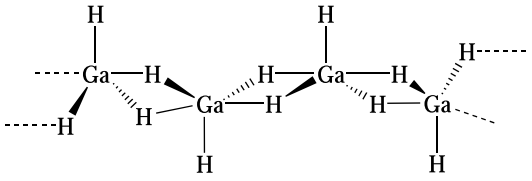

(**2**)

Although no structural details have been reported for the oligomeric form of gallane, $[GaH_3]_x$, IR spectroscopic evidence suggests the retention of terminal Ga–H bonds. This is unlike the all-bridging hydride six-coordinate structure of $[AlH_3]_x$, suggesting the gallium in $[GaH_3]_x$ is perhaps five-coordinate with a single terminal Ga–H bond along with doubly hydride-bridged $Ga(\mu\text{-}H)_2Ga$ units (**2**), similar to that observed in the structure of $HGa(BH_4)_2$.[93]

The adduct $[GaH_3(NMe_3)]$ is a colorless, crystalline compound (mp 70.5 °C), which is formed quantitatively by the reaction of ethereal solutions of $Li[GaH_4]$ and $[NHMe_3]Cl$; like the aluminum analog, it takes up a further mole of ligand to give the trigonal bipyramidal $[GaH_3(NMe_3)_2]$. Numerous complexes with other Lewis base ligands may be prepared from $[GaH_3(NMe_3)]$, and the structures of some of these have been determined by X-ray crystallography, for example, (**3**) and (**4**).[94] The stabilities of the 1:1 adducts have been determined to decrease in the sequences: $NHMe_2 > NMe_3 >$ pyridine $> NEt_3 > NMe_2Ph > NPh_3$; $NMe_3 \sim PMe_3 > PHMe_2$; $PPh_3 > NPh_3 > AsPh_3$; NR_3 or $PR_3 > OR_2$ or SR_2.

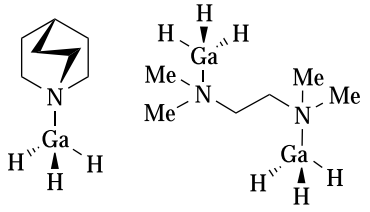

(**3**) (**4**)

Gallane and its Lewis base complexes react readily with protic acids to eliminate hydrogen. Thus complexes of the type $GaH_2X(NMe_3)$ and $GaHX_2(NMe_3)$ (X = Cl, Br) are readily prepared by reaction of HX on the gallane complex at low temperatures. The reactions shown in Scheme 2[94] are examples of an elimination–condensation reaction with a secondary amine and the reduction of an imine; both reaction types have been observed for aluminum hydrides.

Gallium hydride complexes have also been studied for their use in fabricating binary thin films. $[H_3Ga(HNMe_2)]$ has been used in the growth of GaAs and AlGaAs film in low-pressure CVD type processes, which demonstrates reduced carbon contamination in the III-V films.[95] Unfortunately, as like most amine adducts of gallane they are very labile and require storage at low temperatures, therefore these GaAs films grown from $[H_3Ga(HNMe_2)]$ with AsH_3 or H_2AsBu^t have *p*-type behavior.[95]

Dichlorogallane $(HGaCl_2)_2$ was recently readily prepared from $GaCl_3$ and triethylsilane in high yields. Single-crystal X-ray diffraction revealed the Cl-bridged dimers as having C_{2h} symmetry, with the terminal H atoms in trans geometry. In the reaction of dichlorogallane with 2 equivalents of triethylphosphine, mononuclear $[(Et_3P)GaHCl_2]$ is formed.[96]

The reactions of trichlorogermane $HGeCl_3$ and dichlorogallane $HGaCl_2$ with pyridine donors has been recently studied. Pyridine was found to deprotonate $HGeCl_3$ to afford pyridinium trichlorogermanate(II), $PyH^+[GeCl_3]^-$.

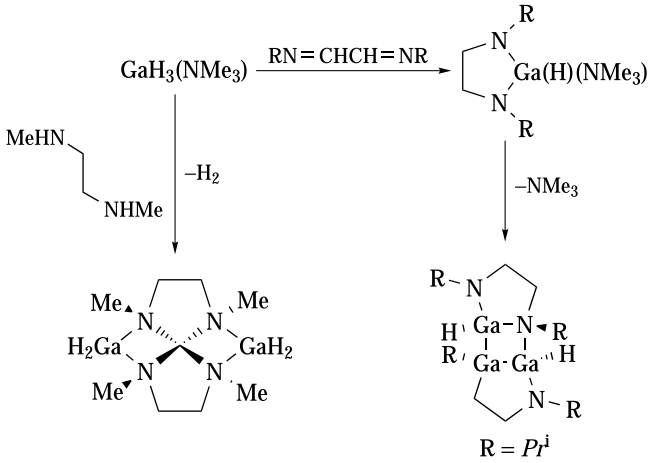

Scheme 2

This course of the reaction was examined and supports the assignment of an inverse polarization (−)Ge-H(+) of the bond in $HGeCl_3$ as compared to the (+)Si-H(−) bond in trichlorosilane $HSiCl_3$, which is known to form a 1:2 adduct with pyridine instead. Dichlorogallane was found to form 1:1 coordination compounds ($HGaCl_2L$), where L = pyridine, 4-dimethylaminopyridine, 4-cyanopyridine, and 3,5-dimethylpyridine.[97]

Dialkylgallium hydrides $[R_2GaH]_n$ (R = Me, Et, $CHMe_2$, CH_2CHMe_2, CH_2CMe_3) have been readily prepared by two different synthetic routes. The methyl and ethyl derivatives were formed by the reaction of LiH with the corresponding dialkylgallium chlorides via lithium dialkyldihydrogallate intermediates; however, they were not isolated in a pure form. In the second route, the trialkylgallium compound was treated with $[H_3Ga(NMe_2Et)]$ to yield the dialkylgallium hydrides by a substituent exchange reaction. The trimeric structure with inner Ga_3H_3-heterocycle was verified for R = $CHMe_2$ by a single-crystal structure determination, whereas for R = CH_2CMe_3, a dimeric structure both in solution and solid state is noted.[98]

The synthesis and structural characterization of a thermally stable group 13 hydride complexes derived from a gallium(I) carbene analog was achieved.[99] The reactivity of $[Ga\{NC(R)C(H)\}_2]^-$ (R = $C_6H_3(Pr^i)_2$) with $[AlH_3(NMe_3)]$ in an ethereal solution yielded $[Ga\{[NC(R)C(H)]_2\}_2][K(DME)_4]$. In addition, the reaction with tertiary amine adducts of GaH_3 and InH_3 in a 2:1 stoichiometry were found to give the respective salt complexes.

The first gallane-coordinated metal complex, $[(OC)5W(\eta^1\text{-}GaH_3{\cdot}quinuclidine)]$, was synthesized by photolysis of a near 1:1 mixture of $W(CO)_6$ and $H_3Ga{\cdot}$(quinuclidine), in toluene and THF.[100] X-ray crystal-structure analysis revealed that product is bound to the W fragment via a W–H–Ga three-center-two-electron bond. Controlled test reactions indicated that the gallane ligand complex is inert toward direct substitution reactions and decomposes without releasing free $H_3Ga{\cdot}$(quinuclidine). The synthesis of Lewis acid/base-stabilized phosphanylgallanes $[(CO)_5WPH_2MH_2(NMe_3)]$ (M = Al, Ga) has been obtained via H_2 elimination reactions between $[(CO)_5WPH_3]$ and H_3MNMe_3. Crystal structures were determined for both complexes and comprehensive density functional theory (DFT) calculations on the aluminum systems were used to verify the high stability of the complexes.[101] In addition, a complete series of intermetallic gallane hydrides has been synthesized and studied with their potential aspect for depositing mixed metal gallium films.[102]

The preparation of $[Bu^t(H)Ga(\mu\text{-}NEt_2)]_2$ was accomplished by the metathesis reaction between Bu^tLi with $[Cl_2Ga(\mu\text{-}NEt_2)]_2$. Evidence suggests that two Bu^t groups are lost as isobutylene and result in Ga–H bond formation. The gallium hydride demonstrates high stability toward ambient air, oxygen, photolysis, and moderate heating; however, in $CHCl_3$ the hydride is replaced by chloride, producing $[Bu^t(Cl)Ga(\mu\text{-}NEt_2)]_2$. $[Bu^t(H)Ga(\mu\text{-}NEt_2)]_2$ was also synthesized by sequential additions of Bu^tLi to $[Cl_2Ga(\mu\text{-}NEt_2)]_2$. A singly substituted *tert*-Bu dimer, $[Bu^t(Cl)Ga(\mu\text{-}NEt_2)_2GaCl_2]$, was also isolated, and interconversions between three gallium hydrides were reported as was its utility in fabricating GaN. However, it was found to yield nitrogen deficient films as a consequence of facile Et_2NH elimination.[103]

8 GROUP 14, 15, AND 16 DONOR LIGANDS

8.1 Introduction

The majority of compounds reported in the literature containing ligands with either a group 15 or 16 donor atom are derived from a gallium alkyl, and as such they are covered in (*see* ***Gallium: Organometallic Chemistry***). However, a number of purely inorganic compounds and complexes are relevant to the present discussion. Where compounds contain both a group 15 or 16 donor ligand and either a hydride or halide ligand, they (and any relevant references) are included in the appropriate section depending on the ligand type of primary importance.

8.2 Silyl Gallium Compounds

Clearly, alkyl (and aryl) groups make up the largest contingent of group 14 ligands; however, surprisingly little work has been reported on compounds of gallium with silicon containing ligands, and no nonalkyl-based compounds with germanium or tin ligands are known. Tris(trimethylsilyl)gallium is produced by treating $GaCl_3$ and three equivalents of Me_3SiCl in the presence of lithium metal in THF. The initial solvated adduct, $Ga(SiMe_3)_3{\cdot}THF$, is converted to $Ga(SiMe_3)_3$ by vacuum sublimation. $Ga(SiMe_3)_3$ is monomeric, with a planar $GaSi_3$ framework, characterized by vibrational bands $\nu(Ga\text{–}Si)_{sym} = 312\,cm^{-1}$ (Raman) and $\nu(Ga\text{–}Si)_{deg} = 349\,cm^{-1}$. The area of Si gallium chemistry that has been explored thoroughly is the use of bulky silane groups to encourage cluster formation, and as such is reported in detail in ***Electronic Structure of Clusters***; ***Silicon: Inorganic Chemistry***; ***Silicon: Organosilicon Chemistry***.

Recently the first compounds containing Si=Ga or Si=In double bonds, 1,3-disila-2-gallata- and -indataallenic anions respectively, were obtained in the form of lithium salts as dark red crystals by the reaction of *bis*(di-*tert*-butylmethylsilyl)dilithiosilane, with the respective M(III) halide (Figure 18).[104] X-ray crystallographic analysis of gallium and indium salt derivatives showed that the >SiMSi< frameworks (M = Ga, In) are not linear and the two Si=M

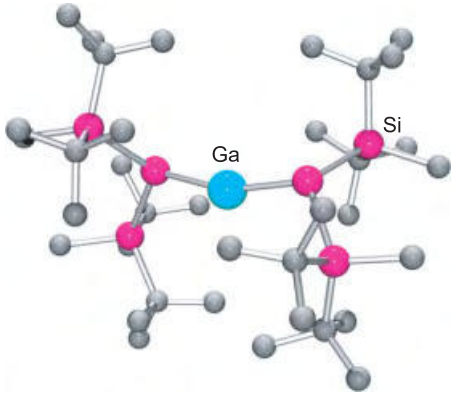

Figure 18 Li[(Bu^t_2MeSi)$_2$SiGaSi(Bu^t_2MeSi)$_2$]: hydrogen atoms and the cationic fragment $[Li(thf)_4]^+$ are omitted for clarity: Si-Ga-Si = 161.61(3) deg

bond lengths are about 9% shorter than typical Si–M single bonds (Figure 18). The ^{29}Si NMR spectra show the signals of the terminal Si atoms in both compounds are greatly shifted upfield (Ga: −79.9; In: −77.6 ppm). In addition, the gallium salt was found to react with MeI to give the corresponding iodogallane in nearly quantitative yield, thus confirming that the allenic $[>SiMSi<]^-$ fragments are highly polarized.

8.3 Nitrogen Derivatives

8.3.1 Amine and Amido Ligands

As discussed earlier, gallane and the trihalides all form Lewis acid–base complexes with amines and N-heterocyclic ligands. While the majority of these compounds are neutral and have a general formula of $GaX_3(L)_n$ ($n = 1, 2$), complexes formed with bidentate ligands such as 1,10-phenanthroline and 2,2′-bipyridyl are typically ionic. A common feature of these complexes is the presence of a gallium cation, for example, $[Ga(bipy)_3]^{3+}$ or $[GaCl_2(bipy)_2]^+$. Thus the crystal structure of '$GaCl_3$(bipy)' shows it to be *cis*-$[GaCl_2(bipy)_2]^+[GaCl_4]^-$.[4]

Potassium amidogallate, $K[Ga(NH_2)_4]$, is prepared by dissolving gallium in a solution of KOH in liquid ammonia. Heating this compound to 300 °C under vacuum removes two moles of ammonia, forming the imido complex $K[Ga(NH)_2]$, while partial neutralization of the ammonia solution of $K[Ga(NH_2)_4]$ with NH_4Cl yields $Ga(NH_2)_3$. The anion $[Ga(NH_2)_4]^-$ has tetrahedral symmetry, according to the single-crystal Raman spectrum in which ν(Ga–N) appears near 550 cm^{-1}. $NaGa(NH_2)_4$ crystallizes isotypic in space group P21/c was obtained by the reaction of the metals with NH_3 in autoclaves at 100 °C and P(NH_3) = 60 bar within 7 days.[105] A more highly coordinated complex, $Na_2[Ga(NH_2)_5]$, has also been prepared. From evidence of IR spectra, this contains six-coordinate gallium, with a structure based on linked $Ga(NH_2)_6$ octahedra with both bridging and nonbridging NH_2 groups.[4]

Dialkylamido compounds, $GaX_2(NR_2)$, $GaX(NR_2)_2$ (X = halide), and $Ga(NR_2)_3$, are obtained from the reaction of GaX_3 with the appropriate equivalents of $LiNR_2$; unless precluded owing to steric hindrance, an excess yields $Li[Ga(NR_2)_4]$. Hydrido-substituted amido compounds, $[H_2Ga(NXR)]_n$ (X = H or R, $n = 2$ or 3), may be prepared from the reaction of primary or secondary amines with $GaH_3(NMe_3)$. In the absence of steric hindrance, gallium amido compounds oligomerize as a result of the amido ligands bridging ability.[4] Thus for $Ga(NR_2)_3$ when R = Me, a dimerization through bridging dimethylamido ligands occurs, while in the case of R = $SiMe_3$ a monomeric structure is observed.

Gallane complexes with amido-amine ligands $-N(R)CH_2CMe_2CH_2NMe_2$ [R = H or $SiMe_3$ (TMS)], (**5**) $\{H_2Ga[N(H)CH_2CMe_2CH_2NMe_2]\}_2$, (**6**) $H_2Ga[N(TMS)CH_2CMe_2CH_2NMe_2]$, (**7**) $\{H(Cl)Ga[N(H)CH_2CMe_2CH_2NMe_2]\}_2$, (**8**) $\{[(TMS)_2N](H)Ga[N(H)CH_2CMe_2CH_2NMe_2]\}_2$, (**9**) and $HGa[N(TMS)CH_2CMe_2CH_2NMe_2]_2$, (**10**) were synthesized from the reactions of the quinuclidine adducts of mono- and dichlorogallane with the corresponding lithium amides. Structural determinations of compounds (**5**), (**7**), (**8**) showed they were dimeric with bridging amido groups. The tertiary amine groups in (**5**) and (**8**) were hydrogen-bonded to the amido N–H rather than being bonded directly to gallium center. In the structure of compound (**7**), the amine group was found to occupy an axial position in the trigonal bipyramidal geometry of the five-coordinate gallium. These results were rationalized in terms of the steric and electronic properties of respective gallium ligands.[106]

Base-free tris(primary amido) compounds of the type $M[N(H)Mes^*]_3$ (M = Al, Ga, In; Mes^* = 2,4,6-tri-*tert*-butylphenyl) have been synthesized via the salt elimination reaction of $Mes^*N(H)Li$ with the respective MCl_3. Whereas the singly base-stabilized *tris*(primary amido) derivatives, $[M\{N(H)Dipp\}_3(py)]$ (Dipp = 2,6-diisopropylphenyl), have been prepared via an amine elimination reaction of H_2NDipp with $[E(NMe_2)_3]_2$. These derivatives were also to be examined for their potential as III-V precursors.[107]

In compounds where oligomerization occurs, the formation of dimeric versus trimeric species, as well as *cis* (**11**) and *trans* (**12**) isomers for compounds derived from primary (or asymmetric secondary) amines, is governed by the steric hindrance at both nitrogen and gallium.

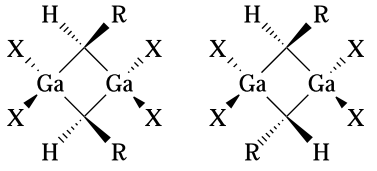

For example, an equilibrium mixture of the *trans* trimer, and the *cis* and *trans* dimers of $GaCl_2[NH(SiMe_3)]$, has been observed in toluene solution. When a methyl group is

substituted for the hydrogen atom on the nitrogen, only the *cis* and *trans* dimers of $GaCl_2[NMe(SiMe_3)]$ were found in solution.[108] Substituted aminogallanes exhibit a similar trend. $GaH_2(NHMe)$ is trimeric in solution while $GaH_2(NMe_2)$ exists as a dimer. Apparently the introduction of a second substituent on the nitrogen atom creates sufficient steric strain to prohibit the formation of the trimer. The effect of the substituents bonded to the nitrogen on the degree of association and the conformational properties of aminogallanes has been examined extensively; however, the manner in which the substituents on the gallium atom influence the trimer–dimer equilibrium and the isomerization of the dimer has only been recently explored. One such study showed that the trimer–dimer equilibrium present for $GaCl_2[NH(SiMe_3)]$ is absent for $GaBr_2[NH(SiMe_3)]$, *cis* and *trans* isomers of the dimer being the only species observed.[109] Although the van der Waals radii of the chlorine and bromine atoms (1.70–1.90 and 1.80–2.00 Å) differ only slightly, the increase in the steric requirements of the bromide atoms compared with the chloride atoms is clearly sufficient to prohibit the formation of the trimer, leading to the exclusive formation of $[Br_3Ga(NHSiMe_3)]_2$.

8.3.2 *Miscellaneous*

While the transition metal chemistry of the pyrazolylborate ligands, $[H_xB(pz)_{4-x}]^-$ ($x = 0 - 2$, pz = pyrazolyl) has been extensively studied, it is only recently that the first gallium compounds have been reported. Reaction of $GaCl_3$ with the bis(pyrazolyl)borato ligands (equation 15) yields a five-coordinate complex (Figure 19).[110]

$$2K[H_2B(pz)_2] + GaCl_3 \longrightarrow [H_2B(pz)_2]_2GaCl + 2KCl \qquad (15)$$

In contrast, the substituted tris(pyrazolyl)borate ligand allows for the formation of the six-coordinate complex cation (**13**) (equation 16).[111] The 3,5-dimethylpyrazolate analog has also been reported.

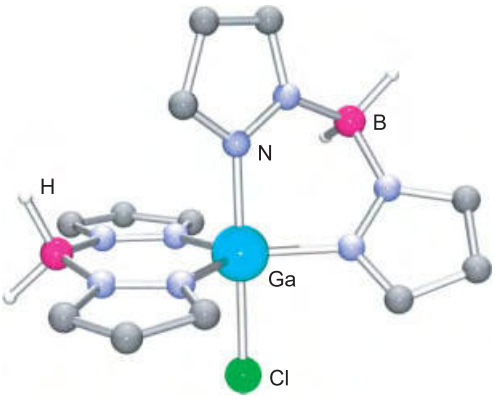

Figure 19 Molecular structure of $[H_2B(pz)_2]_2GaCl$

$$2K[HB(pz)_3] + 2GaCl_3 \longrightarrow [GaH\{(pz)_3BH\}_2]^+ + [GaCl_4]^- + 2KCl \qquad (16)$$

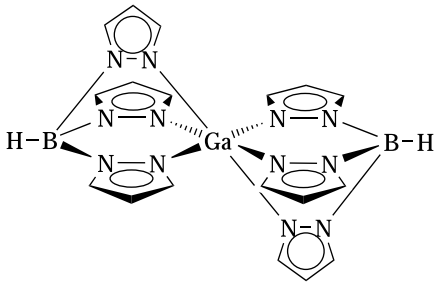

(**13**)

$[GaCl_2(pyrazole)_4]Cl$ and $[GaCl_2(pyrazole)_4]GaCl_4$ are formed in the reaction of pyrazole and anhydrous $GaCl_3$ in toluene/Et_2O solution. The crystal structure of the chloride salt shows the cations in a trans-configuration which are associated with the chloride counterions through N-H–Cl H bonds.

The triazenide anion, $RN{=}N{-}NR^-$, is formally isolobal with the carboxylate anion. However, while there are no well-characterized examples of gallium tris-carboxylates (see Section 8.7), the *tris*(1,3-diphenyltriazenide) complex $Ga(dpt)_3$ (**14**) has been isolated and fully characterized.[112]

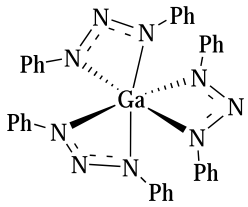

(**14**)

A number of simple N-donor ligand complexes are known; for example, azide, $[Ga(N_3)]$, thiocyanate, $[Ga(NCS)_4]^-$, and selenocyanate, $[Ga(NCSe)_4]^-$. However, spectroscopic evidence suggests that the cyanate anions coordinate via the oxygen.[5] The gallium secondary amines adducts $TMPH{\cdot}GaCl_3$ and $Pr^i_2NH{\cdot}GaCl_3$ (TMPH = tetramethylpiperidine) were achieved through synthesis from the respective reagents in toluene at −78 °C in very high yields of 80%. Characterization via single-crystal determinations revealed $TMPH{\cdot}GaCl_3$ having short Ga···H–N distances (2.28(9) Å).[113]

A series of group 13 metal complexes featuring the β-diketiminate ligand $[\{(C_6H_3\text{-}2,6\text{-}Pr^i_2)NC(Me)\}_2CH]^-$ (i.e. $[Dipp_2nacnac]^-$, Dipp = C_6H_3-2,6-i-Pr^i_2) have been prepared and fully characterized. The chloride derivative $Dipp_2nacnacGaCl_2$ was isolated by the reaction of 1 equivalent of $Dipp_2nacnacLi{\cdot}Et_2O$ and the respective metal halides. The iodide derivatives $Dipp_2nacnacGaI_2$, which are useful for

reduction to afford M(I) species, were made by a variety of routes. Their X-ray crystal structures feature nearly planar C_3N_2 arrays in the Dipp$_2$nacnac ligand backbone with short C–C and C–N distances that are consistent with a delocalized structure. However, there are large dihedral angles between the C_3N_2 plane and the N_2Ga metal coordination plane, which have been attributed mainly to steric effects. The relatively short Ga–N distances are consistent with the coordination numbers of the metals and the normal/dative character of the nitrogen ligands.[114]

8.4 Phosphines and Arsines

While there are a large number of phosphines and arsine adducts of GaX_3, the number of nonorganometallic phosphide and arsenide compounds are few, and of those the steric bulk of the group 15 substitutes is of critical importance in controlling their isolation. Reaction of $GaCl_3$ with three equivalents of lithium dimesitylarsenide yields the monomeric triarsenide compound Ga[As(Mes$_2$)]$_3$,[115] whose structure has been shown by X-ray crystallography (Figure 20) to consist of a gallium atom bonded to three arsenic atoms in a trigonal-planar configuration. The Ga–As distances [2.470(1) – 2.508(1) Å] are significantly shorter than those observed for four-coordinate gallium (below). A monomeric gallium phosphide, Ga[P(t-Bu)$_2$]$_3$, has also been reported but no structural elucidation presented.

Reaction of four equivalents of $LiEPh_2$ (E = P, As) with $GaCl_3$ in THF yields the anionic perphosphido and perarsenido complexes $[Li(THF)_4][Ga(EPPh_2)_4]$. While the gallium atoms are in a tetrahedral GaE_4 coordination environment, analogous to those in the binary compounds GaP and GaAs, the bond lengths are slightly longer in the anions than the binary compounds (e.g. Ga–As, 2.497(4) vs. 2.448 Å). However, these small differences are presumably due to the steric repulsion between the phenyl rings in the anions as opposed to any significant electronic interactions.

The coordination of pnictogen ligands to gallium alkyl compounds has also been used in purification techniques similar to those implemented for its indium analogs (*see* ***Indium: Organometallic Chemistry***). For example, $[R_yGa_xL]$ where L = PPh_3, dppe, triphos ($Ph_2P(CH_2)_2P(Ph)(CH_2)_2PPh_2$), tetraphos ($Ph_2P(CH_2)_2P(Ph)(CH_2)_2P(Ph)(CH_2)_2PPh_2$), and MBDA 4,4′-methylene-bis(*N*,*N*′-dimethylaniline).[9] Subsequent controlled heating liberates the highly pure metal derivative, which is used for fabricating high quality Ga alloy thin films. It is commonplace to also use gallium pnictogen coordination complexes for III-V film growth. The adduct $[ClEt_2Ga(AsEt_3)]$ has been used in conjunction with $HPEt_2$, for epitaxial growth of $GaAs_{1-x}P_x$ at 500 – 650 °C, whereas GaAs thin films have been grown from the halide derivatives, $[(C_6F_5)Me_2Ga(AsEt_3)]$ and $[\{ClEt_2Ga(AsEt_2)\}_2CH_2]$ at 600 – 700 °C and 500 – 625 °C, respectively.[9]

The metathesis reaction of potassium (tris(*tert*-butyl)silyl) phosphanide with $GaCl_3$ in a 1:1 affords $[Cl_2GaP(H)SiBu^t_3]_2$ as a mixture of *cis* and *trans*. The molecular structure reveals a Ga_2P_2 moiety cycle with nearly planar coordinated phosphorus atoms neglecting hydrogen atoms and Ga–P distances of 2.39 Å. The reaction of $GaCl_3$ with 3 equivilents of potassium (tris(*tert*-butyl)silyl)phosphanide as well as the reaction of 1 with 2 equiv of $KP(H)SiBu^t_3$ yields $[Bu^t_3SiP(H)Ga(\text{-}PSiBu^t_3)]_2$. The central moiety comprises a four-membered Ga_2P_2 cycle with one planar P atom and extremely short Ga–P bonds of approximately 2.26 Å. The structure of $[Bu^t_3SiP(H)Ga(\text{-}PSiBu^t_3)]_2$ is described as a GaPGa heteroallyl system which is bonded to a phosphanidyl substituent.[116]

The gallium chloro complex $[GaCl\{Fe(CO)_2Cp\}_2]$ (Cp = η^5-C_5H_5) was reacted with $MP(SiMe_3)_2$, (M = K, Li) under special conditions to yield the complexes $[\{CpFe(CO)\}_2\{\text{-}(CO)\}[\text{-}Ga\{CpFe(CO)_2\}]]$ and $[\{CpFe(CO)_2\}GaP(SiMe_3)]_4$, whereas $[[\{CpFe(CO)_2\}ClGa](\text{-}PPh_2)_2FeCpCO]$ was obtained by the reaction of $[GaCl\{Fe(CO)_2Cp\}_2]$ with $LiPPh_2$. Complex $[\{CpFe(CO)_2\}GaP(SiMe_3)]_4$ represents an ideal Ga_4P_4-heterocubane, the first Ga-containing example of this structural type with organometallic substituted group 13 elements. In addition, in the solid state, $[[\{CpFe(CO)_2\}ClGa](\text{-}PPh_2)_2FeCpCO]$ possesses a near planar GaPFeP four-membered ring, which is a novel structural motif in mixed group 13/15 chemistry (Scheme 3).[117]

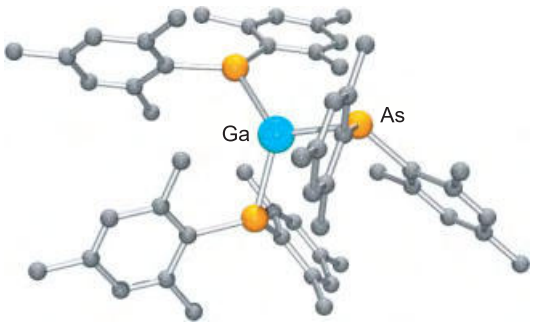

Figure 20 Molecular structure of Ga[As(Mes$_2$)]$_3$

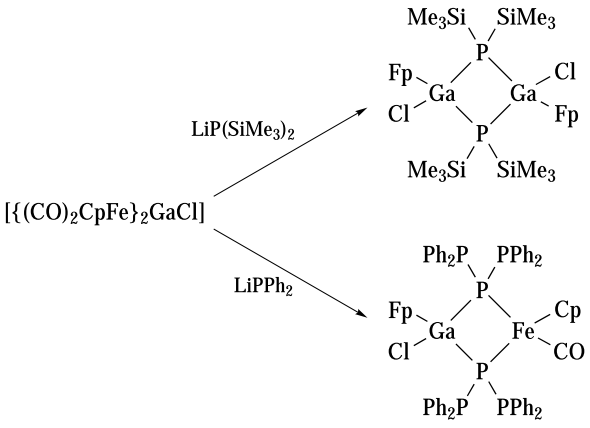

Scheme 3 Formation of mixed group 13/15 Fe derivatives

Examples of Ga derivatives with double bond character to group 15 centers have attracted much attention and review.[118–124] Power and coworkers recently published compounds with gallium–nitrogen multiple bonds,[125] and the first example of a Ga=As derivative, $[\{Li(THF)_3\}_2Ga_2\{As(SiPr^i_3)\}_4]$, has recently been synthesized and contains two As=Ga double bonds from the reaction of $GaCl_3$ with $Li_2AsSiPr^i_3$.[126]

8.5 Aqua ions and related

In acidic solutions, gallium exists as the hexaaqua cation $[Ga(H_2O)_6]^{3+}$ which, based on ^{17}O NMR studies, occurs in the hydrated crystals of oxyanion salts, for example, $Ga(X)_3{\cdot}xH_2O$ ($X = NO_3$, $x = 9$; $X = SO_4$, $x = 18$; $X = ClO_4$; $x = 6$).[5] Ligand exchange at 25 °C ($k_1 = 0.17\,s^{-1}$) is much faster in $[Ga(H_2O)_6]^{3+}$ than the associated exchange in $[Al(H_2O)_6]^{3+}$ ($k_1 = 1.8 \times 10^3\,s^{-1}$), thus reflecting the lesser affinity for oxygen donor ligands of Ga^{3+} versus Al^{3+}. A S_N2 type of mechanism, involving $[Ga(H_2O)_n]^{3+}$, has been suggested for ligand exchange. The gallium cation $[Ga(H_2O)_6]^{3+}$, with K_a of 2.5×10^{-3}, is a stronger acid than $[Al(H_2O)_6]^{3+}$ ($K_a = 1.1 \times 10^{-5}$).[5]

8.6 Alkoxides

Gallium alkoxides can be prepared by the methods employed for aluminum (*see* ***Aluminum: Inorganic Chemistry***). $Ga(OMe)_3$, a polymeric material, decomposes without melting but can be sublimed under vacuum. $Ga(OEt)_3$, $Ga(O\text{-}n\text{-}Pr)_3$, and $Ga(O\text{-}n\text{-}Bu)_3$ are more volatile than $Ga(OMe)_3$ and are tetrameric in solution. According to NMR studies, $Ga(O\text{-}i\text{-}Pr)_3$ and $Ga(O\text{-}t\text{-}Bu)_3$ have dimeric structures bridged by alkoxide ligands. The bulky trimethylsilyl ligand results in $Ga(OSiMe_3)_3$ being monomeric, but does not prevent the formation of a complex anion, $[Ga(OSiMe_3)_4]^-$. Aryloxides, for example, $Ga(OPh)_3$, are obtained by prolonged heating of Ga metal with the phenol at 180–220 °C. Like group 13 alkoxides generally, these compounds are Lewis acids and form 1:1 adducts with ammonia, pyridine, and other bases.

$$Ga_2X_4 + 3EtOH \xrightarrow{0\,^\circ C} [GaX(OEt)_2] + [GaX_3(HOEt)] + H_2 \quad (17)$$

Reaction of gallium trihalides, GaX_3 (X = Cl or Br), with less than three moles of alcohol initially gives the Lewis acid–base adducts $GaX_3(HOR)$. However, these are readily converted into oligomeric halide–alkoxide compounds, $GaX_n(OR)_{3-n}$ ($n = 1$ or 2), in which the alkoxide ligands are bridging. Alcoholysis of the mixed valent dihalides, Ga_2X_4, involves oxidation of the Ga^+ by the alcohol (equations 17 and 18).

$$Ga_2X_4 + 2EtOH \xrightarrow{25\,^\circ C} 2[GaX_2(OEt)] + H_2 \quad (18)$$

Like their aluminum counterparts, gallium alkoxides are susceptible to hydrolysis, giving ill-defined products. Methanolysis of hydrated Ga^{3+} ions produces $Ga(OMe)^{2+}$ and $Ga(OMe)_2{}^+$ in solvated forms, as well as polymeric complexes. $Ga(OPh)_3$ reacts with boiling MeOH or EtOH to form the corresponding alkoxide. Reaction of the trialkoxide compounds with other metal alkoxides, for example, LiOR, results in the formation of four-coordinate complex anions of the type $[Ga(OR)_4]^-$.[5] A recent review of sesquihalides/oxides of group 13 derivatives has been published. The review covers the major synthetic routes and the structures of the corresponding products, and also reactions with compounds having sesquialkoxides as educts.[127]

Owing to the importance of Ga_2O_3 thin films, Ga alkoxides have also been examined as viable compounds to Ga_2O_3 materials. A general synthetic route to Ga alkoxide complexes involving reactions between Ga *tris*(dimethylamide) with alcohols has been developed. Their utility in a CVD process to deposit Ga oxide films was demonstrated.[128] $[Ga(NMe_2)_3]_2$ reacted with *i*-BuOH and *i*-PrOH to yield the tetramers $Ga[(\mu\text{-}OR)_2Ga(OR)_2]_3$ (R = *i*-Bu, *i*-Pr). In contrast to the results obtained using *i*-BuOH and *i*-PrOH, the bulkier alcohols *t*-BuOH and $EtMe_2COH$ reacted with $[Ga(NMe_2)_3]_2$ at room temperature to yield mixtures of the dimer $[Ga(\mu\text{-}OR)(OR)_2]_2$ and the amine adduct $[Ga(OR)_3(HNMe_2)]$, while *i*-$PrMe_2COH$ and Et_2MeCOH gave $[Ga(OR)_3(HNMe_2)]$ derivatives exclusively. The amine could be removed from the $[Ga(OR)_3(HNMe_2)]$ compound to yield the corresponding homoleptic alkoxide dimers. Low-pressure CVD using $[Ga(OBu^t)(OBu^t)]$ and O precursors gave GaO films at substrate temperature between 300–700 °C, which were carbon-free, amorphous, and highly transparent in the 350–800-nm region.[129,130]

8.7 Carboxylates

A number of patents and publications have addressed the synthesis, properties, and application of gallium carboxylates.[10,131,132] Gallium carboxylates, $Ga(O_2CR)_3$, may be prepared by a variety of synthetic methods, including the reaction of the carboxylic acid with Ga_2O_3 (equation 19), $GaCl_3$ (equation 20), or directly with the metal (equation 21).[5] Basic carboxylates result if aqueous acids are employed (see below).

$$Ga_2O_3 + 3HO_2CR \longrightarrow [Ga(O_2CR)_3] + 3H_2O \quad (19)$$

$$GaCl_3 + 3HO_2CR \longrightarrow [Ga(O_2CR)_3] + 3HCl \quad (20)$$

$$Ga + 3HO_2CR \longrightarrow [Ga(O_2CR)_3] + 1.5H_2 \quad (21)$$

However, the gallium oxalate system has also been examined. $Ga(C_2O_4)_3{\cdot}4H_2O$ crystallizes from hot aqueous $Ga(NO_3)_3$ solution containing oxalic acid. On heating (>140 °C), a dihydrate and then anhydrous $Ga_2(C_2O_4)_3$

are produced. The latter decomposes to Ga_2O_3 at 200 °C. Complex salts containing $[Ga(C_2O_4)_2]^-$ and $[Ga(C_2O_4)_3]^{3-}$ anions have been prepared and the formation of these and the cation $[Ga(C_2O_4)]^+$, presumably hydrated, have been studied to obtain stability constants. It is thought that basic complexes are probably present in these aqueous solutions (see below). Raman spectra of gallium oxalate solutions confirm the presence of $[Ga(C_2O_4)_3]^{3-}$: $\nu(M\text{–}O)_{sym} = 573\ cm^{-1}$ compared to 585 cm^{-1} in $[Al(C_2O_4)_3]^{3-}$.[5]

While no crystallographic data have been obtained for a gallium tricarboxylate, Hepp, Duraj and co-workers have reported the synthesis and structural characterization of an oxo-centered trinuclear carboxylate, of the well-established class of complexes commonly referred to as 'basic carboxylates', $[M_3(O)(O_2CR)_6(L)_3]^+$.[133] The reaction of Ga_2Cl_4 with sodium benzoate in the presence of 4-methylpyridine (4-Mepy) allows the isolation of $[Ga_3(O)(O_2CPh)_6(4\text{-}Mepy)_3][GaCl_4]$ in high yield. The solid-state structure of the cation, $[Ga_3(O)(O_2CPh)_6(4\text{-}Mepy)_3]$ consists of a planar oxo-centered Ga_3O core; each edge is bridged by two benzoate ligands, and the sixth coordination site of each gallium is occupied by a terminal pyridine ligand.

There are many reports of complexes between gallium and hydroxy acids (including those derived from carboxylic acids) and other related organic chelating agents. The lactate, tartrate, and citrate have all been used in physiological studies involving gallium radioisotopes. According to NMR studies (^1H, ^{13}C, and ^{71}Ga), the 1:1 Ga/citrate complex predominates at low pH (<2), while oligomeric species exist in the range pH 2–6, unlike the aluminum citrate system.[134] The structural characterization for the gallium citrate complex has recently been realized; the gallium citrate complex $(NH_4)_3[Ga(C_6H_5O_7)_2]\cdot 4H_2O$ hydrate has been prepared from the reaction of gallium nitrate with citric acid. The X-ray crystal structure of the complex revealed it to exist as discrete ions, with the 6-coordinate gallium center bonded to two deprotonated carboxylate groups and one alcoholate group from each citrate ligand leaving one protonated pendent carboxy group.[135]

A range of other systems of Ga^{3+} with chelating organic acids has been studied and solution equilibria data have been obtained.[5] Based on these investigations it is clear that in all cases basic complexes (i.e. those containing oxo or hydroxo ligands) are involved, and the hydrated hydroxide cation $[Ga(OH)]^{2+}$ shows greater reactivity compared with the hydrated ion of Ga^{3+}.

8.8 β-Diketonates

Gallium tris-β-diketonate complexes are formed by the addition of acetylacetonate ions to aqueous solutions of Ga^{3+} (e.g. equation 22). However, at β-diketonate to gallium ratios less than three, basic hydroxo complexes are also formed.

$$Ga_2(SO_4)_3 + 3Hacac \xrightarrow{[NH_4][OH]aq.} [Ga(acac)_3] + 3[NH_4]_2[SO_4] \quad (22)$$

Rates of ligand exchange have been measured for some β-diketonate complexes.[136] Exchange between $Ga(acac)_3$ and ^{14}C-labeled Hacac in THF solution is much faster than in the case of $Al(acac)_3$. A dissociative mechanism proceeds via a five-coordinate transition state in which one ligand is unidentate (Scheme 4). In addition, activation energies for cis–trans ligand rearrangements have been determined from NMR measurements. As expected, these studies place gallium between aluminum and indium in the order of decreasing bond strength, that is, Al–O > Ga–O > In–O. This result is consistent with Raman studies of $M(acac)_3$.[5] When $Ga(acac)_3$ is added to a solution of $Ga(ClO_4)_3$ in DMF, the NMR spectrum shows new signals attributable to $[Ga(acac)(DMF)_4]^{2+}$ and $[Ga(acac)_2(DMF)_2]^+$.

Tris(acetylacetonato)gallium(III) exists in two crystallographic modifications, differing slightly in density. The X-ray crystal-structure determination shows the central GaO_6 core to be close to octahedral, with an average Ga–O distance of 1.95 Å.

The dichlorogallium(III) β-diketonato derivatives of the type $GaCl_2L$ [L = acac (2,4-pentanedionato) and tmhd

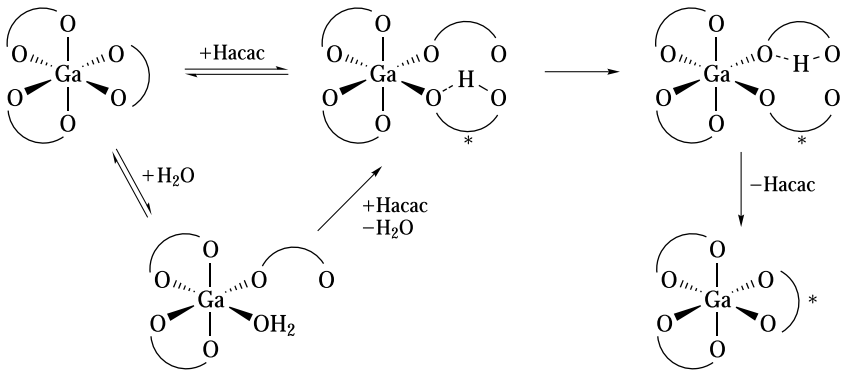

Scheme 4 Proposed mechanism for the ligand exchange of [Ga{acac}3] with excess acac ligand, in THF solution, (*14-C labeled)

(2,2,6,6-tetramethylheptanedionato)] were prepared and characterized by a variety of spectroscopic techniques. The four-coordinate Ga compounds were found to react with THF to form $GaCl_2L{\cdot}THF$ derivatives. Single-crystal X-ray diffraction study identified $[GaCl_2(acac){\cdot}THF]$ to be the ion-pair [*trans*-$Ga(acac)_2(THF)_2]^+$ $[GaCl_4]^-$. The Ga atom in the cation is six-coordinate, whereas in the anion it is four-coordinate. Variable-temperature ^1H NMR spectral studies suggest that multiple processes including (i) a stereochemical rearrangement, (ii) THF exchange, and (iii) equilibria between $[GaL_2(THF)_2]^+[GaCl_4]^-$, $[GaCl_2L]$, and other species such as $[GaL_2(THF)]^+[GaCl_4]^-$ occur in solution. In contrast, the fluorinated derivatives $GaX_2(hfac)$ (X = Cl, Br; hfac = 1,1,1,5,5,5-hexafluoro-2,4-pentanedionato) cannot be isolated since they undergo ligand redistribution reactions to form $[Ga(hfac)_3]$.[137]

The gallium(II) derivatives $[GaCl(acac)]_2$, and $[GaCl(tmhd)]_2$ were prepared and characterized by X-ray structural studies.[138] Both compounds have direct gallium–gallium bonds between two tetracoordinated gallium atoms with each in the +2 oxidation state and each gallium bonded to a chloride and chelated to a β-diketonate ligand. Metal–metal bond lengths are Ga(1)-Ga(1a) = 2.396(3) Å. for the acac derivative, which has crystallographic imposed C2 symmetry and Ga(1)-Ga(2) = 2.391(2) Å. for the tmhd derivative.[138]

8.9 Pyridinones

The discovery that ^{67}Ga administered as the citrate localized in soft tumor tissue[139] initiated considerable clinical interest in gallium coordination chemistry. In fact the citrate complex is now widely used in oncological nuclear medicine for tumor detection; however, the mechanism of uptake is still to be determined. Despite this early success and the ready availability of both ^{67}Ga and ^{68}Ga, the application of gallium in medicine has been limited. One of the reasons for this is the complex hydrolysis chemistry of gallium compounds, and the majority of studies have been performed under acidic conditions. Clearly if the coordination chemistry of gallium is to be understood *in vivo*, then complexes stable at pH 7.4 are of great interest. While some researchers have concentrated on polydentate ligands, such as cryptands, others have investigated bidentate chelating ligands of biological relevance. The most successful work in this area is by Orvig and coworkers on complexes of gallium with hydroxypyrones and hydroxypyridinones.[140–142]

A series of tris(3-hydroxy-4-pyranato)gallium(III) complexes has been prepared by the neutralization of solutions of $GaCl_3$ and substituted pyrones (**15a–d**). The complexes of larixinic acid (**15b**) and kojic acid (**15c**) are water soluble but retain their neutral charge.

The known sequestering ability of various hydroxypyridinones for iron(III) prompted investigation of the gallium complexes. The tris complexes have been prepared with a wide

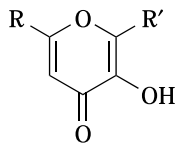

(**15a**) R = R′ = H; pyromeconic acid
(**15b**) R = H, R′ = Me; maltol (larixinic acid)
(**15c**) R = CH_2OH, R′ = H; kojic acid
(**15d**) R = CH_2Cl, R′ = H; chlorokojic acid

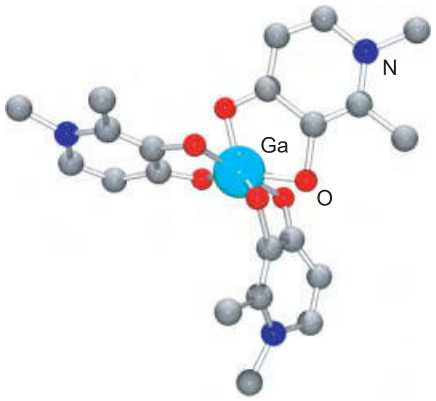

Figure 21 Molecular structure of $Ga(dpp)_3$; Hdpp = 3-hydroxy-1, 2-dimethyl-4-pyridinonate

range of substituted hydroxypyridinones (**16**).[140] The molecular structure of one such compound is shown in Figure 21. All the complexes form a rigid *fac* geometry, are water soluble, and have a wide window of stability to hydrolysis. Their lipophilicity is increased by the substitution of an aryl group at the nitrogen (see **17**).[141]

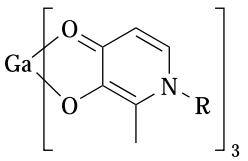

(**16**) R = H, Me, *n*-C_6H_{13}

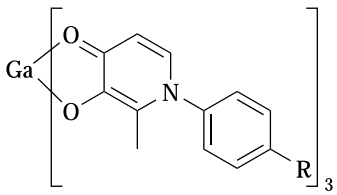

(**17**) R = H, Me, OMe, NO_2

Aqueous solution stability constants for the aryl substituted complexes have been determined. The ML_3 complexes are highly stable; at 25 °C the overall stability constant (β_3) for the parent complex (**17**); R = H is $10^{36.3}$. At ligand to metal ratios ≥ 1, the ligands prevent gallium hydrolysis even at millimolar concentrations and under slightly basic conditions; the effective formation constant (β_{3eff}) for ML_3 at physiological pH is $10^{30.3}$. As a practical application of these data, comparative metal binding in a simple blood plasma model has been simulated, which in turn allowed for the design of biodistribution experiments in mice. The

concentration of ligand required to inhibit removal of gallium from the GaL_3 complexes and the excretion pathway have been determined.[142]

8.10 Chalcogen Donor Ligands

While the donor chemistry for the heavier chalcogens with group 13 elements is generally poorly developed in comparison to the lighter chalcogen oxygen donor ligand chemistry, in the case of gallium there has been significant interest in non-oxide chalcogen-containing compounds with chalcogenide, and in particular sulfur, donor ligands for III-VI binary alloy formation. This anomaly for gallium is as a function of the similarities in its coordination chemistry to that of high-spin iron(III), and the biological importance of iron–sulfur proteins (*see* ***Iron: Heme Proteins & Dioxygen Transport & Storage***; ***Iron: Heme Proteins & Electron Transport***; ***Iron: Heme Proteins, Mono- & Dioxygenases***; ***Iron: Heme Proteins, Peroxidases, Catalases & Catalase-peroxidases***). The anionic gallium tetrathiolate complexes, $[Ga(SR)_4]^-$, may be prepared by the reaction of either $GaCl_3$ or $[GaCl_4]^-$ with five equivalents of LiSR, where R = Me, Et, *i*-Pr, Ph, 2,3,5,6-Me_4C_6H, or 2,4,6-*i*-$Pr_3C_6H_2$.[143] Because of the inaccessibility of the +2 oxidation state of gallium, the tetrathiolate complexes do not undergo the redox reaction (equation 23) that is responsible for the instability of many of the iron analogs.

$$2M^{3+} + 2RS^- \longrightarrow 2M^{2+} + RSSR \qquad (23)$$

The structure of $[(n\text{-Pr})_4N][Ga(SEt)_4]$ has been determined by X-ray crystallography to be isomorphous to the iron analog; however, although isostructural, $[Et_4N][Ga(SPh)_4]$ is not isomorphous with its iron analog. This difference has been rationalized with regard to the presence of steric interactions between the *ortho* hydrogens of two of the phenyl rings and the GaS_4 core. Although no examples of neutral three-coordinate gallium alkoxides have been reported, thiolate and selenolate derivatives, $Ga[E(2,4,6\text{-}t\text{-}Bu_3C_6H_2)]_3$ (E = S, Se), have been crystallographically characterized,[144] and the thiolate compound is shown in Figure 22. Structural data show that the gallium centers are three coordinate and almost planar. The slight distortion from idealized trigonal-planar coordination has been explained on the basis of ionic M–S bonding character and some agostic Ga···H interactions involving the *ortho t*-butyl groups of the ligand.

In addition to a variety of organometallic gallium thiolates (*see* ***Gallium: Organometallic Chemistry***), there are a number of mixed thiolate compounds, for example, the halide–thiolate dimers $[I_2Ga(SMe)]_2$ and $[I_2Ga(S\text{-}i\text{-}Pr)]_2$. The latter compound has the unusual feature of having a butterfly Ga_2S_2 core.[145] The first gallium thiolato compound to be structurally characterized was the adamantane cluster $Ga_4I_4(SMe)_4S_2$ (Figure 23), prepared from the reaction of Me_2S_2 with Ga_2I_4.[146] The Ga–S

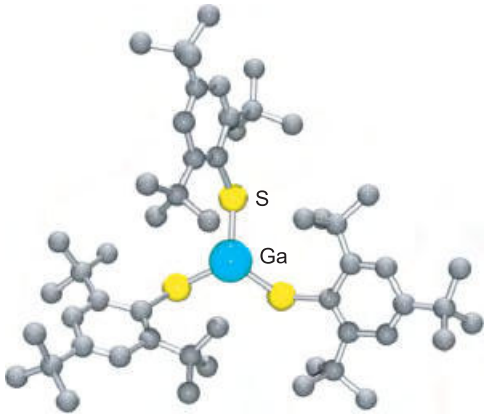

Figure 22 Molecular structure of $Ga[S(2,4,6\text{-}t\text{-}Bu_3C_6H_2)]_3$

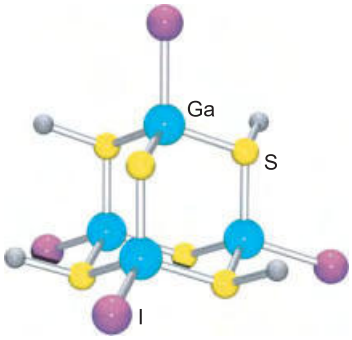

Figure 23 Molecular structure of $Ga_4I_4(SMe)_4(S)_2$

distances fall into two groups, those to the sulfide (average = 2.20 Å) and those to the methylthiolate ligands (average = 2.33 Å). The $[Ga_2S_2(SPh)_4]^{2-}$ anion has been prepared and structurally characterized (Figure 24). The structure is that of a centrosymmetric dimer consisting of two edge-sharing tetrahedra.

Figure 24 Structure of the $[Ga_2S_2(SPh)_4]^{2-}$ anion

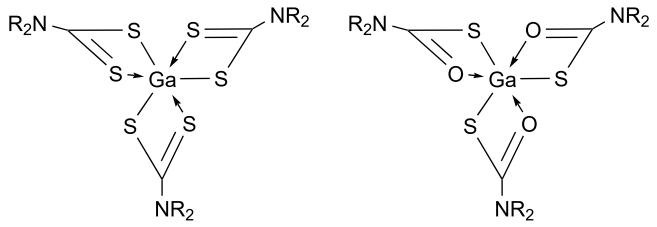

Figure 25 Schematic of $[Ga(S_2CNR_2)_3]$ & $[Ga(SOCNR_2)_3]$ derivatives

A number of gallium dithiocarbamate coordination complexes have been investigated for their potential suitability as single-source III-VI precursors. These type of compounds are often referred to as Mitsubishi™ compounds owing to their structural resemblance to the respective company logo (Figure 25). Additionally this area has recently been reviewed.[145]

The gallium *tris*-dialkyldithiocarbamates are monomeric solids that possess relatively low volatility. Improved volatility is achieved with asymmetric secondary amines derivatives; for example, the use of $[Ga\{S_2CN(Me)Hex\}_3]$ in a LP-MOCVD affords α-Ga_2S_3 thin films at 500 °C on GaAs(111).[147] Whereas the monothiocarbamato coordination complex $[Ga(SOCNEt_2)_3]$ affords thin films of GaS at 450 °C.[148] Again a more comprehensive array of the analogous indium derivatives has been synthesized and studied in comparison to gallium. The ^{71}Ga NMR studies have been preformed on a number of Mitsubishi™ complexes of the type $[Ga\{S_2CNR\}_3]$, $[Ga\{S_2CNR\}\{(SCH_2CH_2)_2O\}]$, where R=$CH_2CH_2OCH_2CH_2$, $CH_2CH_2N(Me)CH_2CH_2$, and $[GaCl_2\{S_2CN(CH_2CH_2)_2O\}]$, $[GaCl\{S_2CN(CH_2CH_2)_2O\}_2]$, and $[Ga\{S_2CN(CH_2CH_2)_2O\}\{S_2P(OR)_2\}_2]$ where R = Et, Pr^i have been investigated. The ^{71}Ga NMR chemical shifts and half line widths were found to be influenced by the coordination number of gallium and the substituents on the ligand moiety; additionally, an in-depth study of their spectroscopic properties has been reported.[149]

Dithiophosphinato complexes have found application as solvent extraction reagents for metals, insecticides, and pesticides, flotation agents for mineral ores, and additives to lubricant oils and can be used as precursors in metal-organic chemical vapor deposition (MOCVD).[150] The related indium compounds $[In(S_2PR)_3]$ (R = Me, Et, OEt, Ph) are monomeric in the solid state in contrast to the dinuclear species seen for the related group 12 zinc and cadmium species. The analogous group 13 derivatives $[In(S_2PBu^i_2)_3]$ and $[Ga(S_2PBu^i_2)_3]$ were prepared and characterized. Whereas the In metal center was found to be six-coordinate, the Ga metal center is four-coordinate, being bound to only one chelating and two pendant diisobutyldithiophosphinate ligands in a distorted tetrahedral geometry.

The sterically encumbering β-diketiminate ligand [{HC(MeCDippN)$_2$Ga}] (Dipp = C_6H_3-2,6-Pr^i_2) has been used to stabilize the first dimeric galloxane derivative $[\{HC(MeCDippN)_2\}GaO]_2$, as well as its S analog $[\{HC(MeCDippN)_2\}GaS]_2$. Treatment of $\{HC(MeCDippN)_2\}Ga$ with N_2O or S_8 in a toluene solution at room temperature produced the respective compounds as colorless crystals. The Ga_2S_2 core is planar and has an average Ga–S bond length of 2.26(1) Å, which is just within the currently known range (2.20–2.27 Å) for low-coordinate Ga-S species.[151]

The reactions of $Ga(CH_2CH_3)_3$ with variable amounts of elemental sulfur, S_8, in toluene or benzene at different temperatures results in the insertion of sulfur into the Ga–C bonds to form the $Ga[(S\text{-}S)CH_2CH_3]_3$ and $Ga[(S\text{-}S\text{-}S)CH_2CH_3]_3$. Even when the reactions were carried out with more than 9.0 equiv of sulfur, the maximum extent of sulfur insertion was found to be three S units. However, the reactions of $Ga(CH_3)_3$ with various molar ratios of S in toluene or benzene only gave $Ga[(S\text{-}S)CH_3]_3$. In pyridine at −30 °C, deinsertion of the sulfur atoms from Ga-S-S-C bonds was noted for the first time from $Ga[(S\text{-}S)CH_2CH_3]_3$ and $Ga[(S\text{-}S\text{-}S)CH_2CH_3]_3$, resulting in formation of the six-membered Ga–S ring compounds $[PyEtGaS]_3$ and $[PyMeGaS]_3$ respectively.[152]

9 HALIDES

9.1 Ga(III) Halides

9.1.1 Synthesis and Structure

The halides (especially the chloride) are the most commonly employed synthons in the chemistry of gallium. This is undoubtedly due to their ease of synthesis and high reactivity. While the trihalides have been traditionally the most extensively studied, the mono- and dihalides have come under recent scrutiny.

Gallium fluoride differs markedly from the other halides of gallium and in this it resembles the fluorides of aluminum and indium. For example, the melting points of the fluorides are several hundred degrees above those of the chlorides, though this difference decreases from 1097 °C for aluminum, to 872 °C for gallium, to 584 °C for indium. The compound GaF_3 is produced by the thermal decomposition of either $[NH_4]_3[GaF]_6$ or $GaF_3(NH_3)_3$ in the absence of moisture; the latter brings about the formation of $(NH_4)_2GaF_3(OH)_2$. The GaF_3 molecule is planar with a Ga–F distance of 1.88 Å. This species and the dimer Ga_2F_6 have been examined in the vapor phase by mass spectrometry.[5]

The trihalides $GaCl_3$ and $GaBr_3$ are usually prepared directly from the elements, by burning the metal in a stream of Cl_2 (or Br_2) in an apparatus that uses all-glass, or greaseless, connections. GaI_3 can be obtained by dissolving

Table 6 Physical properties of gallium trihalides

Property	$GaCl_3$	$GaBr_3$	GaI_3
Mp (°C)	77.75 ± 0.05	122.3 ± 0.05	211.5 ± 0.1
Bp (°C)	201.2	279	346
Vapor pressure (mm Hg)	10.4 (at 78 °C)	4.7 (at 125 °C)	19.2 (at 215 °C)
Density ($g\,cm^{-3}$)	2.47	3.69	4.15
$\Delta H°_f$ ($kJ\,mol^{-1}$)	523	386	255
ΔH_{dimer} ($kJ\,mol^{-1}$)	87 (per Ga_2Cl_6)	77 (per Ga_2Br_6)	46 (per Ga_2I_6)

Ga in a refluxing solution of I_2 in CS_2. The trichloride and tribromide of gallium have some advantages over $AlCl_3$ as Friedel–Crafts catalysts, in particular, their high solubility in organic solvents.[4] All three halides are colorless, deliquescent, low-melting solids, whose physical properties are shown in Table 6. In solid and liquid states, and in noncoordinating solvents, the GaX_3 (X = Cl, Br, I) molecules are dimeric with bridging ligands spanning four-coordinate gallium atoms. In the vapor, there is increasing dissociation of Ga_2X_6 to GaX_3 for X = Cl (0.4%), Br (14%), or I (96%), in accord with the decreased ΔH of dimer formation (see Table 6). Molecular dimensions are known for the monomers $GaBr_3$ and GaI_3, and the dimers Ga_2Cl_6 and Ga_2I_6, but precise values are lacking for $GaCl_3$ and Ga_2Br_6. Vibrational assignments are available for the GaX_3 monomers (from gas-phase and matrix-isolation studies) and the Ga_2X_6 dimers.[4]

9.1.2 Complexes

The trihalides (except the fluorides) all function as Lewis acids, forming 1:1 adducts with a great variety of Lewis bases. This is one of the most important aspects of the chemistry of the gallium halides. The Lewis acidity of the GaX_3 groups has been extensively studied thermodynamically, and basicity sequences for a variety of donors have been established.

Neutral Adducts. Being powerful acceptors, the gallium trihalides react with donor molecules L to form the adducts $GaX_3(L)$, and in some instances $GaX_3(L)_2$. In the trigonal bipyramidal 2:1 complexes, the halogen atoms are usually equatorial. The 1:1 complexes of trimethylamine with gallium trichloride and tribromide are solids, stable above 200 °C, while the complexes with two moles of trimethylamine decompose above −48 °C to give the 1:1 complex. Pyridine and piperidine form 1:1 and 2:1 adducts with $GaCl_3$, but only the 1:1 complex with $GaBr_3$.[4,5] Ethers form stable complexes with GaX_3, and there seems to be less tendency than with the aluminum analogs for thermal elimination of alkyl halides. However, caution should be observed when dissolving $GaCl_3$ in coordinating ether solvents, for example, Et_2O or THF, since the formation of the $GaCl_3(L)$ complex is sufficiently exothermic to boil the solvent. While the donor atom is generally from group 15 or 16, several examples of neutral complexes between $GaCl_3$ and alkyl halides have been reported.[4]

Anionic Complexes. Gallium, like aluminum, forms tetrahedral tetrahalide ions, $[GaX_4]^-$. Crystalline salts can be obtained, for example, by the action of alkali metal halides or ammonium halides on Ga_2Cl_6. However, oxonium salts, for example, $[(Et_2O)_nH][GaCl_4]$, isolated from the reaction of $GaCl_3$ with HCl in ether, are viscous oils.[4] That the tetrahalogallates can be regarded as typical Lewis acid–base complexes is seen by the ease with which the halide is replaced by neutral donor ligands (e.g. equation 24).

$$M[GaCl_4] + L \xrightarrow[M = Li,\ NH_4;\ L = NR_3,\ py]{} GaCl_3(L) + MCl \qquad (24)$$

While the tetrahaloaluminates are unstable under acid conditions, the gallium analogs are readily extracted from aqueous solutions of gallium salts, into ethers, by 8 M HCl; the resulting ether phase contains $[GaCl_4]^-$ ions. This suggests the presence of a series of equilibria (equation 25):

$$[Ga(H_2O)_6]^{3+} \xrightarrow{+n\text{HCl}} [GaCl_n(H_2O)_m]^{3-n} \xrightarrow{+m\text{HCl}} [GaCl_4]^- \qquad (25)$$

In addition to crystallographic data for solids containing the $[GaX_4]^-$ ion, characteristic absorption spectra, vibrational frequencies, NMR chemical shifts, and NQR parameters are well established. These properties can be used to study effects such as ligand exchange processes of $[GaX_4]^-$ with Cl^-, ion pairing in nonaqueous solutions of alkylammonium chlorogallates, polymorphism of $K[GaCl_4]$, and solid-state interactions in the crystalline solids $[NO][GaCl_4]$ and $[Ga][GaCl_4]$. Bond dissociation energies $\Delta(X_3Ga–X)$ are 364 and 314 $kJ\,mol^{-1}$ for X = Cl and Br, respectively.

[GaSBr] and [GaSeBr] have been synthesized from $Ga[GaBr_4]$ and elemental S/Se in toluene or THF, respectively, with the formation of the by-product $GaBr_3(THF)_2$. The two ternary Ga bromides are insoluble in most common organic solvents, but are readily dissolved in pyridine and substituted pyridines (L) to give trinuclear $[GaSBr(L)]_3$

with L = 3,5-dimethylpyridine, 4-*tert*-butylpyridine, and 4-dimethylaminopyridine, and $[GaSeBr(L)]_3$ with L = 3,5-dimethylpyridine, respectively. The core units are six-membered rings with different substitution patterns and were found to depend largely on the steric requirements of the ligands L, and on the mode of crystallization undertaken. Similar studies have been preformed for the chloride analog.[153]

Cationic Complexes. Apart from the aqua ions and partially substituted species such as $[GaCl(H_2O)_5]^{2+}$, cationic complexes of gallium halides with pyridine, bipyridine, or phenanthroline are known, for example, $[GaCl_2(phen)_2]^+$ and $[Ga(phen)_3]^+$. Furthermore, given the steric hindrance about the gallium center in complexes formulated as $GaX_3(NH_3)_n$ (X = Cl, n = 1, 3, 5, 6, 7, 14; X = Br, n = 1, 5, 7, 9, 14; X = I, n = 1, 5, 6, 7, 9, 13, 20), it is likely that where n is greater than 3 these are also cationic solvates.[154]

9.2 Lower Oxidation State (I) & (II) halides

All four halides GaX (X = F, Cl, Br or I) are known as vapor-phase species, but tend to disproportionate when condensed, producing elementary gallium. The solid once thought to be GaI has been shown to be Ga_2I_3. Gallium forms a number of mixed valence halides containing gallium(I) cations. In these compounds, the Ga^+ cation is stabilized by the presence of the anion formed when the strong Lewis acid GaX_3 combines with halide ligands. Examples are the so-called 'dihalides' [Ga][GaX_4] and the compounds Ga_3X_7, that is, [Ga][Ga_2X_7] (X = Cl, Br, I). In the subhalides, Ga_2X_3, the stabilizing anion is $[Ga_2X_6]^{2-}$, the constitution being $[Ga]_2[Ga_2X_6]$ (X = Cl, Br, I).

The crystal structure of Ga_2Cl_4 shows each of the Ga^+ cations surrounded by eight chlorides of the $[GaCl_4]^-$ counterions. The gallium(I) chloride distance is more than 3.00 Å, to be compared with the Ga–Cl bond length of 2.19 Å in $[GaCl_4]^-$, and implies that the Ga^+ cation is not coordinated but 'solvated'. However, when Ga_2Cl_4 is vaporized, the vapor consists solely of GaCl and $GaCl_3$ molecules. Recent structural analyses of Ga_2I_4 and Ga_2I_3 have directed attention to the influence on these structures of the $4s^2$ electron pair of the Ga^+ ion, and confirm that in the case of the iodide no coordination is observed to the lower oxidation state center.

The halides Ga_2X_4 combine with various donor ligands to give products since shown to be molecular adducts of the metal–metal bonded Ga^{II} state. For example, the treatment of Ga_2Cl_4 with dioxane gives a crystalline solvate (**18**), in which each Ga atom has a distorted tetrahedral configuration and the Ga–Ga distance is 2.406(1) Å.

There are reports of reactions of the halides Ga_2X_4 with alcohols, water, aqueous NaOH, HCl or HF, and H_2S gas. Oxidative addition usually occurs, although there is evidence of the initial precipitation of Ga^I containing solids in the reactions of Ga_2Cl_4 in benzene solution with H_2O or H_2S.

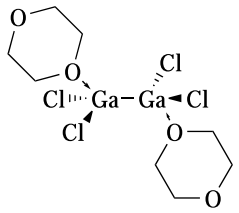

(**18**)

The crystalline solid Ga_2Cl_4 is soluble in benzene. Under regulated conditions this solution yields crystals that prove to contain the complex $[Ga(C_6H_6)_2][GaCl_4]$, and X-ray studies show the cation to be the η^6-bis(benzene) complex of Ga^I (*see* ***Gallium: Organometallic Chemistry***). The $[GaCl_4]^-$ ions interact weakly with Ga^+ to provide bridging chlorine atoms between the Ga^I centers. The anodic dissolution of gallium in 6 M HCl or HBr at 0 °C followed by addition of $[Me_4N]X$ precipitates white crystalline salts of the ion $[Ga_2X_6]^{2-}$ that are stable and diamagnetic owing to the presence of a Ga–Ga bond (2.39 Å for X = Cl and 2.41 Å when X = Br).[155]

Mixed metal derivatives of gallium have become novel target compounds for investigation. [Tetra(*n*-ethyl)-1,1′-diphosphaferrocene $GaCl_2]^+$ $[GaCl_4]^-$ was prepared by the reaction of the ferrocene derivative and $GaCl_3$ at room temperature. The synthesis of the corresponding complex incorporating octa(*n*-propyl)-1,1′-diphosphaferrocene was carried out to try an ascertain the bonding structure in these molecules the [octa(*n*-propyl)-1,1′-diphosphaferrocene-$GaCl_2]^+$ $[GaCl_4]^-$ complex, which was successfully characterized by X-ray crystallography. In octa derivative, the diphosphaferrocene ligand acts as a chelate and the overall geometry around the gallium is tetrahedral. Theoretical calculations indicated that the bonding of the diphosphaferrocene ligand to the $[GaCl_2]^+$ fragment involves the lone pairs on the phosphorus atoms and a contribution of the P–Fe bond.[156]

$[[(\eta 5\text{-Cp}^*)Fe(CO)_2]_2GaCl]$ is a useful reagent that is readily prepared by a metathesis reaction with 2 equivalents of $Na[(\eta 5\text{-Cp}^*)Fe(CO)_2]$ with $GaCl_3$ at room temperature. Treatment of the aforementioned with a boron anion allows for the formation of the unique cationic Fe complex $[[(\eta 5\text{-Cp}^*)Fe(CO)_2]_2Ga]^+$ $[BAr^f_4]^-$ ($Ar^f = C_6H_3(CF_3)_2$-3,5) (Scheme 5), which contains a symmetrically bridging two-coordinate Ga atom and a delocalized Fe-Ga-Fe π system having partial Fe–Ga multiple bond character. DFT (BLYP/TZP) computational analysis showed that the fully optimized geometry is consistent with that for the crystallographically solved structure.[157]

10 POLYDENTATE LIGANDS

Kinetically stable complexes of gallium are being examined for use as imaging agents in diagnostic nuclear medicine

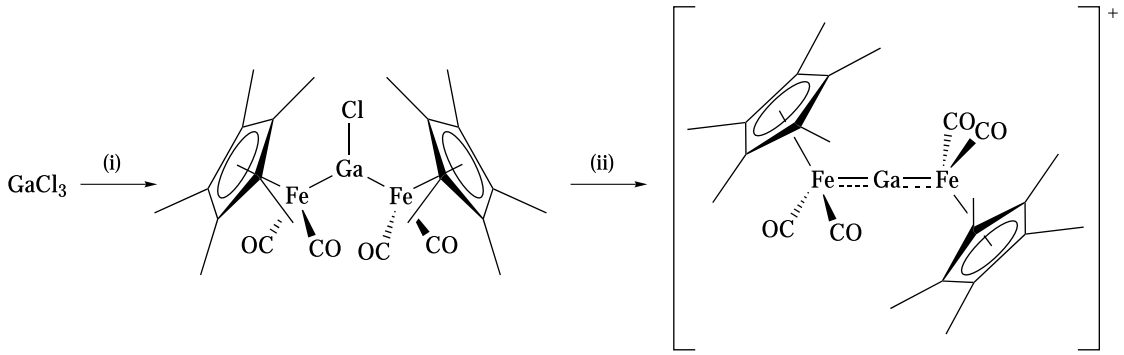

Scheme 5 Syntheses of $[[(\eta 5\text{-Cp}^*)\text{Fe(CO)}_2]_2\text{GaCl}]$ and $[[(\eta 5\text{-Cp}^*)\text{Fe(CO)}_2]_2\text{Ga}]^+$ $[\text{BAr}^f{}_4]^-$. Reagents and conditions: (i) $\text{Na}[(\eta 5\text{-Cp}^*)\text{Fe(CO)}_2]$ 2 equiv., toluene, 20 °C, 12 h; (ii) $\text{Na}[\text{BAr}^f{}_4]$ 1 equiv., dichloromethane, 278 °C to 20 °C, 30 min

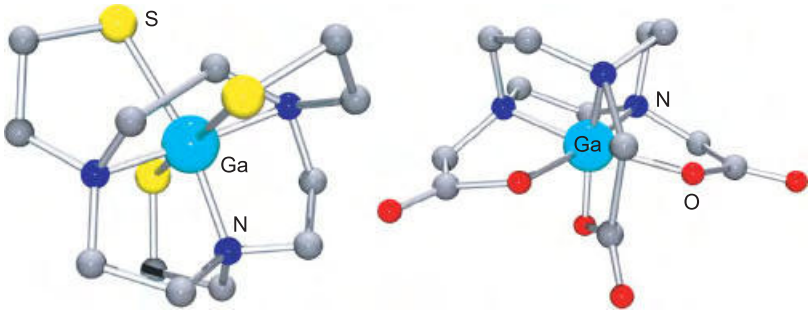

Figure 26 Molecular structure of Ga(TS-TACN); H_3TS-TACN = 1,4,7-tris(2-mercaptoethyl)-1,4,7-triazacyclononane and Ga(NOTA) (NOTAH_3 = 1,4,7-triazacyclononante-1,4,7-trisacetic acid)

(^{67}Ga, γ, $t_{1/2} = 3.25$ days; ^{68}Ga, β^+, $t_{1/2} = 68$ min). In order for these complexes to be used in vivo, they should resist acid (or cation) mediated decomplexation in the pH range 2–8. The synthesis of oxygen, nitrogen, and recently sulfur functionalized polydentate ligands, especially those that may be attached to tumor-localizing antibodies, has been investigated.

10.1 Cryptand Ligands

The development of new metal-chelating agents for medical applications is an actively growing area of research in gallium coordination chemistry. While much effort has been put into the synthesis and determination of stability constants of ethylenediamine derivatives, these ligands yield a potential coordination sphere consisting of an $[N_2O_4]^{4-}$ core, which produces an anionic complex when bound to gallium(III).[158,159] Accordingly, these complexes are not very lipophilic. Hydrophilicity may be the principal reason that some radio-labeled complexes of Ga^{3+} are unable to cross the blood–brain barrier. Research has therefore been directed toward the development of cryptand ligands that possess a potential coordination sphere consisting of an $[N_3O_3]^{3-}$ core, thereby producing neutral, highly lipophilic complexes of Ga^{3+}. Several groups have reported a variety of triprotic ligands with $[O_6]^{3-}$, $[N_3O_3]^{3-}$, and $[N_3S_3]^{3-}$ cores,[160–162] examples are shown in Figure 26.

10.2 Porphyrin and Related Ligands

Chlorogallium(III) porphyrins, Ga(Por)Cl, are obtained in good yield by treating the corresponding free bases with gallium trichloride. The action of the hydrogen halides HX (X = F or I) on the chloro derivatives Ga(Por)Cl led to the corresponding halogeno complexes Ga(Por)X. The crystal structure of the tetraphenylporphyrin derivative has been determined by X-ray diffraction methods and shows a square pyramidal coordination for the gallium.[163] The reactions of the Lewis bases (L) *N*-methylimidazole and pyridine with Ga(Por)X [H_2Por = octaethylporphyrin (OEP, (**19b**)), tetraphenylporphyrin (TPP, (**19a**)); X = Cl^-, OAc^-, OH^-, F^-] have been investigated, and demonstrated the stepwise formation of hexacoordinate gallium porphyrin species of the type [Ga(Por)(X)(L)] and $[\text{Ga(Por)(L)}_2]^+$ (Scheme 6).[164] These compounds represent the first monomeric, hexacoordinated gallium(III) porphyrins to be reported. Equilibrium constants for ligand binding by Ga(Por)X and Ga(Por)(X)(L) were calculated from the electronic absorption spectra.

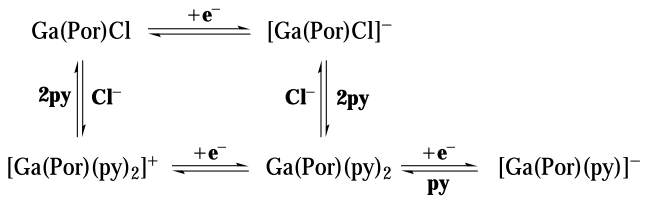

Scheme 6 Electrochemical reactions of gallium porphyrin complexes

The synthesis, spectroscopic, and structural characterization of the stable Ga hydride porphyrin [Ga(TPP)H] (TPP = 5,10,15,20-tetraphenylporphyrinato) was synthesized in high yield (85%) by reducing [Ga(TPP)Cl] with $NaBH_4$ in DMF. Infrared (IR) studies determined the Ga–H stretch at 1864 cm^{-1}, and the hydride ^1H NMR resonance located at −6.47 ppm. The Ga–H distance is 1.48(4) Å, whereas the Ga atom lies 0.46(1) Å from the perfect porphyrin plane.[165]

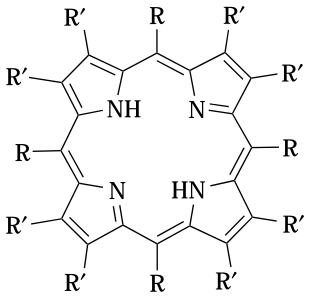

(**19a**) TPP; R = Ph, R′ = H
(**19b**) OEP; R = H, R′ = Et

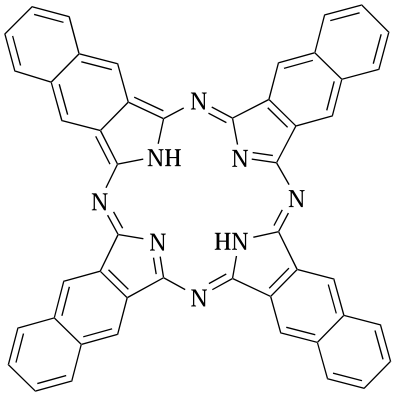

(**20**) H_2Nc

Gallium complexes of naphalocyanine (H_2Nc, (**20**)) have been investigated with respect to their application in photodynamic therapy agents for neoplastic disease. Compounds of the general formula Ga(Nc)X were prepared for X = F, Cl, OH, or OSi(*n*-C_6H_{13})$_3$.

Corroles are tetrapyrrole macrocycles that are closely related to porphyrins, with one carbon atom less in the outer periphery and one NH proton more in their inner core. They may also be considered as the aromatic version (identical skeleton) of the only partially conjugated corrin, the cobalt-coordinating ligand in Vitamin B_{12}. Two potential application of corroles are in tumor detection and their use in photovoltaic devices. Selective substitution of corroles via nitration, hydroformylation, and chlorosulfonation for the gallium were studied in detail and the respective mechanistic pathways and spectroscopic data were reported, (an example is shown in Figure 27). Overall, over 139 various corroles were synthesized and the effect of various metal complexation pertaining to their selective reactivity examined.[166,167]

The first highly characterized Ga and In halide complexes of tetraazamacrocycles have been reported. Gallium(III) and indium(III) complexes of cross-bridged cyclam and cyclen tetraaza macrocyclic ligands have been prepared and structurally characterized. In the crystalline state, both the $GaCl_3$ (cross-bridged cyclam) (**21**) and $InBr_3$ (cross-bridged cyclen) (**22**) complexes feature hexacoordinate cations in cis-folded tetradentate ligand clefts with ancillary cis-dihalides.[168]

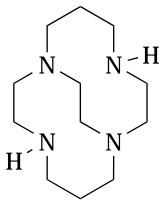

(**21**)

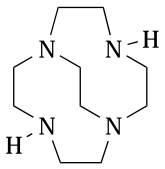

(**22**)

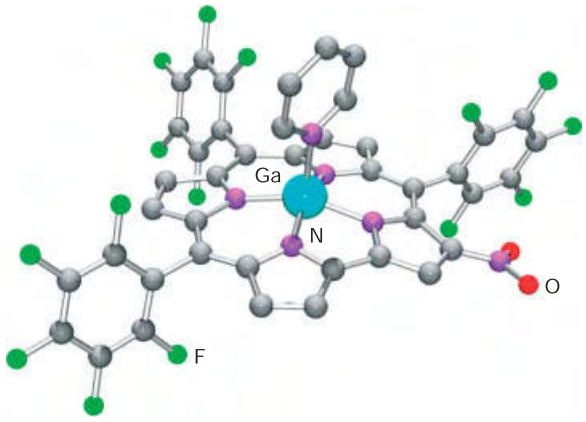

Figure 27 $C_{42}H_{12}F_{15}GaN_6O_2\cdot(C_6H_6)$, $M = 1065.4$, orthorhombic, space group $P2_12_12_1$, $a = 12.0410(2)$, $b = 18.2040(3)$, $c = 18.5900(3)$ Å, $V = 4074.8(1)$ Å^3, $D_c = 1.737$ g cm^{-3}, μ(Mo Kα) = 0.80 mm^{-1}. The observed Ga–N coordination distances to the four pyrrole and the pyridyl nitrogens are 1.972, 1.926, 1.942, 1.938, and 2.039(4) Å, respectively

Three hexadentate, asymmetric pendent arm macrocycles containing a 1,4,7-triazacyclononane-1,4-diacetate backbone and a third, *N*-bound phenolate or thiophenolate arm have been synthesized. In $[L^1]^{3-}$ the third arm is 3,5-di-*tert*-butyl-2-hydroxybenzyl, in $[L^2]^{3-}$ it is 2-mercaptobenzyl, and in $[L^3]^{3-}$ it is 3,5-di-*tert*-butyl-2-mercaptobenzyl. With trivalent metal ions these ligands form very stable neutral mononuclear complexes $[Ga^{III}L^{1to3}]$ where the gallium complexes possess an $S = 0$ ground state. Cyclic voltammetry studies revealed that all three $[Ga^{III}L^1]$ complexes undergo a reversible, ligand-based, one-electron oxidation generating the monocations $[GaL^1]^+$, which contain a coordinated phenoxyl radical as was unambiguously established by their electronic absorption, EPR, and Mössbauer spectra. In contrast, $[Ga^{III}L^2]$ complexes in CH_3CN solution undergo an irreversible one-electron oxidation where the putative thiyl radical monocationic intermediates dimerize with S–S bond formation yielding dinuclear disulfide species $[Ga^{III}L^2\text{-}L^2Ga^{III}]^{2+}$. $[GaL^3]$ behaves similarly despite the steric bulk of two tertiary butyl groups at the 3,5-positions of the thiophenolate.[169] Similar work has been performed on various gallium triazacyclononane with modified pendent arms and their crystal structures have been elucidated.[170]

11 Ga(III): A DIAMAGNETIC MIMIC OF IRON(III)

The hydrolytic behavior and aqueous chemistry of the Ga^{3+} ion is similar to that of the Fe^{3+} ion. In fact, useful extrapolations of properties have been made between the two. For instance, diamagnetic gallium analogs of the microbial iron chelates (siderophores) have been useful in NMR studies,[171] since the native Fe^{3+} ion complexes are paramagnetic. In reverse, the knowledge gained from studies of Fe^{3+} ion transport has been applied to the development of ^{67}Ga radiopharmaceuticals.[172] The basis for this replacement of Fe^{3+} by Ga^{3+} lies in the physical and chemical similarities of the two ions. Both have the same charge and similar ionic radii in six-coordinate complexes (0.620 Å for Ga^{3+} compared to 0.645 Å for Fe^{3+}). Neither ion is perturbed by crystal field effects. The Fe^{3+} ion configuration is high-spin d^5 while the gallium is diamagnetic d^{10}. Moreover, since neither have any crystal field stabilization and both have similar ionic radii, they are similar in many of their ligand exchange rates. However, there are some significant differences in the stabilities of Ga^{3+} and Fe^{3+} complexes. The formation constants of a series of catecholate complexes have been determined and the gallium complexes are found to be consistently less stable than the analogous iron complexes. The stabilities of the benzohydroxamate complexes show a similar disparity.

One notable difference in the properties of Ga^{3+} and Fe^{3+} is that while the Fe^{3+}/Fe^{2+} redox system is very important in biological systems, the absence of a stable divalent state for gallium removes from consideration any processes that involve one-electron reduction of Ga^{3+}.

12 RELATED ARTICLES

Aluminum: Inorganic Chemistry; Aluminum: Organometallic Chemistry; Boron Hydrides; Boron: Inorganic Chemistry; Gallium: Organometallic Chemistry; Indium: Inorganic Chemistry; Indium: Organometallic Chemistry; Iron: Heme Proteins & Dioxygen Transport & Storage; Iron: Heme Proteins, Peroxidases, Catalases & Catalase-peroxidases; Main Group: Multiple Bonding.

13 FURTHER READING

S. M. Bradley, R. A. Kydd, and R. Yamdagni, *J. Chem. Soc., Dalton Trans.*, 1990, 413.

Z. Liliental-Weber, C. W. Wilmsen, K. M. Geib, P. D. Kirchner, J. M. Baker, and J. M. Woodall, *J. Appl. Phys.*, 1990, **67**, 1863.

S. Nogai, A. Schier, and H. Schmidbaur, *Z. Naturforsch., B: Chem. Sci.*, 2002, **57**(2), 183.

K.-N. Tu, J. W. Mayer, L. C. Feldman, 'Electronic Thin Film Science for Electrical Engineers & Material Scientists', Prentice Hall College Div: 1st edition (December 2), 1996, p. 127.

K.-N. Tu, J. W. Mayer, L. C. Feldman, 'Electronic Thin Film Science for Electrical Engineers & Material Scientists', Prentice Hall College Div: 1st edition (December 2), 1996, p. 157.

K.-N. Tu, J. W. Mayer, L. C. Feldman, 'Electronic Thin Film Science for Electrical Engineers & Material Scientists', Prentice Hall College Div: 1st edition (December 2), 1996, , p. 194.

14 REFERENCES

1. Gmelin, 'Handbuch der Anorganischen Chemie', Syst. No. 36, Gallium, Springer, Berlin, 1936.
2. E. Einecke, 'Das Gallium', Voss, Leipzig, 1937.
3. N. Saunders, 'Aluminum and the elements of group 13', Heinemann Library, Chicago, IL, 2004, ISBN 1403416613.
4. N. N. Greenwood and A. Earnshaw, 'Chemistry of the Elements', Butterworth-Heinemann, 1997, ISBN 0750633654.
5. F. A. Cotton, G. Wilkinson, C. A. Murillo, and M. Bochmann, 'Advanced Inorganic Chemistry', John Wiley & Sons, New York, 1999, ISBN 0471199575.
6. D. A. Atwood, in 'Group 13 chemistry III: Industrial Applications', eds. H. W. Roesky and D. A. Atwood, Springer, Berlin, 2003, ISBN 3540441050.

7. H. Schnockel and C. Klemp, in 'Inorganic Chemistry Highlights', eds. G. Meyer, D. Naumann, and L. Wesemann, Wiley-VCH, Cambridge, 2002, p. 245, ISBN 3527302654.
8. P. J. Shapiro, and D. A. Atwood eds. 'group 13 Chemistry: From Fundamentals to Applications', ACS Symposium series; 822, Oxford University Press, Washington, DC, 2002, ISBN 0841237859.
9. P. O'Brien and N. L. Pickett, Coordination Complexes as Precursors for Semiconductor Films and Nanoparticles, in 'Comprehensive Coordination Chemistry II: from Biology to Nanotechnology', eds. J. A. McCleverty, and T. J. Meyer, Elsevier Science, 2004, p. 1005, ISBN 0080437486.
10. G. H. Robinson, Aluminum and Gallium, in 'Comprehensive Coordination Chemistry II: From Biology to Nanotechnology', eds. J. A. McCleverty and T. J. Meyer, Elsevier Science, 2004, p. 347, ISBN 0080437486.
11. J. P. Maher, *Annu. Rep. Prog. Chem., Sec. A: Inorg. Chem.*, 2003, **99**, 43.
12. J. P. Maher, *Annu. Rep. Prog. Chem., Sec. A: Inorg. Chem.*, 2002, **98**, 45.
13. J. P. Maher, *Annu. Rep. Prog. Chem., Sec. A: Inorg. Chem.*, 2001, **97**, 49.
14. J. P. Maher, *Annu. Rep. Prog. Chem., Sec. A: Inorg. Chem.*, 2000, **96**, 45.
15. J. P. Maher, *Annu. Rep. Prog. Chem., Sec. A: Inorg. Chem.*, 1999, **95**, 45.
16. J. P. Maher, *Annu. Rep. Prog. Chem., Sec. A: Inorg. Chem.*, 1998, **94**, 43.
17. J. P. Maher, *Annu. Rep. Prog. Chem., Sec. A: Inorg. Chem.*, 1997, **93**, 45.
18. J. P. Maher, *Annu. Rep. Prog. Chem., Sec. A: Inorg. Chem.*, 1996, **92**, 41.
19. J. P. Maher, *Annu. Rep. Prog. Chem., Sec. A: Inorg. Chem.*, 1995, **91**, 41.
20. J. P. Maher, *Annu. Rep. Prog. Chem., Sec. A: Inorg. Chem.*, 1994, **90**, 25.
21. P. P. Power, *Chem. Rev.*, 1999, **99**(12), 3463.
22. H. Curien, A. Rimsky, and A. Defrain, *Bull. Soc. Fr. Mineral. Crystallogr.*, 1961, **84**, 260.
23. J. P. Yesinowski and A. P. Purdy, *J. Am. Chem. Soc.*, 2004, **126**, 9166.
24. M.-C. Hsien, H.-M. Kao, and K.-H. Lii, *Chem. Mater.*, 2001, **13**, 2584.
25. A. Breuer and D. Siebert, *Berichte der Bunsen-Gesellschaft*, 1996, **100**, 1736.
26. P. P. Man, 2004, http://www.pascal-man.com/periodic-table/gallium.html.
27. M. Winter, 2004, http://www.webelements.com.
28. 2004, http://arrhenius.rider.edu/nmr/NMR_tutor/periodic_table/nmr_pt_frameset.html.
29. K. Weiß, R. Köppe, and H. Schnöckel, *Int. J. Mass Spectrom.*, 2002, **214**(3), 383.
30. Cv. Hanisch and O. Hampe, *Angew. Chem., Int. Ed.*, 2002, **41**(12), 2095.
31. J.-W. Hwang, S. A. Hanson, D. Britton, J. F. Evans, K. F. Jensen, and W. L. Gladfelter, *Chem. Mater.*, 1990, **2**, 342.
32. R. A. Logan, B. Schwartz, and W. J. Sundburg, *J. Electrochem. Soc.*, 1973, **120**, 1385.
33. H. Hasegawa, K. E. Forward, and H. L. Hartnagel, *Appl. Phys. Lett.*, 1975, **26**, 567.
34. M. A. Hoffbauer, J. B. Cross, and U. M. Bermudez, *Appl. Phys. Lett.*, 1990, **57**, 2193.
35. E. Yablonovitch, C. J. Sandroff, R. Bhat, and T. Gmitter, *Appl. Phys. Lett.*, 1987, **51**, 439.
36. A. N. MacInnes, M. B. Power, and A. R. Barron, *Chem. Mater.*, 1992, **4**, 11.
37. A. N. MacInnes, M. B. Power, A. R. Barron, P. P. Jenkins, and A. F. Hepp, *Appl. Phys. Lett.*, 1993, **62**, 711.
38. M. Tabib-Azar, A. N. MacInnes, M. B. Power, A. R. Barron, P. P. Jenkins, and A. Hepp, *Appl. Phys. Lett.*, 1993, **63**(5), 625.
39. M. Passlack, E. F. Schubert, W. S. Hobson, M. Hong, N. Moriya, S. N. G. Chu, K. Konstadinidis, J. P. Mannaerts, M. L. Schnoes, and G. J. Zydzik, *J. Appl. Phys.*, 1995, **77**(2), 686.
40. L. I. Berger, 'Semiconductor Materials', CRC Press, New York, 1997, ISBN 0-849389127.
41. E. Villora, K. Shimamura, Y. Yoshikawa, K. Aoki, and N. Ichinose, *J. Cryst. Growth*, 2004, **270**(3–4), 420.
42. S. Schulz, E. G. Gillan, J. L. Ross, L. M. Rogers, R. D. Rogers, and A. R. Barron, *Organometallics*, 1996, **15**(22), 4880.
43. S. Shigetomi and T. Ikari, *J. Appl. Phys.*, 2004, **95**(11), 6480.
44. L. I. Man, R. M. Imanov, and S. A. Semiletov, *Sov. Phys. Crystallogr.*, 1976, **21**, 255.
45. C. C. Landry, A. Hynes, A. R. Barron, I. Haiduc, and C. Silvestru, *Polyhedron*, 1996, **15**(3), 391.
46. C. C. Landry and A. R. Barron, 1992, unpublished results.
47. A. Kuhn and A. Chevy, *Acta Crystallogr.*, 1976, **B32**, 983.
48. M. P. Pardo and J. Flauhaut, *Mater. Res. Bull.*, 1987, **22**, 323.
49. A. R. Barron, *Comments Inorg. Chem.*, 1993, **14**, 123.
50. M. Burgelman, F. Engelhardt, J. F. Guillemoles, R. Herberholz, M. Igalson, R. Klenk, M. Lampert, T. Meyer, V. Nadenau, A. Niemegeers, J. Parisi, U. Rau, H. W. Schock, M. Schmitt, O. Seifert, T. Walter, and S. Zott, *Prog. Photovolt. Res. Appl.*, 1997, **5**(2), 121.
51. A. Niemegeers, M. Burgelman, R. Herberholz, U. Rau, D. Hariskos, and H.-W. Schock, *Prog. Photovolt. Res. Appl.*, 1998, **6**(6), 407.
52. S. B. Zhang, S.-H. Wei, A. Zunger, and Y. H. Katayama, *Phys. Rev. B*, 1998, **57**(16), 9642.
53. S.-H. Wei, S. B. Zhang, and A. Zunger, *Appl. Phys. Lett.*, 1998, **72**(24), 3199.

54. S. G. Bailey and D. J. Flood, *Prog. Photovolt. Res. Appl.*, 1998, **6**, 1.
55. K. Ramanathan, M. Contreras, C. L. Perkins, S. Asher, F. S. Hasoon, J. Keane, D. Young, M. Romero, W. Metzger, R. Noufi, J. Ward, and A. Duda, *Prog. Photovolt. Res. Appl.*, 2003, **11**(4), 225.
56. B. M. Basol, V. K. Kapur, A. Halani, C. R. Leidholm, J. Sharp, J. R. Sites, A. Swartzlander, R. Matson, and H. Ullal, *J. Vac. Sci. Technol. A*, 1996, **14**, 2251.
57. S. C. Park, D. Y. Lee, B. T. Ahn, K. H. Yoon, and J. Song, *J. Sol. Energy Mater. Sol. Cells*, 2001, **69**, 99.
58. C. Guillen and J. Herrero, *Thin Solid Films*, 2001, **387**, 57.
59. C. Eberspacher, K. Fredic, K. Paula, and J. Serra, *Thin Solid Films*, 2001, **387**, 18.
60. M. Klenk, O. Schenker, V. Alberts, and E. Bucher, *Thin Solid Films*, 2001, **387**, 47.
61. J. A. Hollingsworth, Chemical Routes to Nanocrystalline and Thin Film III-VI and I-III-VI Semiconductors, PhD Thesis, Washington University, 1999, Chap. 2–3.
62. T. C. Deivaraj, J. H. Park, M. Afzaal, P. O'Brien, and J. J. Vittal, *Chem. Mater.*, 2003, **15**(12), 2383.
63. T. C. Deivaraj, M. Lin, K. P. Loh, M. Yeadon, and J. J. Vittal, *J. Mater. Chem.*, 2003, **13**(5), 1149.
64. A. J. Nozik, *Annu. Rev. Phys. Chem.*, 2001, **52**, 193.
65. M. Green and P. O'Brien, *J. Mater. Chem.*, 2004, **14**, 629.
66. U. Brin, Synthesis and Characterisation of III-V Semiconductor Nanoparticles, in 'Nanoparticles: From Theory to Application', ed. G. Schmid, John Wiley & Sons, New York, 2004, p. 79, ISBN 3527305076.
67. U. Brin and O. Millo, Optical and Electronic Properties of III-V and II-VI Nanoparticles, in 'Nanoparticles: From Theory to Application', ed. G. Schmid, John Wiley & Sons, New York, 2004, p. 305, ISBN 3527305076.
68. R. L. Wells, C. G. Pitt, A. T. McPhail, A. P. Purdy, S. Shafieezad, and R. B. Hallock, *Chem. Mater.*, 1989, **1**, 4.
69. M. D. Healy, P. E. Laibinis, P. D. Stupik, and A. R. Barron, *J. Chem. Soc., Chem. Commun.*, 1989, 359.
70. M. A. Olshavsky, A. N. Goldstein, and A. P. Alivisatos, *J. Am. Chem. Soc.*, 1990, **112**, 9438.
71. H. Uchida, C. J. Curtis, P. V. Kamat, K. M. Jones, and A. J. Nozik, *J. Phys. Chem.*, 1992, **96**, 1156.
72. A. A. Guzelian, J. E. B. Katari, A. V. Kadavanich, U. Banin, K. Hamad, E. Juban, A. P. Alivisatos, R. H. Wolters and C. C. Heath, 1996, **100**, 7212.
73. O. I. Micic, S. P. Ahrenkiel, D. Bertram, and A. J. Nozik, *J. Appl. Phys. Lett.*, 1999, **75**, 478.
74. Y. Xie, Y. T. Qian, W. Z. Wang, S. Y. Zhang, and Y. H. Zhang, *Science*, 1996, **272**, 1926. Y. H.
75. J. Xiao, Y. Xie, R. Tang, and W. Luo, *Inorg. Chem.*, 2003, **42**(1), 107.
76. J. F. Janik, R. L. Wells, V. G. Young, A. L. Rheingold, and I. A. Guzei, *J. Am. Chem. Soc.*, 1998, **120**, 532.
77. M. Green, *Curr. Opin. Solid State Mater. Sci.*, 2002, **6**, 355.
78. M. C. Hanna, Z. H. Lu, A. F. Cahill, M. J. Heben, and A. J. Nozik, *J. Cryst. Growth*, 1997, **174**, 605.
79. Y. Banto and R. Ma, JP 2004182547, 2004.
80. Y. Banto and Y. Gao, JP 2004182546, 2004.
81. S. Gao, Y. Xie, L. Zhu, and X. Tian, *Inorg. Chem.*, 2003, **42**(17), 5442.
82. J. H. Chun, Y. S. Choi, S. Y. Bae, H. W. Seo, J. S. Hong, J. Park, and H. Yang, *J. Phys. Chem. B*, 2003, **107**, 9042.
83. M. Lazell, P. O'Brien, D. J. Otway, and J.-H. Park, *J. Chem. Soc., Dalton Trans.*, 2000, 4479.
84. S. L. Stoll, E. G. Gillan, and A. R. Barron, *Chem. Vap. Dep.*, 1996, **2**, 182.
85. S. L. Castro, S. G. Bailey, R. P. Raffaelle, K. K. Banger, and A. F. Hepp, *J. Phys. Chem. B*, 2004, **108**(33), 12429.
86. S. L. Castro, S. G. Bailey, R. P. Raffaelle, K. K. Banger, and A. F. Hepp, *Chem. Mater.*, 2003, **15**(16), 3142.
87. Q. Lu, J. Hu, K. Tang, Y. Qian, G. Zhou, and X. Liu, *Inorg. Chem.*, 2000, **39**, 1606.
88. Y. Cui, J. Ren, G. Chen, Y. Qian, and Y. Xie, *Chem. Lett.*, 2001, 236.
89. Y. Jiang, Y. Wu, S. Yuan, B. Xie, S. Zhang, and Y. Qian, *J. Mater. Res.*, 2001, **16**, 2805.
90. J. Olkowska-Oetzel, D. Fenske, P. Scheer, and A. Eichhoefer, *Z. Anorg. Allg. Chem.*, 2003, **629**(3), 415.
91. E. Wiberg and M. Schmidt, *Zeitschrift fuer Naturforschung*, 1951, **6**(b), 172.
92. E. Wiberg and T. Johannsen, *Naturwissenchaften*, 1941, **29**, 320.
93. M. T. Barlow, C. J. Dain, A. J. Downs, G. S. Laurenson, and D. W. H. Rankin, *J. Chem. Soc., Dalton Trans.*, 1982, 597.
94. J. L. Atwood, S. G. Bott, C. Jones, and C. L. Raston, *Inorg. Chem.*, 1991, **30**, 4868, and references therein.
95. H. Protzmann, T. Marschner, O. Zsebok, W. Stolz, E. O. Gobel, R. Dorn, and J. Lorberth, *J. Cryst. Growth*, 1991, **115**, 248.
96. S. Nogai and H. Schmidbaur, *Inorg. Chem.*, 2002, **41**(18), 4770.
97. S. Nogai, A. Schriewer, and H. Schmidbaur, *Dalton Trans.*, 2003, 3165.
98. W. Uhl, L. Cuypers, G. Geisler, K. Harms, and W. Massa, *Z. Anorg. Allg. Chem.*, 2002, **628**(5), 1001.
99. R. J. Baker, C. Jones, M. Kloth, and J. A. Platts, *Angew. Chem., Int. Ed.*, 2003, **42**(23), 2660.
100. K. Ueno, T. Yamaguchi, K. Uchiyama, and H. Ogino, *Organometallics*, 2002, **21**(12), 2347.
101. U. Vogel, A. Y. Timoshkin, and M. Scheer, *Angew. Chem., Int. Ed.*, 2001, **40**(23), 4409.
102. R. A. Fischer, A. Miehr, and T. Priermeier, *Chem. Ber.*, 1995, **128**(8), 831.

103. L. Grocholl, S. A. Cullison, J. Wang, D. C. Swenson, and E. G. Gillan, *Inorg. Chem.*, 2002, **41**(11), 2920.

104. N. Nakata, R. Izumi, V. Y. Lee, M. Ichinohe, and A. Sekiguchi, *J. Am. Chem. Soc.*, 2004, **126**(16), 5058.

105. H. Jacobs and B. Noecker, *Z. Anorg. Allg. Chem.*, 1993, **619**(2), 381.

106. B. Luo, M. Pink, and G. W. Gladfelter, *Inorg. Chem.*, 2001, **40**(2), 307.

107. J. S. Silverman, C. J. Carmalt, A. H. Cowley, R. D. Culp, R. A. Jones, and B. G. McBurnett, *Inorg. Chem.*, 1999, **38**(2), 296.

108. W. R. Nutt, J. A. Anderson, J. D. Odom, M. M. Williamson, and B. H. Rubin, *Inorg. Chem.*, 1985, **24**, 159.

109. W. R. Nutt, J. S. Blanton, F. O. Kroh, and J. D. Odom, *Inorg. Chem.*, 1989, **28**, 2224.

110. D. L. Reger, S. J. Knox, and L. Lebioda, *Inorg. Chem.*, 1989, **28**, 3092.

111. D. L. Reger, *Coord. Chem. Rev.*, 1996, **147**, 571.

112. J. T. Leman, A. R. Barron, J. W. Ziller, and R. M. Kren, *Polyhedron*, 1989, **8**, 1909.

113. D. A. Atwood, V. O. Atwood, D. F. Carriker, A. H. Cowley, F. P. Gabbai, R. A. Jones, M. R. Bond, and C. J. Carrano, *J. Organomet. Chem.*, 1993, **463**(1–2), 29.

114. M. Stender, B. E. Eichler, N. J. Hardman, P. P. Power, J. Prust, M. Noltemeyer, and H. W. Roesky, *Inorg. Chem.*, 2001, **40**(12), 2794.

115. C. G. Pitt, K. T. Higa, A. T. McPhail, and R. L. Wells, *Inorg. Chem.*, 1986, **25**, 2484.

116. S. Weinrich, H. Piotrowski, M. Vogt, A. Schulz, and M. Westerhausen, *Inorg. Chem.*, 2004, **43**(12), 3756.

117. E. Leiner and M. Scheer, *Organometallics*, 2002, **21**(21), 4448.

118. G. Trinquier, *J. Am. Chem. Soc.*, 1990, **112**, 2130.

119. M. Driess and H. Gratzmacher, *Angew. Chem., Int. Ed.*, 1996, **35**, 828.

120. J. Su, X.-W. Li, and R. C. Robinson, *J. Am. Chem. Soc.*, 1997, **119**, 5471.

121. R. J. Wehmschulte and P. P. Power, *Angew. Chem., Int. Ed.*, 1998, **37**, 3152.

122. S. Loss, C. Widauer, and H. Gratzmacher, *Angew. Chem., Int. Ed.*, 1999, **38**, 3329.

123. B. Twamley and P. P. Power, *Angew. Chem., Int. Ed.*, 2000, **39**, 3500.

124. P. P. Power, *Chem. Rev.*, 1999, **99**, 3463.

125. N. J. Hardman, C. Cui, H. W. Roesky, W. H. Fink, and P. P. Power, *Angew. Chem., Int. Ed.*, 2001, **40**, 2172.

126. C. Von Hanisch and O. Hampe, *Angew. Chem., Int. Ed.*, 2002, **41**(12), 2095.

127. B. Neumueller, *Chem. Soc. Rev.*, 2003, **32**(1), 50.

128. J. P. Oliver, R. Kumar, and M. Taghiof, The chemistry of Alkoxides, Thiolates, and the Heavier group 16 Derivatives of Aluminum and Gallium, in 'Coordination Chemistry of Aluminum', eds. R. Gregory Heagward, VCH, New York, 1993, p. 167.

129. M. Valet and D. M. Hoffman, *Chem. Mater.*, 2001, **13**(6), 2135.

130. J. W. Huang, D. F. Gaines, T. F. Kuech, R. M. Potemski, and F. Cardone, *J. Electron. Mater.*, 1994, **23**(7), 659.

131. H. W. Heuer and R. Wehrmann, Five-Coordinate of Gallium(III) Carboxylate Complexes With Blue/Blue–Green Photo- and Electroluminescence, Procedures for their Production as Well as their Use, DE 10225826, 2003.

132. L. V. Budaragin, V. Leonid, Cost-Effective Method for Coating Substrate with Metal Oxide Coating., US 20020041928, 2002.

133. M. T. Andras, S. A. Duraj, A. F. Hepp, P. E. Fanwick, and M. M. Bodnar, *J. Am. Chem. Soc.*, 1992, **114**, 786.

134. T. L. Feng, P. L. Gurian, M. D. Healy, and A. R. Barron, *Inorg. Chem.*, 1990, **29**, 408.

135. P. O'Brien, H. Salacinski, and M. Motevalli, *J. Am. Chem. Soc.*, 1997, **119**(51), 12695.

136. K. Saito and A. Nagasawa, *Polyhedron*, 1990, **9**, 215.

137. O. T. Beachley, J. R. Gardinier, and M. R. Churchill, *Organometallics*, 2003, **22**(5), 1145.

138. O. T. Beachley, J. R. Gardinier, and M. R. Churchill, *Organometallics*, 2000, **19**(22), 4544.

139. C. L. Edwards and R. L. Hayes, *J. Nucl. Med.*, 1969, **10**, 103.

140. W. O. Nelson, T. B. Karpishin, S. J. Rettig, and C. Orvig, *Inorg. Chem.*, 1988, **27**, 1045.

141. Z. Zhang, S. J. Rettig, and C. Orvig, *Inorg. Chem.*, 1991, **30**, 509.

142. D. J. Clevette, D. M. Lyster, W. O. Nelson, T. Rihela, G. A. Webb, and C. Orvig, *Inorg. Chem.*, 1990, **29**, 667.

143. L. E. Maelia and S. A. Koch, *Inorg. Chem.*, 1986, **25**, 1896.

144. K. Ruhlandt-Senge and P. P. Power, *Inorg. Chem.*, 1991, **30**, 2633, 3683.

145. M.-A. Munoz-Hernandez, P. Wei, S. Liu, and D. A. Atwood, *Coord. Chem. Rev.*, 2000, **210**, 1.

146. G. G. Hoffmann and C. Burschka, *Angew. Chem.*, 1985, **97**, 965; *Angew. Chem., Int. Ed. Engl.*, 1985, **24**, 970.

147. M. R. Lazell, P. O'Brien, D. J. Otway, and J.-H. Park, *Chem. Mater.*, 1999, **11**, 3430.

148. A. Horley, M. R. Lazell, and P. O'Brien, *Adv. Mater., Chem. Vap. Dep.*, 1999, **5**, 203.

149. D. P. Dutta, V. K. Jain, A. Knoedler, and W. Kaim, *Polyhedron*, 2002, **21**(2), 239.

150. J.-H. Park, P. O'Brien, A. J. P. White, and D. J. Williams, *Inorg. Chem.*, 2001, **40**(14), 3629.

151. N. J. Hardman and P. P. Power, *Inorg. Chem.*, 2001, **40**(11), 2474.

152. G. Shang, M. J. Hampden-Smith, and E. N. Duesler, *Inorg. Chem.*, 1996, **35**(9), 2611.

153. S. D. Nogai and H. Schmidbaur, *Dalton Trans.*, 2003, 2488.

154. W. Klemm, W. Tilk, and H. Jacobi, *Z. Anorg. Chem.*, 1932, **207**, 187.

155. R. J. Baker, H. Bettentrup, and C. Jones, *Eur. J. Inorg. Chem.*, 2003, **13**, 2446.

156. X. Sava, M. Melaimi, N. Mezailles, L. Ricard, and F. Mathey, *New J. Chem.*, 2002, **26**(10), 1378.

157. N. R. Bunn, S. Aldridge, D. L. Coombs, A. Rossin, D. J. Willock, C. Jones, and L. Ooi, *Chem. Commun.*, 2004, 1732.

158. D. J. Clevette and C. Orvig, *Polyhedron*, 1990, **9**, 151.

159. R. J. Motekaitis, Y. Sun, A. E. Martell, and M. J. Welch, *Inorg. Chem.*, 1991, **30**(13), 2737, and references therein.

160. D. A. Moore, P. E. Fanwick, and M. J. Welch, *Inorg. Chem.*, 1990, **29**, 672.

161. R. C. Matthews, D. Parker, G. Ferguson, B. Kaitner, A. Harrison, and L. Royle, *Polyhedron*, 1991, **10**, 1951.

162. R. J. Motekaitis, Y. Sun, and A. E. Martell, *Inorg. Chem.*, 1991, **30**, 1554.

163. A. Coutsolelos, R. Guilard, D. Bayeul, and C. Lecomte, *Polyhedron*, 1986, **5**, 1157.

164. K. M. Kadish, J.-L. Cornillon, A. Coutsolelos, and R. Guilard, *Inorg. Chem.*, 1987, **26**, 4167.

165. Y. Feng, S.-L. Ong, J. Hu, and W.-J. Ng, *Inorg. Chem. Commun.*, 2003, **6**(5), 466.

166. Z. Gross, A. Mahammed, and I. Saltsman, PCT Int. Appl. (2003), 47 pp. WO 2003004021.

167. I. Saltsman, A. Mahammed, I. Goldberg, E. Tkachenko, M. G. Botoshansky, and Z. Gross, *J. Am. Chem. Soc.*, 2002, **124**(25), 7411.

168. W. Niu, E. H. Wong, G. R. Weisman, R. D. Sommer, and A. L. Rheingold, *Inorg. Chem. Commun.*, 2002, **5**(1), 1.

169. S. Kimura, E. Bill, E. Bothe, T. Weyhermueller, and K. Wieghardt, *J. Am. Chem. Soc.*, 2001, **123**(25), 6025.

170. S. Y. Bylikin, D. A. Robson, N. A. Male, L. H. Rees, P. Mountford, and M. Schroder, *J. Chem. Soc., Dalton Trans.*, 2001, 170.

171. M. Linas, D. M. Wilson, and J. B. Neilands, *Biochemistry*, 1973, **112**, 3836.

172. S. M. Moerlien, M. L. Welch, K. N. Raymond, and F. L. Weitl, *J. Nucl. Med.*, 1982, **22**, 720.

Gallium: Organometallic Chemistry

Gregory H. Robinson
The University of Georgia, Athens, GA, USA

Based in part on the article Gallium: Organometallic Chemistry by Andrew R. Barron which appeared in the Encyclopedia of Inorganic Chemistry, First Edition.

1 INTRODUCTION

The organometallic chemistry of gallium has experienced substantial growth in the intervening decade since publication of the first edition of the *Encyclopedia of Inorganic Chemistry*. One could legitimately argue that the organometallic chemistry of gallium has only just begun to be studied with a critical hand and vigilant eye in the last two decades. It seems that much of the activity in the organometallic chemistry of gallium during this period was driven by the quest for single-source molecular precursors to advanced materials (e.g. semiconductors) and the utilization of organogallium compounds in *Metal-Organic Chemical Vapor Deposition* (MOCVD) procedures.[1] Although it is evident that the breadth of the organometallic chemistry of gallium is as wide as it is varied, fundamental issues relating to structure and bonding have been a substantial driving force in this field much of the past decade. Perhaps more than could ever have been imagined when Paul-E'mile Lecoq de Boisbaudran discovered this rare and oddly mercurial element in 1875, the organometallic chemistry of gallium has been proven to be engaging and exciting. This contribution does not seek to cover the same fundamental material so eloquently presented in the original chapter, *Gallium: Organometallic Chemistry*, authored by A.R. Barron. Rather, this contribution seeks to utilize the original chapter as a template and bring sharper focus to some of the more noteworthy advances in the organometallic chemistry of gallium of the past decade. Specifically, this contribution seeks to highlight two prominent areas: (1) Organogallium compounds utilizing sterically demanding ligands; and (2) Organogallium cluster compounds. However, for historical perspective it is important to first contrast the synthesis of sterically demanding organogallium compounds with that of simple trialkyl and triaryl organogallium compounds.

2 SIMPLE TRIALKYL AND TRIARYL ORGANOGALLIUM COMPOUNDS

2.1 Syntheses

Triethylgallium monoetherate, $Et_3Ga{\cdot}(Et_2O)$, the first reported organometallic compound of gallium, was isolated from reaction of ethylmagnesium bromide with gallium bromide in 1932 (equation 1).[2]

$$3EtMgBr + GaBr_3 \xrightarrow[Et_2O]{} Et_3Ga{\cdot}(Et_2O) \quad (1)$$

Triethylgallium monoetherate was isolated as a colorless, moderately viscous, pyrophoric liquid. The workers also reported that ether-free triethylgallium, Et_3Ga, could be prepared from reaction of gallium metal with diethylmercury. These two synthetic methods – reaction of a gallium halide with a Grignard Reagent and reaction of metallic gallium with a dialkylmercury reagent – are indicative of the often straightforward manner in which simple gallium alkyls and aryls may be prepared. Generally, simple gallium alkyls and gallium aryls may be approached synthetically by variations of these methods. However, some methods are significantly more effective than others.

2.1.1 Grignard Reagents

The utilization of Grignard Reagents, RMgX, with gallium halides, GaX_3, is perhaps the most versatile synthetic method to approach simple gallium alkyls and aryls. Indeed, not only was this the preparative method of choice for triethylgallium[2] in 1932, but it was also used to prepare trimesitylgallium, Mes_3Ga (Mesityl = 1,3,5-trimethylphenyl) – arguably the first sterically demanding organogallium compound – more than five decades later (equation 2).[3]

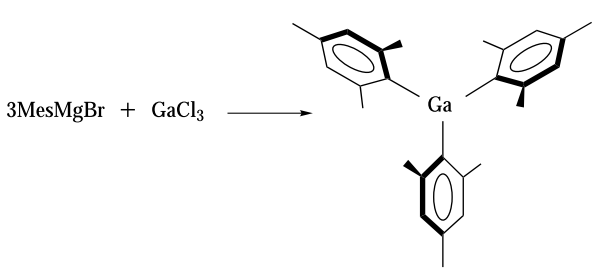

(2)

Mesitylmagnesium bromide was also utilized to prepare dichloromesitylgallium derivatives, which were reported as an inorganic polymer.[4] The following sterically demanding

organogallium compounds, R_3Ga, have been prepared (where R =: -neopentyl[5] and $-CH_2CMe_2Ph$).[6] One of the more recent sterically demanding organogallium species to be prepared by this route is the bis(adamantyl)-based gallate anions, $[Ada_2GaMe_2]^-$ and $[Ada_2GaBr_2]^-$ (Ada = adamantyl).[7] As is widely known, diethyl ether is often present in the organogallium products of such reaction products. However, it is often possible to obtain the ether-free moiety after prolonged exposure to vacuum. In addition, if the ligand is sufficiently sterically demanding, such as (Me_5C_6) Ga, ether complexation with the metal center is often prevented.

2.1.2 Lithium Reagents

The utilization of organolithium reagents, RLi (R = alkyl or aryl), with gallium halides is also a fruitful route to organogallium compounds. The overall reaction is quite similar to that of the Grignard Reagents: for example, reaction of phenyllithium with gallium chloride readily yields triphenylgallium, Ph_3Ga (equation 3).

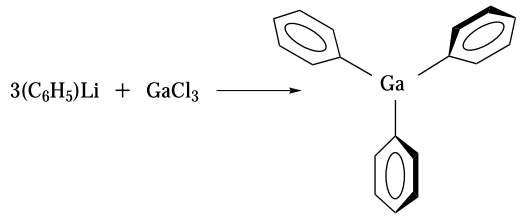

(3)

This method bears some similarities to the Grignard Reagent method in that product formation is often accomplished with solvent association. In particular, this method has been useful in preparing sterically demanding organogallium compounds, $(Aryl)_3Ga$ (vide infra).

2.1.3 Organomercury Reagents

Although organomercury reagents such as dimethylmercury, Me_2Hg, present significant toxicity concerns, these compounds offer a straightforward route to simple organogallium compounds. As demonstrated by the reaction of dimethylmercury with gallium metal, these reactions may be regarded as organometallic redox systems: the gallium metal is oxidized to R_3Ga while the mercury in Me_2Hg is reduced to elemental mercury (equation 4).

$$3Me_2Hg + 2Ga \longrightarrow 2Me_3Ga + 3Hg \qquad (4)$$

This method can also be utilized to prepare trimethylindium. It should be noted, however, that this preparative method is quite limited, being restricted to the simplest of alkyls.

2.1.4 Ligand Redistribution

Preparation of organogallium compounds by ligand redistribution between gallium halides and alkyls of metals such as zinc and mercury is severely limited. A noteworthy example is the preparation of $(CF_3)_3Ga$, isolated from reaction of $GaCl_3$ with $(CF_3)_2Cd$.[8,9] It should be noted that a potentially important class of organogallium compounds is the mixed trialkyls, $R_2R'Ga$. For example, ligand redistribution reactions involving Cp_3Ga and Me_3Ga, to give Me_2GaCp and $MeGaCp_2$, have been examined.[10]

2.2 Structural Characterization

In one sense, the coordination chemistry of simple gallium alkyls and aryls is rather restricted to three-coordinate trigonal planar. Although single-crystal X-ray diffraction remains the most important structural technique in the organometallic chemistry realm, gas-phase electron diffraction data of Me_3Ga unambiguously confirms a monomeric species with the gallium center residing in a trigonal planar environment.[11] While single-crystal X-ray diffraction data confirms the coordination of the gallium center in triphenylgallium, Ph_3Ga, as trigonal planar (Figure 1),[12] it is interesting to note one phenyl ring is observed to be coplanar with the GaC_3 plane while a second phenyl ring resides slightly out of the GaC_3 plane at 13°. In contrast, the third phenyl ring is found to reside considerably out of plane at 31°. Indeed, a more expansive view of the unit cell reveals significant secondary interactions of each gallium center with meta carbon atoms of other Ph_3Ga units (3.42 Å). This effectively results in the coordination approaching five-coordinate trigonal bipyramidal.

A similar intermolecular stabilization has also been observed in $(t\text{-}Bu)_2Ga(OCPh_3)$[13] wherein the carbon atom of one of the phenyl rings approaches the gallium center offering

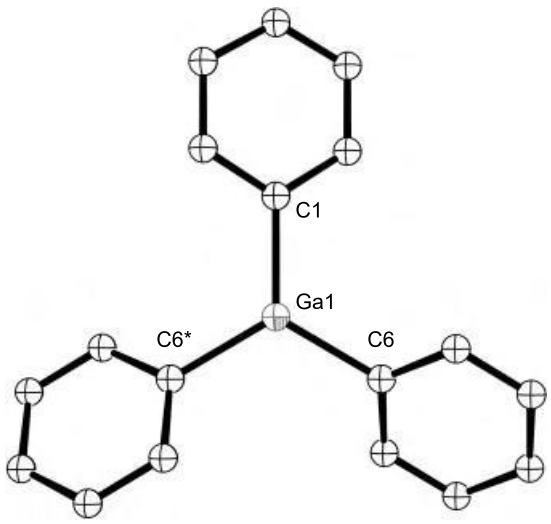

Figure 1 Solid-state structure of Ph_3Ga

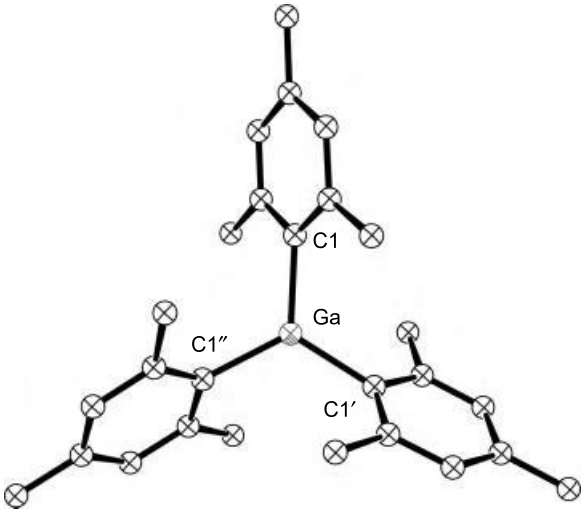

Figure 2 Solid-state structure of Mes_3Ga

additional electron density. Effectively, the coordination of the gallium center may be described as 'trigonal pyramidal': the gallium atom resides in a normal trigonal planar environment with further stabilization from one of the carbon atoms of a phenyl ring.

The solid-state structure of Mes_3Ga stands as a benchmark in organogallium chemistry.[3] The structure reveals the gallium atom in an almost idealized trigonal planar environment (C–Ga–C bond angle: 120°) (Figure 2). While the Ga–C bond distances are unremarkable (Ga–C: 1.968 Å), the mesityl rings of Mes_3Ga reside in a propeller arrangement at angles of 55.9° relative to the GaC_3 basal plane. Unlike Ph_3Ga, the steric bulk of the mesityl groups in Mes_3Ga preclude any significant secondary interaction from neighboring molecules in the unit cell or solvent donor interactions.

In notable contrast to Mes_3Ga, the solid-state structure of mesitylgallium dichloride, $MesGaCl_2$, reveals a one-dimensional polymer.[14]

3 STERICALLY DEMANDING ORGANOGALLIUM COMPOUNDS

3.1 Syntheses

Considerable activity in the synthesis of sterically demanding organogallium compounds has taken place in the past decade. In particular, there has been significant activity concerning sterically demanding *m*-terphenyl ligands. The synthesis of such organogallium compounds has predominantly been accomplished *via* the lithium reagent route. In particular, the lithium reagent method is often preferred to the Grignard reagent route by workers as it frequently provides uncomplicated reaction products. For example, the Grignard reagent method often yields ionic salts accompanied by $[Mg(Et_2O)_x]^+$ cations. Nonetheless, both Grignard reagents and lithium reagents have greatly contributed to the synthesis of sterically demanding organogallium compounds.

3.1.1 Grignard Reagents and Lithium Reagents

It is interesting that, arguably, the ligand most similar to mesityl, pentamethylphenyl, has only recently been utilized in organogallium chemistry. The synthesis of tris(pentamethylphenyl)gallium, $(C_6Me_5)_3Ga$, is cleanly achieved by reaction of the pentamethylphenylmagnesium bromide Grignard reagent with $GaCl_3$ in diethyl ether (equation 5).[15] Tris(pentamethylphenyl)gallium was isolated as colorless, needle crystals in modest yield.

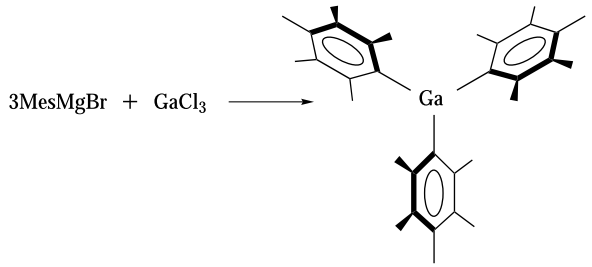

(5)

A particularly intriguing aryllithium reagent is the bis(etherate) of 2,6-diphenylphenyllithium, $(2,6\text{-}Ph_2C_6H_3)Li(Et_2O)_2$. This reagent, readily prepared by reaction of (2,6-diphenyl)-1-iodobenzene with *n*-butyllithium, is isolated as a white crystalline solid (equation 6).[16]

$$(2,6\text{-}Ph_2C_6H_3)I + n\text{-}BuLi \xrightarrow[Et_2O]{} (2,6\text{-}Ph_2C_6H_3)Li(Et_2O)_2 \quad (6)$$

The solid-state structure of $(2,6\text{-}Ph_2C_6H_3)Li(Et_2O)_2$ reveals the lithium atom in a trigonal planar environment with the Li–C bond (2.106(9) Å) being complemented by two Li–O interactions (1.943(5) Å). Reaction of $(2,6\text{-}Ph_2C_6H_3)Li$ with GaI_3 gives the neutral trigonal planar complex bis(2,6-diphenylphenyl)gallium iodide, $(2,6\text{-}Ph_2C_6H_3)_2GaI$ (equation 7).[16]

$$2(2,6\text{-}Ph_2C_6H_3)Li(Et_2O)_2 + GaI_3 \longrightarrow (2,6\text{-}Ph_2C_6H_3)_2GaI \quad (7)$$

It is noteworthy that when gallium(III) chloride, $GaCl_3$, instead of GaI_3, is allowed to react with $(2,6\text{-}Ph_2C_6H_3)Li(Et_2O)_2$, the ionic complex $[Li(Et_2O)_2][(2,6\text{-}Ph_2C_6H_3)GaCl_3]$ is obtained (instead of the neutral chloride analog of $(2,6\text{-}Ph_2C_6H_3)_2GaI$).[16] Indeed, the analogous ionic compound, $[Li(Et_2O)_2][(1,3,5\text{-}Ph_3C_6H_3)GaCl_3]$, is also isolated from reaction of the related lithium aryl 1,3,5-triphenylphenyllithium, $(1,3,5\text{-}Ph_3C_6H_2)Li$, with $GaCl_3$.[16] Thus, it appears that the propensity to obtain the neutral trigonal planar diarylgallium halide is enhanced when iodide is used instead of chloride.

Arguably, the most prominent aryllithium reagent in organogallium chemistry of the past decade is 2,6-dimesitylphenyllithium, (2,6-$Mes_2C_6H_3$)Li. The previous statement is justifiable owing to the significant organogallium compounds prepared using this sterically demanding *m*-terphenyl ligand. This reagent is conveniently prepared in a straightforward fashion from reaction of 2,6-dimesityl-1-iodobenzene[17] with *n*-butyllithium.[18] Reaction of 2,6-dimesitylphenyllithium with gallium chloride readily affords bis(2,6-dimesitylphenyl)gallium chloride, (2,6-$Mes_2C_6H_3)_2GaCl$, (equation 8) in high yield.[19]

$$2(2,6\text{-}Mes_2C_6H_3)Li + GaCl_3 \longrightarrow (2,6\text{-}Mes_2C_6H_3)_2GaCl \quad (8)$$

This compound was noteworthy for two reasons: (1) The isolation of (2,6-$Mes_2C_6H_3)_2GaCl$ demonstrated that it was possible to affix two of these large *m*-terphenyl ligands about a gallium center; and (2) The T-shaped coordination geometry about the gallium center in (2,6-$Mes_2C_6H_3)_2GaCl$ was the first reported for a gallium center. Notably, both the corresponding bis(2,6-dimesitylphenyl)gallium bromide, (2,6-$Mes_2C_6H_3)_2GaBr$, and the dimeric (2,6-dimesitylphenyl)gallium dichloride complex, [(2,6-$MesC_6H_3)GaCl_2]_2$, have also been prepared and their solid-state structures determined.[20]

A variation on this method produces perhaps the most sterically protected gallium center reported in dimesityl-(2,6-dimesitylphenyl)gallium, $(Mes)_2$(2,6-$Mes_2C_6H_3$) Ga.[20] This compound was prepared by reaction of (2,6-$Mes_2C_6H_3$)Li with $GaCl_3$ followed by the in situ reaction with mesityllithium.

3.2 Structural Characterization

The structural characterization of sterically demanding organogallium compounds is arguably the most significant development in this area of the past decade. The fact that gallium atoms have been observed in a variety of coordination environments over the past decade underscores the fact that the organometallic chemistry of gallium is as varied as it is exciting.

It is perhaps expected that the pentamethylphenyl ligand has received considerably less attention than the closely related mesityl ligand. Indeed, the addition of two additional methyl groups in the two meta positions of a mesityl moiety would hardly be expected to result in any significant structural changes. The facts, however, bespeak as to why experiments are necessary. The coordination of the gallium center in $(C_6Me_5)_3Ga$ is almost idealized trigonal planar with a C–Ga–C bond angle of 120.1(2)°. The structure of $(C_6Me_5)_3Ga$ (Figure 3) is most easily compared to that of Mes_3Ga. Both $(C_6Me_5)_3Ga$ and Mes_3Ga approximate D_3 symmetry. It is surprising that the mean Ga–C bond distance of 1.981 Å in $(C_6Me_5)_3Ga$ is considerably longer than the reported values for either Ph_3Ga (1.957 Å) or Mes_3Ga (1.968 Å). The mesityl rings

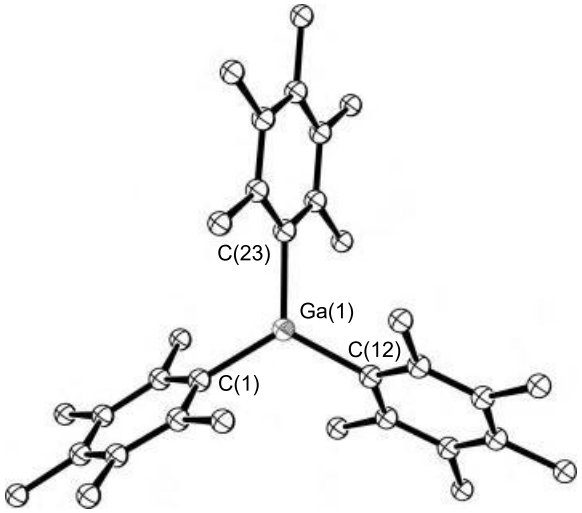

Figure 3 Solid-state structure of $(C_6Me_5)_3Ga$

of Mes_3Ga reside in a propeller arrangement at angles of 55.9°. However, the angles of the (C_6Me_5)-rings in $(C_6Me_5)_3Ga$ are 67.3°, 62.3°, and 60.9°. Contributing factors to this may be a weak aromatic–aromatic interaction, at a distance of 4.1 Å, between parallel rings of two molecules in the unit cell.

The solid-state structure of bis(2,6-diphenylphenyl)gallium iodide, (2,6-$Ph_2C_6H_3)_2GaI$,[16] displays the gallium atom in a somewhat distorted trigonal planar environment (C–Ga–C: 134.3(3)°). The Ga–I bond distance of 2.550(1) Å is unremarkable (Figure 4).

Perhaps the most telling comparison of (2,6-$Ph_2C_6H_3$)- is with the closely related, but even more sterically demanding ligand system of 2,6-dimesitylphenyl, (2,6-$Mes_2C_6H_3$)-. The solid-state structures of both bis(2,6-dimesitylphenyl)gallium

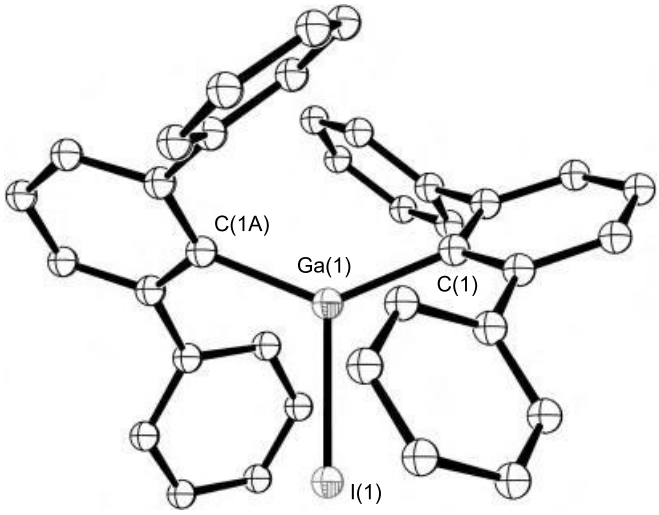

Figure 4 Solid-state structure of (2,6-$Ph_2C_6H_3)_2GaI$

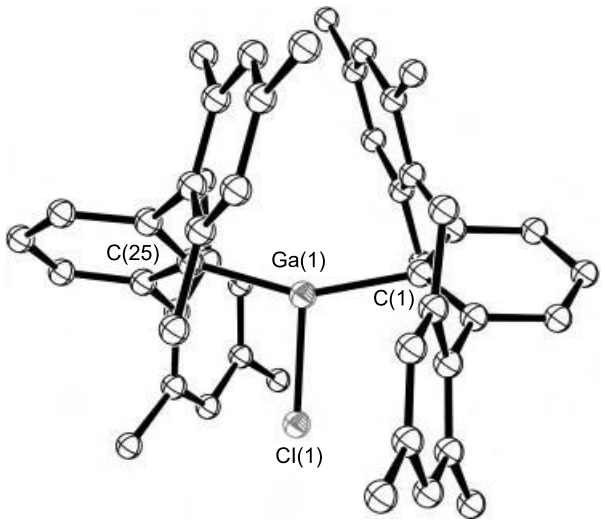

Figure 5 Solid-state structure of $(2,6\text{-}Mes_2C_6H_3)_2GaCl$

chloride, $(2,6\text{-}Mes_2C_6H_3)_2GaCl$ (Figure 5),[19] and bis(2,6-dimesitylphenyl)gallium bromide, $(2,6\text{-}Mes_2C_6H_3)_2GaBr$,[20] have been determined. They are isostructural. Although the Ga–X bond distances are rather long (X = Cl: 2.177(5) Å; X = Br: 2.3183(1) Å), the singular most striking feature of these compounds is the C–Ga–C bond angles of 153.5(5)°. The normal coordination for three-coordinate gallium is trigonal planar with bond angles about the metallic center approximating 120°. However, the C–Ga–C bond angles in these two compounds substantially exceed the 120° benchmark sufficiently to justify the T-shaped description. The T-shaped structure is almost exclusively reserved for interhalogen compounds such as ClF_3 and BrF_3 wherein the coordination is facilitated by the steric repulsion of the two lone pairs of electrons about the central halide ion. Thus, $(2,6\text{-}Mes_2C_6H_3)_2GaCl$ and $(2,6\text{-}Mes_2C_6H_3)_2GaBr$ are significant in that they represent rare examples of three-coordinate gallium atoms assuming the uncommon T-shaped coordination environment through sheer ligand steric repulsion (*without* the aid of lone pair–lone pair repulsion).

4 ORGANOMETALLIC COMPOUNDS CONTAINING GALLIUM–GALLIUM BONDS

The stabilization of the Ga–Ga bond is, arguably, the most important development of the past decade in the organometallic chemistry of gallium. Perhaps the most significant factor in the stabilization of these compounds is the utilization of sterically demanding ligands. Such ligands are necessary as they provide kinetic stabilization. It is anticipated that this field will only continue to grow as workers realize the variety of compounds that may be isolated.

4.1 Synthesis

4.1.1 Gallium Dimers and Tetrahedra

A notable difference between gallium and aluminum lies in the 2+ oxidation state: while aluminum(II) halides are not known, those of gallium are stable and well known. Indeed, the solid-state structures of bis-dioxane adducts of both gallium(II) chloride[21] and gallium(II) bromide[22] have been shown to reside about Ga–Ga bonds. Gallium(II) bromide was utilized with bis(trimethylsilyl)methyllithium in the preparation of the first organometallic compound unambiguously shown to possess a Ga–Ga bond: tetrakis[bis(trimethylsilyl)methyl]digallane, $[(Me_3Si)_2HC]_2Ga\text{–}Ga[(CH(SiMe_3)_2)]_2$ (equation 9).[23]

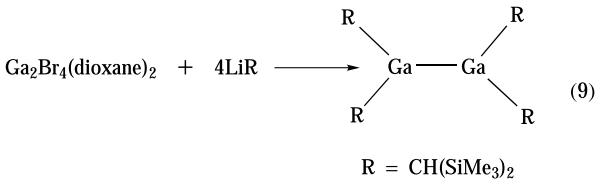

This novel compound was isolated as yellow crystals from pentane.

The first tetraaryldigallane, $[Pr_3C_6H_2]_2Ga\text{–}Ga[C_6H_2Pr_3]_2$, was prepared by reaction of $Ga_2Cl_4(dioxane)_2$ with the corresponding Grignard reagent.[24] Treatment of this digallane with an excess of lithium powder gave a dark solution. The addition of 12-crown-4 and workup produced a radical anion, $[Pr_3C_6H_2]_2Ga\text{–}Ga[C_6H_2Pr_3]_2^{\bullet -}$, that was held to possess a measure of multiple bond character in the Ga–Ga bond.

A particularly interesting synthesis concerns reaction of $Ga_2Br_4(dioxane)_2$ with ether-free $LiC(SiMe_3)_3$: this reaction gives the novel $[\{GaC(SiMe_3)_3\}_4]$ tetramer.[25] $[\{GaC(SiMe_3)_3\}_4]$, isolated as a dark red crystalline compound, is noteworthy as it represents the first example of gallium assuming the 1+ oxidation state in an organometallic compound. In addition, this remarkable compound demonstrated unusual thermal stability (only decomposing above 255 °C) and could be stored in air for months without decomposition.

Perhaps the organogallium compound most closely related to the tetrahedral metallic core of $[\{GaC(SiMe_3)_3\}_4]$ is $[\{(Me_3Si)_3C\}_6Ga]_8$.[26] The critical point in this synthesis is the utilization of gallium(I) bromide, GaBr. Reaction of trimethylsilyllithium (dissolved in toluene at −78 °C) with GaBr, after considerable workup, affords $[\{(Me_3Si)_3C\}_6Ga_8]$. This dark red/black crystalline compound contains a Ga_8 core: two Ga_4-tetrahedra linked by a single Ga–Ga bond.

4.1.2 Gallium Rings

Organometallic compounds containing gallium rings were first reported in 1995: sodium metal reduction of (2,6-$Mes_2C_6H_3$)$GaCl_2$[27] resulted in a deeply red colored solution from which a red (almost black) crystalline compound was isolated (equation 10). These crystals were determined to be Na_2[(2,6-$Mes_2C_6H_3$)Ga]$_3$.[28]

$$3(2,6\text{-}Mes_2C_6H_3)GaCl_2 + 8Na \xrightarrow[-6NaCl]{} Na_2[(2,6\text{-}Mes_2C_6H_3)_2Ga]_3 \quad (10)$$

Quite surprisingly, this compound was shown to contain an unprecedented gallium three-membered ring at its core. The potassium analog, K_2[(2,6-$Mes_2C_6H_3$) Ga]$_3$, was subsequently reported by the same laboratory.[29] Similar to the nomenclature used for organic ring compounds (i.e. cyclopropane), this class of organogallium compounds were referred to as *cyclogallanes*. Particularly significant, these compounds were shown to possess a new type of aromaticity – *metalloaromaticity*: traditional aromatic behavior derived from a metallic ring system (instead of carbon).[30–32] A noteworthy Ga_4-based cyclogallane, K_2[(2,6-$Mes_2C_6H_3$) Ga]$_4$,[33] and a 'silagallane',[34] an organometallic cluster with a III–IV skeleton of gallium and silicon atoms, have also been reported. In the silagallane, a trigonal arrangement of three gallium atoms is capped by two silicon atoms in the axial positions.

4.2 Structural Characterization

Certainly unambiguous single-crystal X-ray crystal structures are critical in this area of organogallium chemistry. The solid-state structure of tetrakis[bis(trimethylsilyl)methyl]digallane, [$(Me_3Si)_2HC]_2Ga$–Ga[$(CH(SiMe_3)_2)]_2$ (Figure 6),[23] with its Ga–Ga bond distance of 2.541(1) Å, remains a benchmark in organometallic chemistry. In addition, this gallane possesses a planar C_2Ga–GaC_2 core. Valence bond theory would hold that the gallium atoms are sp^2 hybridized with an empty p orbital orthogonal to the planar C_2Ga–GaC_2 core. It is also noteworthy that the planar C_2Al–AlC_2 core was reported for the corresponding [$(Me_3Si)_2HC]_2Al$–Al[$(CH(SiMe_3)_2)]_2$ alane.[35] This fact will become important as organometallic compounds containing multiple bond character in the Ga–Ga interaction are approached (vide infra). Perhaps expected, the Ga–Ga bond observed in [$(Me_3Si)_2HC]_2Ga$–Ga[$(CH(SiMe_3)_2)]_2$ (2.541(1) Å) was lengthened from that reported for the gallium(II) bromide bis(dioxane), Br_2Ga–$GaBr_2\cdot$(dioxane)$_2$, starting compound (2.395(6) Å).[22] Certainly, the important role of sterically demanding ligands and the manner in which they lend kinetic stabilization to such compounds was critically important in the development of the chemistry of the Ga–Ga bond.

Of all the polyhedra, the tetrahedra hold a unique place. The core of [{$GaC(SiMe_3)_3$}$_4$][25] (Figure 7) bears a striking resemblance to that of white phosphorus, P_4: a nearly idealized tetrahedral core. The Ga–Ga bond distances in [{$GaC(SiMe_3)_3$}$_4$], ranging from 2.678(4) to 2.702(4) Å, are slightly longer than those reported for the initial gallane of 2.541(1) Å.

The Ga_4 tetrahedral of [{$GaC(SiMe_3)_3$}$_4$] readily compared with the striking double gallium tetrahedral, [{$(Me_3Si)_3C$}$_6Ga_8$], reported by Schnöckel in 2001 (Figure 8).[26] The fact that two Ga_4 tetrahedra are connected by a single Ga–Ga bond is stunning and suggests that the Ga–Ga bond is sufficiently robust to possibly link larger polyhedra. All angles within the two tetrahedral approach 60°. The

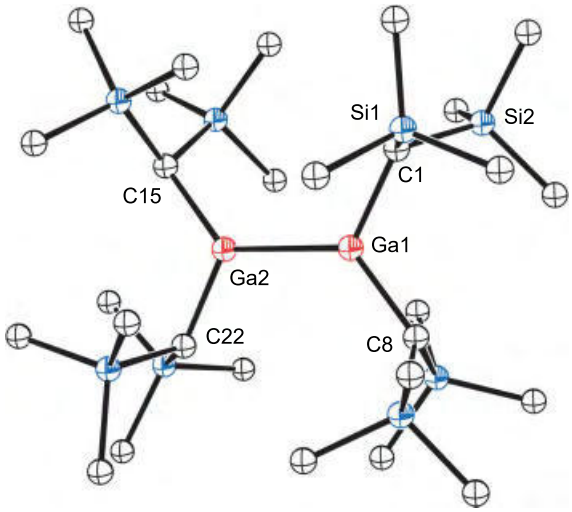

Figure 6 Solid-state structure of [$(Me_3Si)_2HC]_2Ga$–Ga[$(CH(SiMe_3)_2)]_2$

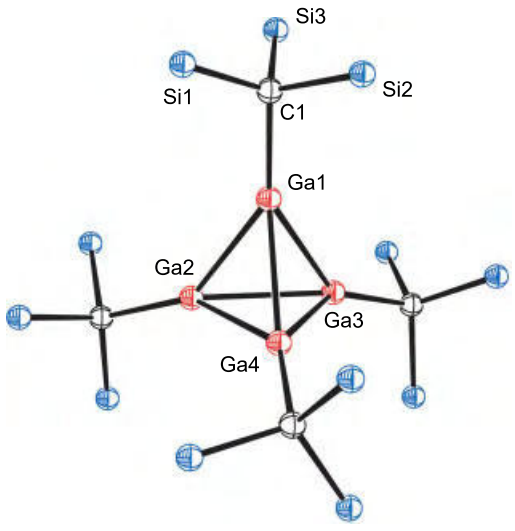

Figure 7 Solid-state structure of [{$GaC(SiMe_3)_3$}$_4$]

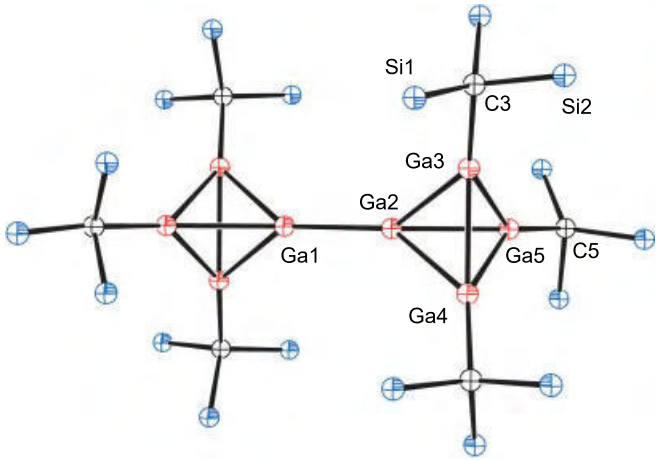

Figure 8 Solid-state structure of $[\{(Me_3Si)_3C\}_6Ga_8]$

Ga–Ga bond distances reside within the somewhat narrow range of 2.605 to 2.648 Å. As the authors stated, this was the first example of 'two tetrahedral R_3M units linked by a single metal–metal bond' in a homonuclear cluster.

The Ga–Ga bond distances in the first reported gallium ring system, $Na_2[(2,6\text{-}Mes_2C_6H_3)Ga]_3$ (Figure 9),[28] were determined to be 2.441(1) Å. The Ga–Ga–Ga bond angles within the metallic triangle were 60.01(1)°. While the sodium atoms do not appear to be engaged in any significant bonding interaction with the gallium atoms (Na···Ga approach: 3.1 Å), the sodium atoms appear to be assisted by subtle, yet significant, interactions with the π-electron cloud of the substituent rings of the *m*-terphenyl ligands.

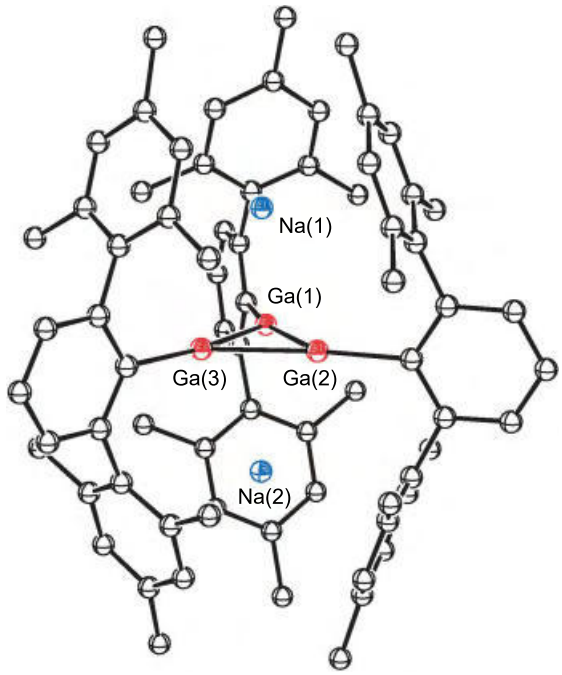

Figure 9 Solid-state structure of $Na_2[(2,6\text{-}Mes_2C_6H_3)Ga]_3$

The structural features of the potassium-based cyclogallane, $K_2[(2,6\text{-}Mes_2C_6H_3)Ga]_3$,[29] are very similar with Ga–Ga–Ga bond angles of 60.0° and Ga–Ga bond distances of 2.4260(5), 2.4317(5), and 2.4187(5) Å. These values are easily compared to $K_2[R_2Ga_4]$(R = 2,6-(2,4,6-*i*-$Pr_3C_6H_2)_2C_6H_3$),[36] which was described as having a 'planar, almost square Ga_4 core'. The Ga–Ga bond distances in this compound were shown to be slightly longer at 2.4624(4) and 2.4685(3) Å while the Ga–Ga–Ga bond angles were shown to be 87.222(11) and 92.778(11)°.

5 RELATED ARTICLES

Main Group: Multiple Bonding.

6 REFERENCES

1. A. C. Jones, *Chemtronics*, 1989, **4**, 15.
2. L. M. Dennis and W. Patnode, *J. Am. Chem. Soc.*, 1932, **54**, 182.
3. O. T. Beachley, M. R. Churchill, J. C. Pazik, and J. W. Ziller, *Organometallics*, 1986, **5**, 1814.
4. O. T. Beachley, M. R. Churchill, J. C. Pazik, and J. W. Ziller, *Organometallics*, 1987, **6**, 2088.
5. O. T. Beachley and J. C. Pazik, *Organometallics*, 1988, **7**, 1516.
6. O. T. Beachley, M. J. Noble, M. R. Churchill, J. C. Pazik, and J. W. Ziller, *Organometallics*, 1992, **11**, 1051.
7. J. K. Vohs, L. E. Downs, M. E. Barfield, K. Latibeaudiere, and G. H. Robinson, *J. Organomet. Chem.*, 2003, **666**, 7.
8. D. Neumann, W. Strauss, and W. Tyrra, *J. Organomet. Chem.*, 1991, **407**, 1.
9. M. A. Guerra, S. K. Mehrotra, D. W. Dyer, and R. J. Lagow, *J. Organomet. Chem.*, 1990, **390**, C37.
10. O. T. Beachley, T. L. Royster, and J. R. Arhar, *J. Organomet. Chem.*, 1992, **434**, 11.
11. B. Beagley, D. G. Schmidling, and I. A. Steer, *J. Mol. Struct.*, 1974, **21**, 437.
12. J. F. Malone and W. S. McDonald, *J. Chem. Soc. (A)*, 1970, 3362.
13. M. A. Petrie, M. M. Olmstead, and P. P. Power, *J. Am. Chem. Soc.*, 1991, **113**, 8704.
14. Z. Zhang, S. J. Rettig, and C. Orvig, *Inorg. Chem.*, 1991, **30**, 509.
15. J. K. Vohs, E. Downs, M. E. Barfield, S. D. Goodwin, and G. H. Robinson, *Polyhedron*, 2002, **21**, 531.

16. R. C. Crittendon, B. C. Beck, J. Su, X.-W. Li, and G. H. Robinson, *Organometallics*, 1999, **18**, 156.
17. C.-J. F. Du, H. Hart, and K.-K. Ng, *J. Org. Chem.*, 1986, **51**, 3162.
18. K. Ruhlandt-Senge, J. J. Ellison, R. J. Wehmschulte, F. Pauer, and P. P. Power, *J. Am. Chem. Soc.*, 1993, 11353.
19. X.-W. Li, W. T. Pennington, and G. H. Robinson, *Organometallics*, 1995, **14**, 2109.
20. R. C. Crittendon, X.-W. Li, J. Su, and G. H. Robinson, *Organometallics*, 1997, **16**, 2443.
21. J. C. Beamish, R. W. H. Small, and I. J. Worrall, *Inorg. Chem.*, 1979, **18**, 220.
22. R. W. H. Small and I. J. Worrall, *Acta Crystallogr., Sect. B*, 1982, **38**, 250.
23. W. Uhl, M. Layh, and T. Hildenbrand, *J. Organomet. Chem.*, 1989, **364**, 289.
24. X. He, R. A. Barlett, M. M. Olmstead, K. Ruhlandt-Senge, B. E. Sturgeon, and P. P. Power, *Angew. Chem., Int. Ed. Engl.*, 1993, **32**, 717.
25. W. Uhl, W. Hiller, M. Layh, and W. Schwarz, *Angew. Chem., Int. Ed. Engl.*, 1992, **31**, 1364.
26. A. Schnepf, R. Köppe, and H. Schnöckel, *Angew. Chem., Int. Ed. Engl.*, 2001, **40**, 1241.
27. J. Su, X.-W. Li, and G. H. Robinson, *Chem. Commun.*, 1998, 2015.
28. X.-W. Li, W. T. Pennington, and G. H. Robinson, *J. Am. Chem. Soc.*, 1995, **117**, 7578.
29. X.-W. Li, Y. Xie, P. R. Schreiner, K. D. Gripper, R. C. Crittendon, C. F. Campana, H. F. Schaefer, and G. H. Robinson, *Organometallics*, 1996, **15**, 3798.
30. Y. Xie, P. R. Schreiner, H. F. Schaefer, X.-W. Li, and G. H. Robinson, *J. Am. Chem. Soc.*, 1996, **118**, 10635.
31. Y. Xie, P. R. Schreiner, H. F. Schaefer, X.-W. Li, and G. H. Robinson, *Organometallics*, 1998, **17**, 114.
32. G. H. Robinson, *Acc. Chem. Res.*, 1999, **32**, 773.
33. B. Twamley and P. P. Power, *Angew. Chem., Int. Ed. Engl.*, 2000, **39**, 3500.
34. G. Linti, W. Köster, H. Piotrowski, and A. Rodig, *Angew. Chem., Int. Ed. Engl.*, 1998, **37**, 2209.
35. W. Uhl, *Z. Naturforsch.*, 1988, **43b**, 1113.
36. B. Twamley and P. P. Power, *Angew. Chem. Int. Ed. Engl.*, 2000, **39**, 3500.

Acknowledgment

The author wishes to thank a number of gifted coworkers and students for their contributions. In addition, gratitude is expressed to the National Science Foundation and to the Petroleum Research Fund, administered by the American Chemical Society, for financial support.